IMPROVED SOIL MOISTURE ACCOUNTING IN HYDROLOGIC MODELS

A Dissertation

Submitted to the Faculty

of

Purdue University

by

Adnan Rajib

In Partial Fulfillment of the

Requirements for the Degree

of

Doctor of Philosophy

May 2017

Purdue University

West Lafayette, Indiana

To my parents

ACKNOWLEDGEMENTS

Dr. Venkatesh Merwade, there was never any doubt in me that you are the best mentor I could ever have. Thank you. I will always attest your immense care to systematically lay out the foundation stone on which I could grow myself as an independent researcher.

I thank Purdue's College of Education for awarding me with the prestigious Bilsland Dissertation Fellowship. I would also like to extend sincere gratitude to my thesis committee members, Dr. Rao Govindaraju, Dr. Indrajeet Chaubey and Dr. Dennis Lyn, who have provided insights and helpful comments for improving the quality of my research. I am grateful to Dr. Cibin Raj for being a mentor in the early stage of my modeling literacy. I also thank all my 'Hydro-group' colleagues who made my PhD journey enjoyable: Zhu Liu, Liuying Du, Sayan Dey, Keighobad Jafarzadegan, Jessica Eisma, Ganesh Mallya, Rebecca Essig, David Cannon and Nikhil Sangwan. Siddharth Saksena, you have been the sounding board since my very first day at the Purdue University. I thank Ms. Kimberly Peterson, department secretary, for proof-reading all the research papers I have co-authored during my PhD.

I cannot find any word to express gratitude to my parents and my parents-in-law, my only sister and brother-in-law – it is their unconditional blessing which has driven me this far. To my wife, Warda, thank you for being with me; let's not forget every little happiness and struggling moments we shared together in the 218, Nimitz Drive at the Purdue Village (2013-2017).

TABLE OF CONTENTS

Contents

LIST OF TABLES

Page

LIST OF FIGURES

ABSTRACT

Rajib, Adnan. Ph.D., Purdue University, May 2017. Improved soil moisture accounting in hydrologic models. Major Professor: Venkatesh M. Merwade

Uncertainty is inherent in any hydrologic prediction; an apparently well-performing model can still be a pseudo-accurate model giving right answers for wrong reasons. Soil Moisture Accounting (SMA), being the integrated framework to partition water balance, regulates the overall physical consistency and predictive skills of a hydrologic model. Given the complex cause-and-effect relationships among soil moisture, surface runoff and evapotranspiration, there is no single solution to enhance the soundness of SMA. It is necessary to explore different "sustainable and replicable" avenues that can improve SMA, thus, enabling maximum predictability by the hydrologic model.

Using Soil and Water Assessment Tool (SWAT) on four US watersheds, this dissertation aims to accomplish three objectives including (1) evaluation of a multi-objective calibration approach for hydrologic models using remotely sensed soil moisture estimates, (2) re-conceptualization of surface runoff mechanism by incorporating a time-dependent, soil moisture-informed Curve Number method, and (3) source-attribution of inaccuracies in model's actual evapotranspiration, accordingly, evaluating a remedial measure by the spatially distributed direction ingestion of remotely sensed potential evapotranspiration. To meet the level of interoperability required between a complex hydrologic model and the remotely sensed "big data" (objectives 1 and 3), a key contribution of this study is the development of a new, adaptive tool that can perform rapid extraction and processing of satellite observations at user-defined spatial resolution.

The first objective involves evaluating the relative potential of spatially distributed surface and root zone soil moisture estimates in the calibration of SWAT model. Considering two agricultural watersheds in Indiana, USA, the proposed calibration

approach is performed using remotely sensed Advanced Microwave Scanning Radiometer-Earth Observing System (AMSR-E) surface soil moisture (~1 cm top soil) estimates in sub-basin/HRU level together with observed streamflow data at the watershed's outlet. Although application of remote sensing data in calibration improves surface soil moisture simulation, other hydrologic components such as streamflow and deeper layer moisture content remain less affected. An extension of this approach to apply root zone soil moisture estimates from limited field sensor data showed considerable improvement in those cases. Difference in relative sensitivity of parameters and reduced extent of uncertainty are also evident from the proposed method, especially for parameters related to the sub-surface hydrologic processes.

The second objective involves incorporating a time-dependent SMA based Curve Number method (SMA_CN) in the SWAT model and compare its performance with the existing CN method by simulating the hydrology of two agricultural watersheds in Indiana, USA. Results show that fusion of the SMA_CN method in SWAT better predicts streamflow in all wetness conditions, thereby addressing issues related to peak and low flow predictions by SWAT in many past studies. Comparison of the calibrated model outputs with field-scale soil moisture observations reveals that the SMA overhauling enables SWAT to represent soil moisture condition more accurately, with better response to the incident rainfall dynamics. While the results from the newly introduced SMA_CN method are promising, functionality of this method would likely to be more pronounced if applied for sub-daily hydrologic forecasting.

Source-attribution of evapotranspiration uncertainty in a hydrologic model and evaluation of a remote sensing based solution are the two main aspects of the third objective. Using SWAT for three US watersheds from Indiana and Arkansas, this study first addresses the effects of parameter equifinality, energy related weather input-uncertainty and lack of geo-spatial representation on evapotranspiration simulation. In every case, remotely sensed 8-day total actual evapotranspiration (AET) estimate from Moderate Resolution Imaging Spectroradiometer (MODIS) is used as the reference to evaluate model outcome. Results from these assessments indicate the

likelihood of a pseudo-accurate model that invariably shows high streamflow prediction skills despite having severely erroneous spatio-temporal dynamics of AET. As a remedial measure, a hybrid daily PET estimate, derived from MODIS and the North American Land Data Assimilation System phase 2 (NLDAS-2), is directly ingested at each Hydrologic Response Units (HRUs) of the SWAT model to create a new configuration called SWAT-PET. Noticeably increased accuracy of three water balance components (soil moisture, AET and streamflow) in SWAT-PET, being evaluated against completely independent sources of observations/reference estimates (i.e. field sensor, satellite and gauge stations), proves the efficacy of the proposed approach towards improving physical consistency of hydrologic modeling. While the proposed approach is evaluated for a past period, the main motivation here is to serve the purpose of hydrologic forecasting once near real-time PET estimates become available.

Although three objectives are accomplished through separate studies, the proposed approaches are designed to function in an integrated way if applied together in a particular hydrologic model. While designing the methodologies, main focus was to ensure replicability such that research results from this dissertation can be readily translated into practice.

CHAPTER 1. INTRDOUCTION

1.1 Background and Motivation

Information of soil moisture and its spatio-temporal dynamics are needed for initialization of weather/climate models, irrigation scheduling and crop yield forecasting, hydroclimatic prediction of flood and droughts, efficient water quality management, as well as natural conservation practices (Walker et al., 2001; Western et al., 2002; Starks et al., 2006; Zucco et al., 2014). Accordingly, precise prediction of soil moisture has been a subject of long-standing research. Soil moisture information can be obtained from in-situ sensor-based point measurements, space-borne remote sensing, and physically-based distributed hydrologic modeling of watersheds. Typically, at large scales, spatio-temporal variability of soil moisture cannot be represented through point measurements from in-situ sensor networks. In comparison, characterizations of surface soil moisture fields captured by the remote sensing techniques have been found sufficient enough to supplement the in-situ point measurements (Njoku and Entekhabi, 1996). However, the shallow sensing depth of remote sensors (~ top 5 cm of soil; Adams et al., 2013; Vereecken et al., 2013) does not fully comply the need in flood forecasting or agricultural water management. Against this background, physics-based hydrologic models retain their value because of their ability to provide root zone soil moisture information over a continuous period of time in large scales (e.g. Chen et al., 2011; Han et al., 2012a; Rajib and Merwade, 2016).

In reality, even the most well-formulated model cannot have the perfect realization of nature mainly because of the semi-empirical process-approximations of hydrologic cycle (Beven, 2012). Hence, uncertainty in model's Soil Moisture Accounting (SMA) is obvious. Unless the uncertainties in SMA can be minimized, an apparently well-performing model can still be a pseudo-accurate, equifinal model giving right answers for wrong reasons (Favis-Mortlock, 2004).

SMA in a hydrologic model is not limited only to the estimation of soil moisture; it essentially represents an integrated framework also constituting surface runoff and evapotranspiration. Given the complex cause-and-effect relationships among these hydrologic processes, lack of precision in SMA would impart unknown degree of persistent inaccuracy in the overall water balance. In such context, there is no single solution to enhance the physical consistency of SMA. It is necessary to explore multiple "sustainable and replicable" avenues that can improve SMA individually and collectively, ensuring the highest predictability by the hydrologic model for "right reasons".

1.2 Research Objectives

Using Soil and Water Assessment Tool (SWAT) on four US watersheds, this dissertation aims to consider three avenues in order to establish improved SMA and hence, enable more realistic realization of water balance in a hydrologic model. The objectives are outlined below.

1. **Multi-objective calibration/parameter uncertainty**: This involves evaluating the performance of a hydrologic model while using both soil moisture information and streamflow for calibration. Specific tasks in this objective include: (i) use of remotely sensed sub-basin scale surface soil moisture estimates along with streamflow observations in a spatially distributed calibration scheme; and (ii) use of root zone soil moisture in similar spatially distributed approach to evaluate the relative improvements in model's SMA, streamflow simulation and parameter uncertainty.
2. **Process re-conceptualization/model uncertainty**: In this objective, a time-dependent soil moisture-based Curve Number hypothesis is incorporated within the existing structure of a hydrologic model, and then the modified model is tested for improved simulation of streamflow regimes and soil moisture in different layers of the soil profile. The hypothesis is originally proposed by Michel et al.

(2005) stating that the fraction of rainfall to be converted into runoff is directly proportional to the current moisture store level. Also, Curve Number equations should be applicable in a continuous model not only at the end of a storm but also at any instant during the storm.

3. **Model's input uncertainty**: The third objective involves source-attribution of inaccuracies in SWAT's AET simulation, and accordingly, proposing an effective solution. The specific tasks include separately analyzing the effects of parameter uncertainty, energy related weather input-uncertainty and lack of geo-spatial/bio-geochemical representation on the prediction accuracy of AET. Ultimately, spatially-distributed direct ingestion of remotely sensed daily PET is introduced as a corrective measure towards enhancing the overall hydrologic response of the model including streamflow, root zone soil moisture and AET. A key contribution here is the development of a modified SWAT source code that is fully integrated with an automatic remote sensing data processor.

SWAT (Arnold et al., 2012; Neitsch et al., 2011) is chosen for this study because it is a semi-distributed, physics-based, integrated hydrology-water quality model that has been extensively tested in different geographic/hydro-climatic settings (e.g. Abbaspour et al., 2015; Daggupati et al., 2016; Schuol et al., 2008; Zang et al., 2012). Considering the wide-ranging applications of SWAT on water availability, flood prediction, sediment/nutrient transport and crop yield, positive outcomes of this research would be beneficial to a large scientific community worldwide. Replicable ways to integrate remote sensing data resources or re-conceptualize model physics, as shown in this dissertation, are valuable contributions augmenting the ongoing developments of the SWAT model.

The first two objectives are accomplished on three agricultural watersheds in Indiana, USA. The third objective requires a comprehensive characterization of model bias in AET simulation before applying remotely sensed PET as an "energy" forcing. Hence, a fourth watershed in Arkansas, USA is considered for this particular objective that has completely different land use and climatic condition compared to the other two watersheds in Indiana.

1.3 Organization of this Dissertation

This dissertation consists of five chapters. Chapters 2-4 are based on the three research objectives. These chapters have evolved from separate studies as such they are presented in self-contained manner, i.e., each chapter has its own abstract, introduction, description of study area, methodology, results, and conclusions. Since these chapters are connected under the auspices of the main theme, i.e., to incorporate advanced SMA in hydrologic models, the overall findings, their applicability and possible future directions are synthesized in Chapter 5.

CHAPTER 2. MULTI-OBJECTIVE CALIBRATION OF A HYDROLOGIC MODEL USING SPATIALLY DISTRIBUTED REMOTELY SENSED AND IN-SITU SOIL MOISTURE

2.1 Abstract

The objective of this study is to evaluate the relative potential of spatially distributed surface and root zone soil moisture estimates in the calibration of Soil and Water Assessment Tool (SWAT) towards improving its hydrologic predictability with reduced equifinality. The Upper Wabash and Cedar Creek, two agriculture-dominated watersheds in Indiana, USA are considered as test beds to implement this multi-objective SWAT calibration. The proposed calibration approach is performed using remotely sensed Advanced Microwave Scanning Radiometer-Earth Observing System surface soil moisture (~1 cm top soil) estimates (NASA's Aqua daily level-3 gridded land surface product-version 2) in sub-basin/HRU level together with observed streamflow data at the watershed's outlet. Although application of remote sensing data in calibration improves surface soil moisture simulation, other hydrologic components such as streamflow and deeper layer moisture content in SWAT remain less affected. An extension of this approach to apply root zone soil moisture estimates from limited field sensor data showed considerable improvement of simulation for those cases. Difference in relative sensitivity of parameters and reduced extent of uncertainty are also evident from the proposed method, especially for parameters related to the subsurface hydrologic processes. Regardless, precise representation of vertical soil moisture stratification at different layers is difficult with current SWAT ET depletion mechanism. While the results from this study show that root zone soil moisture can play a major role in SWAT calibration, more studies including various soil moisture data products or actual evapotranspiration are necessary to validate the proposed approach.

2.2 Introduction

Parameter calibration is a necessary step in setting up a hydrologic model for any study. Regardless of the uncertainties in input weather data and imperfections in model physics, a calibrated model tends to provide an "acceptable" output. Simulation of surface and subsurface fluxes in a hydrologic model is strongly affected by the choice of objective variables in model calibration procedure and resultant parameter values adopted from therein (Abbaspour et al., 2007; Park et al., 2014). Similarly, several parameter combinations are possible during calibration, producing equally reasonable simulation results (equifinality; Beven, 1993). Therefore, parameters associated with subsurface fluxes get poorly optimized when models are typically calibrated against observed streamflow hydrograph (Immerzeel and Droogers, 2008; White and Chaubey, 2005).

Simultaneous use of multiple gauging stations in model calibration can help to reduce parameter uncertainty and improve streamflow simulations (e.g. Bekele and Nicklow, 2007; Chiang et al., 2014; Her and Chaubey, 2015; Zhang et al., 2008), but the outcomes are often region-specific (e.g. Gong et al., 2012) and are also affected by the spatial distribution of gauges included in the study (Migliaccio and Chaubey, 2007). Additionally, there is no literature which shows that use of multiple gauges can lead to better estimation of subsurface fluxes such as soil moisture and evapotranspiration (ET), including the reduction of uncertainty/equifinality of the associated parameters. Therefore, the traditional approach of model calibration using observed streamflow at one or more stations can still lead to a model where several components of the watershed's hydrologic system may remain virtually uncalibrated (Wanders et al., 2014). Considering these issues, good correspondence between observed and simulated streamflow is not sufficient to evaluate the simulation capability of physically based hydrologic models (Demarty et al., 2005; Eckhardt, 2005; Gupta et al., 1998; Kuczera and Mroczkowski, 1998). Alternatively, the trade-off between model fits constrained by multiple hydrologic variables observed at different spatial scale of evolution might lead towards lower parameter uncertainty,

improving model robustness and predictability and implicitly encountering possible deficiencies in model structure. The solution to this multi-objective calibration produces a parameter set that is optimal in a Pareto efficiency sense (Xie et al., 2012). Among different surface/subsurface components, soil moisture plays an important role in energy and water balance of hydrologic cycle (Brocca et al., 2012), and hence, ensuring accurate soil moisture accounting in a hydrologic model can lead to better simulation of hydrologic processes including ET, surface runoff generation, groundwater recharge, and streamflow. While obtaining in-situ monitoring data of soil water fluxes/state variables is a long-standing challenge, remotely sensed surface soil moisture estimates can be obtained at high temporal resolution for the entire globe (Wanders et al., 2014).

Most studies that use surface soil moisture estimates to improve model simulation involves assimilation of in-situ, synthetic or remotely sensed data (e.g. Alvarez-Garreton et al., 2015; Bolten et al., 2010; Brocca et al., 2010; Chen et al., 2011; Draper et al., 2011; Han et al., 2012a, b; Houser et al., 1998; Lei et al., 2014; Pauwels et al., 2001, 2002; Reichle et al., 2002; Sawada et al., 2015; Scipal et al., 2008). Only few recent studies have applied remotely sensed surface soil moisture information in model calibration process (e.g. Milzow et al., 2011; Poovakka et al., 2013; Parajka et al., 2009; Sutanudjaja et al., 2014; Wanders et al., 2014). All these past studies conclude that using surface soil moisture, either in data assimilation or model calibration, improves model simulated surface soil moisture, without causing appreciable change in deeper layer (root zone) soil moisture and streamflow/surface runoff outputs. The limited success in modeling results from using remotely sensed soil moisture estimates is related to the shallow depth of assimilation/calibration which is in fact dependent on the sensing depth of the satellite product being used (1-5 cm top soil), and the model conceptualizations related to coupling of surface and root zone soil layers (e.g. Brocca et al., 2012; Chen et al., 2011; Han et al., 2012a).

Considering the role of root zone soil moisture in regulating subsurface hydrology, Parajka et al. (2006) and Silvestro et al. (2015) showed the use of an empirically derived root zone soil moisture index for calibrating a hydrologic model. Brocca et al.

(2012) and Chen et al. (2011) recommended model calibration using both streamflow and root zone soil moisture prior to assimilating soil moisture data into the model, which can potentially improve the efficiency of data assimilation techniques. Despite the limitation of sensing depth from space-borne satellites and the scarcity of field based information, recent advancements in multi-model land surface data assimilation projects such as National Astronomy and Space Administration (NASA)'s North American Land Data Assimilation Systems (NLDAS; Xia et al., 2015a, b) and Soil Moisture Active Passive (SMAP; Entekhabi et al., 2014; Reichle et al., 2014) mission can lead to high resolution root zone soil moisture estimations. These estimates can ultimately be used to improve the representation of subsurface processes in hydrologic models through multi-objective calibration.

Given the potential availability of root zone soil moisture, the overall goal of this study is to evaluate the performance of the SWAT model while using both soil moisture information and streamflow for calibration. Specific objectives include: (i) use of remotely sensed sub-basin/HRU scale surface soil moisture estimates along with streamflow observations in a spatially distributed calibration scheme; and (ii) use of root zone soil moisture and streamflow in similar spatially distributed model calibration scheme. Accordingly, comparison of the outcomes from these two objectives are used to evaluate the relative influence of surface and root zone soil moisture estimates in improving SWAT’s soil moisture accounting, streamflow simulation and parameter equifinality. Even with the recent remarkable advancements in developing new optimization algorithms and automatic tools specifically designed for SWAT, hydrologic calibrations of SWAT models can still be "conditional" (Abbaspour et al., 2015) and "sub-optimal" (Chen et al., 2011). Application of remote sensing data and/or associated data products, as shown in this study, is expected to overcome these limitations and provide more realistic hydrologic simulations.

2.3 Study Area and Data

The Upper Wabash and Cedar Creek watersheds in Indiana, USA (Figure 2.1) are selected as the test beds for this study. Upper Wabash (18,500 km^2) is suitable for the first objective because of its larger size to capture the variability in surface soil moisture from the coarse resolution satellite data, whereas field sensor-based profile/root zone soil moisture data are available for certain parts of Cedar Creek (700 km^2) to accomplish the second objective of this study. In order to evaluate the "relative" role of surface soil moisture, satellite data are also used for Cedar Creek watershed. Both watersheds have United States Geological Survey's (USGS) streamflow gauge station at the respective outlet as shown in Figure 2.1.

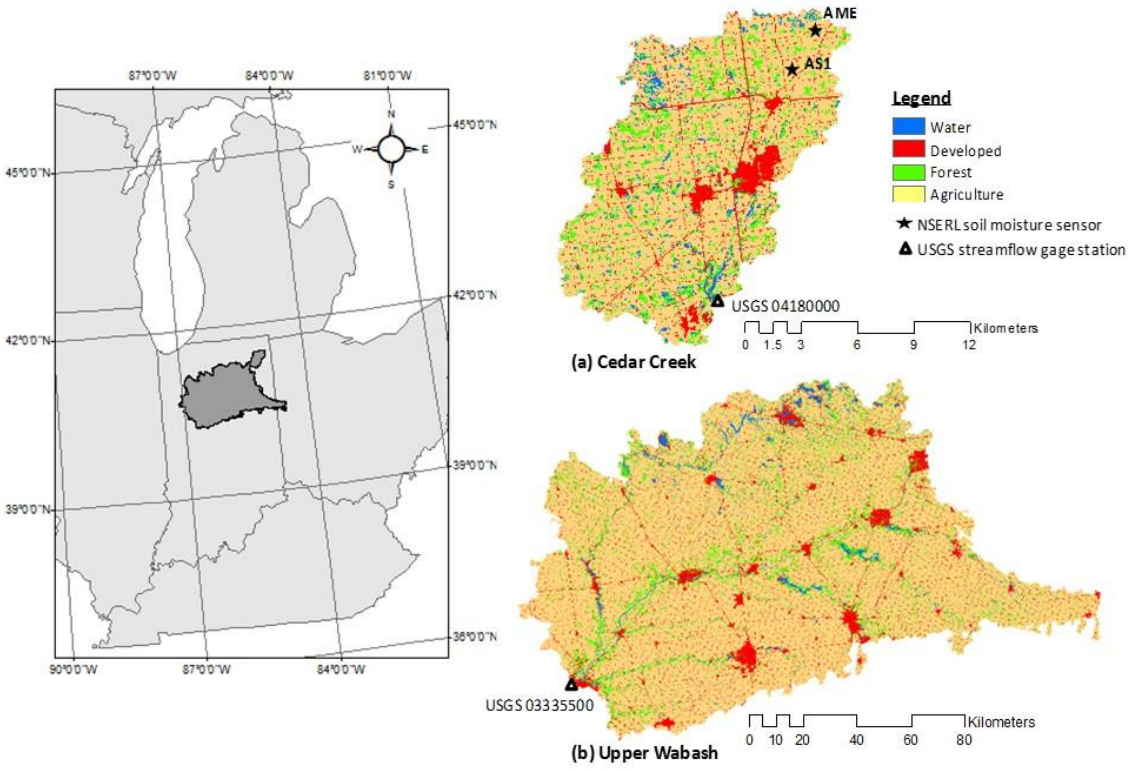

Figure 2. 1 Study areas: (a) Cedar Creek and (b) Upper Wabash watershed with corresponding landuse from 2006 NLCD land use. Streamflow gauge station at the respective watershed outlet is shown here. Map of Cedar Creek also shows the location for soil moisture field-sensors (AS1 and AME) being used in this study.

The landuse in both watersheds is mostly agricultural, although significant difference exists in the forest and developed portion. Table 2.1 presents a summary of their geospatial and hydro-climatic characteristics.

Table 2. 1 Watershed characteristics

	Upper Wabash	Cedar Creek
Drainage area, km^2	18,500	700
No. of Subbasins [a]	36	106
No. of HRUs [b]	36	370
Average Annual Rainfall during 2004-2012, mm	1050	993
Number of weather stations used in the model	6	5
Maximum daily streamflow at the watershed outlet till December 31, 2014, m^3/s	350	163
Landuse as per NLCD 2006 (%)		
Agricultural	80	71
Developed	9	11
Forest	9	14
Wetland/Open Water	2	4

[a] Flow accumulation area threshold: 5% (Upper Wabash), 0.5% (Cedar Creek)

[b] Basis of HRU definition: Upper Wabash (one subbasin-one HRU with dominant landuse, soil type and slope class in a particular subbasin), Cedar Creek (one subbasin-multiple HRUs, 10% threshold to create a unique combination of landuse, soil type and slope class within each subbasin)

SWAT models for both watersheds are created by the ArcSWAT GIS interface by using the following data: (i) 30m digital elevation model (DEM) from the USGS National Elevation Dataset (USGS-NED, 2013); (ii) 30m land cover data for year 2006 from the National Land Cover Database (USGS-NLCD, 2013); and (iii) 1:250,000 scale State Soil Geographic Data (STATSGO) that is included within SWAT 2012 database. Total daily precipitation, average minimum and maximum daily temperature data covering the study period of 2004-2012 are obtained from the National Climatic Data Center for the stations that fall within or adjacent the

watershed boundary. All other related climate variables, including solar radiation, wind speed and relative humidity, are obtained from the internal weather generator within ArcSWAT. Penman-Monteith equation is selected for computing potential evapotranspiration (PET).

For model evaluation, observed daily streamflow time series is obtained from respective USGS station located at each watershed's outlet (Figure 1). Remotely sensed surface soil moisture data (~1 cm top soil) is extracted from the Advanced Microwave Scanning Radiometer - Earth Observing System (AMSR-E). It is noteworthy that several algorithms have been so far applied to retrieve soil moisture information from AMSR–E, the most prominent of which have been developed by Jones et al. (2009), Koike et al. (2004), Njoku et al. (2003) and Owe et al. (2001). The data retrieved by the National Astronomy and Space Administration (NASA) following Njoku et al. (2003) (Aqua daily level-3 gridded land surface product-version 2, AE_Land_3; Njoku, 2004) is used in this study. Metadata associated with this particular estimate, including data format, projection system, spatio-temporal coverage and resolution, as well as the procedure for accessing the data can be found at http://nsidc.org/data/ae_land3. In-situ soil moisture estimates at 5, 20, 40 and 60 cm depths in the Cedar Creek watershed are obtained from http://amarillo.nserl.purdue.edu/ceap/ for two of the permanent field sensors (AS1 and AME in Figure 1). These sensors are part of the National Soil Erosion Research Laboratory's (NSERL) environmental monitoring network (Flanagan et al., 2008; Han et al., 2012c; Heathman et al., 2012a,b).

The STATSGO database is modified while preparing the ArcSWAT model for Cedar Creek so that a uniform stratification of soil profile depth all over the watershed can be maintained from 0-5 cm, 5-20 cm, 20-60 cm, and 60 – 150 cm. This modification makes SWAT simulated soil moisture values at different layers compatible with the placement of field sensors. Such modification is not necessary while using the AMSR-E data because SWAT model invariably considers a 1 cm surface layer for any watershed (Neitsch et al., 2011), which is identical to the approximate sensing depth of the satellite data being used for this watershed. Prior assumptions and

processing are essential to make remotely sensed and field sensor-based soil moisture estimates comparable with SWAT simulations.

2.4 Methodology

2.4.1 Watershed spatial discretization and model setup

While creating a watershed model in the GIS interface of SWAT model (ArcSWAT), spatial heterogeneity is represented through a two-step discretization (Geza and McCray, 2008). A watershed can be first divided into sub-basins, and then each sub-basin is further divided into multiple Hydrologic Response Units (HRUs). Considering the coarse spatial resolution of NASA AMSR-E soil moisture data (25 km x 25 km), sub-basins in the Upper Wabash watershed are not divided into multiple HRUs. Instead only one HRU is created per sub-basin based on dominant landuse, soil type and slope class (Winchell et al., 2010), resulting into total 36 sub-basins (or 36 HRUs). Being a smaller watershed, boundary of Cedar Creek intersects with only four AMSR-E grid cells (not shown here). In order to imitate a condition when fine resolution spatially distributed soil moisture estimates (remotely sensed or model assimilated such as NLDAS/SMAP) are available, Cedar Creek watershed is discretized into 106 sub-basins and 370 HRUs (Table 2.1). HRU level calibration is performed in the Cedar Creek watershed, using both remotely sensed and in-situ soil moisture data. Curve Number and Variable Storage methods (Neitsch et al., 2011) are selected for surface runoff generation and channel routing simulation respectively, invariably in all cases.

2.4.2 Calibration configuration

Evaluating the relative effect of remote sensing and field sensor-based soil moisture estimates in model calibration needs prior consideration of several consistency factors.

For example, drainage areas of the two study watersheds are very different (700 and 18,500 km^2); AMSR-E surface soil moisture estimates are available for the whole basin in both cases, but in-situ estimates are obtained at fixed depths across the root zone and limited only to the few locations of the Cedar Creek watershed. Furthermore, surface soil moisture obtained from remote sensing are "noisier" than in-situ root zone estimates (Draper et al., 2009). Most importantly, in contrast to the field data which are point measurements, remotely sensed data are spatial estimates where the value of a grid cell denotes the average surface moisture of the entire landscape of a cell, ignoring the effects of possible heterogeneity in climate and land use-land cover therein. Thus, the climatology (mean and variance) captured by the satellite-derived soil moisture estimates can be very different from those in the in-situ data and model simulations (Entekhabi et al., 2010; Koster et al., 2009; Reichle and Koster, 2004; Reichle et al., 2004). The differences, traditionally referred as the systematic bias, get enhanced by the physical conceptualizations in satellite's soil moisture retrieval algorithm (Draper et al., 2009); respective retrieval algorithms can generate quite different soil moisture fields, with different degrees of realism (e.g. Tuttle and Salvucci, 2014). Persistence of systematic bias would be a considerable factor while applying other root zone soil moisture products as well including those from the NLDAS or SMAP. Hence, comparison of calibration results involving either remotely sensed, model assimilated or field measured soil moisture estimates should base upon the respective representativeness, scale and inherent uncertainty of these data sources.

The proposed multi-variable spatial calibration scheme is evaluated under two configurations (M1 and M2 in Table 2.2) for each of the study watersheds. The first configuration (M1) involves calibration with streamflow only, and the second configuration (M2) is for the spatial calibration involving both streamflow and soil moisture. As indicated in Table 2.2, M2 configuration for the Upper Wabash watershed includes only the remotely sensed surface soil moisture. To enable a fair evaluation considering the aforementioned consistency issues, M2 in case of Cedar Creek is executed in three separate settings including remotely sensed surface

moisture (~1 cm, same as in Upper Wabash), in-situ surface moisture (5 cm) and in-situ total root zone moisture (60 cm) contents.

Table 2. 2 SWAT calibration configurations

	M1	M2	Source and scale of soil moisture data in calibration
Upper Wabash[a]	Streamflow	Streamflow Surface moisture (~1 cm)	AMSR-E, all sub-basins
Cedar Creek[a]	Streamflow	Streamflow Surface moisture (~1 cm)	AMSR-E, two particular HRUs[b]
		Streamflow Surface moisture (5 cm)	In-situ, two particular HRUs[b]
		Streamflow Total root zone moisture (60 cm)	

M1: calibration only with streamflow

M2: Multi-objective calibration with streamflow and soil moisture

[a] Streamflow observations are at the watershed outlet

[b] Two HRUs within which AS1 and AME field sensors (Figure 1) are located (in all the three M2 setups for Cedar Creek)

2.4.3 Spatial scaling of satellite data and creation of time-series

The AMSR-E data needs to be geo-referenced and processed to enable the comparison between surface soil moisture values in an individual/group of AMSR-E grid cell(s) with the average sub-basin/HRU level model estimates. The geo-processing task is accomplished by creating a python based automatic tool which can account for the heterogeneity in size, shape and location of the sub-basins/HRUs within any watershed. For a given temporal extent in the form of start and end date, and geographic extent in the form of shapefile, the python based tool creates an area averaged time series of AMSR-E soil moisture estimates for all the individual sub-basins (or HRUs). Once the time series is obtained, the data are rescaled using a

statistical method in order to reduce its systematic bias relative to the SWAT model simulations.

2.4.4 Reducing systematic bias in satellite data

Systematic bias mostly arises from resampling the raw data into grid cells, continuously variable sensing depth of satellite instrument as a function of moisture content and the satellite's soil moisture retrieval algorithms (Draper et al., 2009; Reichle et al., 2004). Several approaches, including linear regression (Milzow et al., 2011), cumulative distribution function (CDF) matching (Reichle and Koster, 2004; Scipal et al., 2008; Brocca et al., 2011; Matgen et al., 2012), μ-σ linear rescaling (Brocca et al., 2012, 2010; Dharssi et al., 2011; Draper et al., 2009; Jackson et al., 2010), min-max correction (Albergel et al., 2010) and water holding capacity method (Bisselink et al., 2011; Wanders et al., 2014) can be applied for reducing the bias in remotely sensed soil moisture data. It is noteworthy that the temporally rescaled output might vary depending on the choice of scaling technique.

Sub-basin and HRU scale AMSR-E soil moisture values, respectively for Upper Wabash and Cedar Creek, are first transformed into plant-available water (PAW, in mm H_20 depth unit), because SWAT does not simulate residual water content of soil (DeLiberty and Legates, 2003; Milzow et al., 2011). Following the method used in SWAT source code (Neitsch et al., 2011), water content held at wilting point (WP) is calculated for the top 1 cm layer for a sub-basin/HRU as a function of percent clay content and bulk density, and then this calculated amount is deducted from the respective AMSR-E data, thereby producing sub-basin or HRU scale surface PAW values. These PAW values are then rescaled with the μ-σ linear technique using equation (2.1):

$$\theta'_{(RS)} = [\theta_{(RS)} - \mu(\theta_{(RS)})] \times \sigma(\theta_{(M)})/\sigma(\theta_{(RS)}) + \mu(\theta_{(M)}) \quad \text{..... (2.1)}$$

Here, each AMSR-E PAW value ($\Theta_{(RS)}$) in a sub-basin/HRU is normalized ($\Theta'_{(RS)}$) to match the long-term mean (μ) and variance (σ^2) of the SWAT simulated PAW time-series ($\Theta_{(M)}$), being limited by the period of model simulation. $\Theta_{(M)}$ is obtained after the model parameters are adjusted against observed streamflow data with a small number of trial calibration iterations. This particular step is quite subjective, yet necessary to ensure a reasonable state of SWAT simulation. After the application of eq. (2.1), the resulting rescaled AMSR-E PAW product is used in SWAT calibration along with streamflow data.

2.4.5 Processing field sensor-based soil moisture data

SWAT simulated soil moisture cannot be directly compared with the estimates from field sensors because of two factors: (i) the sensors AS1 and AME (Cedar Creek watershed in Figure 2.1) measure the dielectric permittivity of soil to determine volumetric moisture content (m^3/m^3) for every 10 minutes using the frequency domain reflectometry method (Heathman et al., 2012a), whereas SWAT simulated soil moisture content represents the PAW content in the depth unit (mmH_20) at the end of each simulation time-step (a day) (Deliberty and Legates, 2003); (ii) the sensors deliver point estimates at four different depths (5, 20, 40 and 60 cm) (Han et al., 2012c; Heathman et al., 2012a), but values obtained from SWAT are spatially averaged over particular HRUs. To overcome such limitations, sensor values are transformed into daily averages and then multiplied with the depth interval of sensor placement, producing soil moisture observations in the depth unit (mmH_20) for those particular depth intervals (0-5, 5-20, 20-40 and 40-60 cm). Following the same method as discussed in section 2.4.4, water content held at wilting point is calculated for each layer and then this calculated amount is deducted from the sensor values, thereby producing observed PAW. Total PAW in the top 60 cm of the soil profile is obtained by adding the PAW values in all the four constituent layers. The total PAW in top 5 cm and 60 cm profile from the AS1 and AME locations are employed in HRU-scale calibration of the Cedar Creek model (Table 2.2), assuming that the point

estimates are representative of the average PAW in respective HRUs where these sensors are actually located. To keep the terminology simple, PAW will be referred to as soil moisture in the subsequent sections.

2.4.6 Multi-variable spatial calibration using streamflow and soil moisture

Following a split-sample approach (Klemes, 1986) over a continuous daily simulation period, all the six model setups for the Upper Wabash and Cedar Creek watersheds are calibrated for 2004-2008 and 2004-2010, using year 2004 as the warm-up period in each case. Total 14 parameters involving surface, subsurface and channel hydrologic responses are used for calibration (Table 2.3). The selection of parameters and their initial ranges are based on the review of existing literature and prior knowledge of the study area (e.g. Kumar and Merwade, 2009; Larose et al., 2007; Rajib and Merwade, 2016), as well as suggestions from SWAT developers (Abbaspour, 2015; Neitsch et al., 2011). Calibration is conducted by using the Sequential Uncertainty Fitting algorithm-version 2 (SUFI-2), which is a semi-automated inverse modeling procedure available inside SWAT-CUP. Kling-Gupta Efficiency (KGE) (Gupta et al., 2009; Kling et al., 2012) is used as an objective function to measure the agreement between simulated and observed variables. The KGE statistic decomposes Nash-Sutcliffe Efficiency (NSE) and Mean Squared Error (MSE) into a three-dimensional criteria space and finds out a Pareto front in terms of the shortest Euclidean distance (ED):

$$KGE = 1 - ED = 1 - \sqrt{\{(r-1)^2 + (\beta-1)^2 + (\gamma-1)^2\}} \quad \text{..... (2.2)}$$

$$\beta = \mu_s / \mu_0$$

$$\gamma = \sigma_s / \sigma_0$$

where r represents the correlation, β and γ respectively represent bias and variability ratio between the simulated and observed variable. μ and σ are the mean and standard deviation of the variable; the indices s and o denote simulation and observation,

respectively. KGE ranges from ∞ to 1, with a value closer to 1 produces a more accurate model. Soundness of KGE against the conventional application of NSE in hydrologic model calibration is discussed in detail by Gupta et al. (2009).

Table 2. 3 SWAT calibration parameters

No.	Parameter	Description[a]	Adjustment [b]	Initial Rage
1	CN2	Curve Number, moisture condition II	x	-0.2 – 0.2
2	CH_K2	Channel Hydraulic Conductivity, mm/hr	=	5.0 – 100.0
3	CH_N2	Main Channel Manning's n	=	0.01 – 0.15
4	CANMX	Maximum Canopy Storage, mm	=	0.0 – 25.0
5	SURLAG	Surface Runoff Lag Coefficient, days	=	0.05 – 24.0
6	ESCO	Soil Evaporation Compensation Factor	=	0.01 – 1.0
7	EPCO	Plant Uptake Compensation Factor	=	0.01 – 1.0
8	SOL_AWC	Available Soil Water Capacity, mmH_20 per mm of soil	x	-0.15 – 0.15
9	SOL_K	Saturated Hydraulic Conductivity, mm/hr	x	-0.15 – 0.15
10	ALPHA_BF	Baseflow Recession Constant, days	=	0.01 – 1.0
11	REVAPMN	Re-evaporation (Upward Diffusion) Threshold, mm	=	0.01 – 500.0
12	GW_DELAY	Groundwater Delay, days	+	-10.0 – 10.0
13	GWQMN	Threshold Groundwater Depth for Return Flow, mm	=	0.01 – 5000.0
14	GW_REVAP	Groundwater Re-evaporation Coefficient	=	0.02 – 0.2

[a] Source: Neitsch et al. (2011)

[b] Type of change to be applied over the existing parameter value: 'x' means the original value is multiplied by the adjustment factor (1+a given value within the range), '=' means the original value is to be replaced by a value from the range, '+' means a value from the range is added to the original value

In the first set of iteration, SWAT models for both watersheds are calibrated against daily streamflow records at the watershed outlets. In the case of Upper Wabash watershed, sub-basin scale surface soil moisture output (top 1 cm layer) from this initial streamflow-based calibration is used in the temporal rescaling of corresponding AMSR-E data (eq. (2.1)). After each set of iterations, SUFI-2 produces an updated parameter range which is centered on their best value. Taking the updated parameter range from the initial streamflow-based iteration as input, successive iterations are performed where streamflow at the watershed outlet and rescaled AMSR-E surface soil moisture estimates from all the 36 sub-basins are set as target variables for calibration. A similar approach is followed in the case of Cedar Creek, where the first set of calibration iterations is run only with streamflow; from the second set and onwards, AMSR-E surface moisture (~1 cm), in-situ surface moisture (5 cm) and in-situ total root zone moisture (60 cm) contents at two particular HRUs are added into the calibration process along with streamflow data, in three separate settings. No prior rescaling (eq. (2.1)) of the field sensor-based soil moisture is necessary in this case, because of the relatively less uncertainty and systematic bias in these estimates compared to remote sensing data.

With the addition of soil moisture as objective variable from the second set of iteration and onwards, the goal/objective function, KGE is modified to a weighted mean value, KGE' following the approach shown by Abbaspour et al. (2015):

$$KGE' = \sum_{i=1}^{n_f} w_{f_i}(KGE_{f_i}) + \sum_{j=1}^{n_s} w_{s_j}(KGE_{s_j}) \text{..... (2.3)}$$

where *n* and *w* are the number of objective variables (observational datasets) involved and the weight assigned to each of them, respectively; the indices *f* and *s* stand for streamflow and soil moisture, respectively. Also, *i* denotes the streamflow gauge stations and *j* denotes sub-basins/HRUs with soil moisture estimates brought under calibration. Thus, KGE calculated for individual sets of observed and simulated values are aggregated into KGE' and it is maximized toward an optimal solution. The assignment of weights being subjective, it may affect the outcome of the optimization exercise by SUFI-2 (Abbaspour et al., 1997). On the basis of few test iterations, the

weights in this study are set as w_f = 0.5 (since only one streamflow gauge station for both study areas) and w_{s_j} = 0.5/n_s (n_s is the total number of sub-basins/HRUs in calibration with soil moisture estimates). On the contrary, assigning equal weights to both streamflow and soil moisture components ($w_f = w_{s_j}$=1/(n_f +n_s)) is found to have improved the KGE for soil moisture in individual sub-basins/HRUs, compromising with the KGE of streamflow.

For an even comparison, M1 and M2 configurations are evaluated after equal number of iterations (1500). In each case, maximum three batches are executed each having 500 SUFI-2 iterations. For each of the six calibration setups (Table 2.2), coefficient of determination (R^2) and Percent Bias (PBIAS, Sorooshian et al., 1993) are also calculated to evaluate the goodness of fit between the observations/estimates and the best simulation having maximum objective function value (KGE or KGE' in this case).

2.4.7 Modification of SWAT source code

The default configuration of SWAT-CUP does not allow calibration with respect to estimates in a particular soil layer (e.g. top 1 cm in Upper Wabash and Cedar Creek) or in a portion of the whole soil profile (e.g. top 5 cm and 60 cm in Cedar Creek). To enable this layer-based calibration scheme, subroutine *hruday.f* from the SWAT 2012 version source code (revision 629) is modified such that the simulated soil moisture in top 1 cm layer, and the sum of soil moisture in all the layers up to 5 cm and 60 cm get exported as three new variables in the HRU-level output file (*output.hru*). The edited sub-routine is then compiled with the rest of the source code to get a new SWAT executable file, which can be run in SWAT-CUP.

2.4.8 Relative parameter sensitivity analysis

A relative sensitivity ranking of parameters is performed in order to ascertain the possible reasons behind the changes in simulation results caused from insertion of surface/root zone soil moisture estimates into model calibration process. The global sensitivity analysis technique in SWAT-CUP measures the average changes in objective function due to the changes in one parameter while all other parameters are also simultaneously changing (Abbaspour, 2015). Accordingly, the measure of relative sensitivity is translated in terms of p-values; where a smaller p-value represents more sensitive parameter. Relative sensitivity of parameters depends on the objective variables (soil moisture and/or streamflow) involved in the calibration process. Hence, to identify the effect of soil moisture by comparing the p-values between M1 and M2, this global sensitivity scheme is executed after the second set of 500 iterations for both model configurations.

2.4.9 Measure of parameter uncertainty

Equifinality means that that several parameter combinations from the optimized range can potentially produce behavioral solutions that are considered equally satisfactory in comparison with the observed data (Beven, 1993; Vrugt et al., 2008). In this study, all parameter values staying within their final optimized space and producing a value of the objective function higher than a specified threshold (KGE or KGE' > 0.5) are categorized as behavioral solutions. Then, in order to compare the extent of uncertainty associated with each parameter in the same scale, all these behavioral parameter values are normalized from 0 to 100 using equation (2.4):

$$P_n = \left[\frac{P_b - L_l}{U_l - L_l}\right] x100 \ldots\ldots\ldots (4)$$

where P_n is the normalized uncertainty score, P_b is the behavioral parameter value identified by SUFI-2, U_l and L_l are respectively the upper and lower limit of the corresponding parameter; P_b corresponds to the final batch of iterations producing

optimized parameter set. Example application of this normalized uncertainty scoring technique can be found in Kumar and Merwade (2009) and Rajib and Merwade (2016).

2.4.10 Model validation

The final optimized parameter ranges from the calibration scenarios are used in model validation, with respect to streamflow records and soil moisture estimates. SWAT models for Upper Wabash and Cedar Creek watersheds are validated for the period 2009-2010 and 2011-2012, respectively.

2.5 Results and Discussion

This section presents the findings on the relative improvement in SWAT performance due to the simultaneous application of surface/root zone soil moisture and streamflow data in a spatial calibration approach. Various flow components from the two model configurations (M1 and M2) are compared both at temporal and spatial scale, in terms of their simulated values as well as their goodness of fit statistics with estimates/observations. The possible reasoning behind the differences in simulation results is analyzed in terms of relative parameter sensitivity between M1 and M2. Furthermore, potential reduction in equifinality is evaluated with the corresponding reduction in parameter uncertainty range.

2.5.1 Fitness statistics for streamflow and soil moisture

Table 2.4 compares the goodness of fit scores (KGE, PBIAS and R^2) for the M1 and M2 configurations after equal number of SUFI-2 iterations. Overall, it is evident that high KGE and R^2 with low PBIAS for streamflow can be achieved from M1, without

using any soil moisture information for data assimilation or model calibration (e.g. Immerzeel and Droogers, 2008; Park et al., 2014). Clearly the M1 configuration exhibit higher amount of bias, when the fit scores are compared for soil moisture. This validates the presence of sub-optimality of model calibration practices (Abbaspour et al., 2015) even with acceptable streamflow results. The scores for streamflow are slightly negatively impacted with M2 configuration for Upper Wabash, but this can be attributed to the optimization algorithm. The Upper Wabash has 37 objective functions (one for each sub-basin and the outlet), and optimization algorithm seeks a goal that is best for all the objectives and thereby implicitly imposing an "averaging effect" across scales and the variables involved (White and Chaubey, 2005; Wanders et al., 2014). Having lesser number of objective functions (only 3) compared to the Upper Wabash, streamflow fit scores remain virtually the same for Cedar Creek when calibrated either with satellite or field estimates of surface moisture. This is not the case for Cedar Creek when root zone moisture is employed in the M2 configuration; KGE and R^2 increase from 0.75 to 0.81 and 0.69 to 0.72, respectively, PBIAS shows a substantial decrease from -12.2 to -0.9. Depending on how the relationship between soil wetness and runoff generation within a particular model is conceptualized, it is possible that the stronger influence of root zone moisture on regulating the parameters can overrule the "averaging effect" of multi-objective calibration, thus improving the fitness scores for streamflow simulation.

Improved agreement between simulated soil moisture and the field/satellite estimates is also found in the M2 configuration (Table 2.4), especially in Cedar Creek, when total root zone moisture in upper 60 cm of the soil profile is brought into calibration and compared with the corresponding field estimates; PBIAS decreases from -19.1 to -8.7 with the increase in KGE and R^2 from 0.13 to 0.35 and 0.18 to 0.23, respectively. Similar improvement is evident when watershed-average simulated surface moisture in Upper Wabash is compared with the AMSR-E estimates. These low fitness values may indicate that SWAT is still under-performing in soil moisture simulation even with the multi-objective calibration scheme. From this aspect, it is important to clarify

that these fitness statistics are calculated for the entire duration of simulation and are impacted by the differences in absolute values between the simulations and the observations; hence, they do not represent the actual improvement in the temporal dynamics of soil moisture simulation. However, using either AMSR-E or field sensor-based surface estimates in calibrating the Cedar Creek model does not produce any noticeable difference in fit scores for the 60 cm root zone moisture content, relative to those in the M1 configuration (Table 2.4).

Table 2. 4 Descriptive statistics of calibration and validation schemes [a]

Goodness of fit criteria	Upper Wabash		Cedar Creek			
	M1	M2 AMSR-E: ~ 1 cm	M1	M2 In-situ: 60 cm	M2 In-situ: 5 cm	M2 AMSR-E: ~ 1 cm
Streamflow at watershed outlet						
KGE	0.74 (0.73)	0.72 (0.74)	0.75 (0.71)	0.81 (0.74)	0.75	0.75
PBIAS	- 4.2 (- 9.4)	- 8.6 (1.7)	- 12.2 (- 7.5)	- 0.9 (2.2)	-12	-12.7
R^2	0.68 (0.65)	0.65 (0.67)	0.69 (0.64)	0.72 (0.68)	0.69	0.69
Soil moisture [b, c]						
KGE	0.25 (0.2)	0.31 (0.24)	0.13 (0.11)	0.35 (0.25)	0.14	0.14
PBIAS	8 (12.2)	3.5 (5)	-19.1 (-25.6)	-8.7 (-11.7)	-18.8	-19.1
R^2	0.18 (0.2)	0.3 (0.25)	0.18 (0.19)	0.23 (0.21)	0.18	0.18

[a] Within parentheses are the values from model validation

[b] Upper Wabash: watershed-average statistics for surface soil moisture (~1 cm top soil). Rescaled AMSR-E surface estimates are used in calculation

[c] Cedar Creek: Values are calculated with respect to the in-situ total root zone soil moisture estimates for top 60 cm of the soil profile. Averages of the two sensor locations (AS1 and AME) are reported here

In general, using surface estimates in model calibration can improve the simulation of surface moisture itself, but that may not be influential over the deeper layer moisture content which implicitly refers to the insensitivity of surface moisture to streamflow simulation. Assuming that the available field/satellite soil moisture estimates are representative of actual wetness conditions, calibration with root zone moisture is considered an effective approach as it makes the overall water budget more realistic in terms of the improvement in soil moisture and corresponding enhancement in streamflow prediction.

2.5.2 Enhancement in soil moisture simulation

In the case of Upper Wabash watershed, fitness scores for surface soil moisture listed in Table 2.4 actually represent watershed-average values. Figure 2.2, in contrast, helps to identify the actual extent of model performance improvement in terms of bias removal from individual sub-basins. A spatial comparison of sub-basin scale PBIAS, R^2 and KGE between the simulated daily surface soil moisture and the AMSR-E estimates over the entire simulation period (2005-2010) is presented in Figure 2.2. Clearly, the spatially distributed calibration approach improves model simulation all over the watershed, irrespective of scales. However, the soil and land use characteristics of the sub-basins may have affected this particular spatial pattern of bias removal, but this is not explored further in the current study. Figure 2.3 shows the frequency distribution of the values being mapped in Figure 2.2. As seen from the results of M1 configuration in Figure 2.3, surface soil moisture in 12 out of 36 sub-basins is overestimated by more than 10% (PBIAS), while R^2 in all the sub-basins is less than 0.25. In the M2 configuration, maximum PBIAS in any of the sub-basins decreases to 8%, with almost half of the sub-basins showing much improved R^2 (0.25~0.5). Consequently, KGE in majority of the sub-basins also increases from 0.2 - 0.3 in M1 to 0.25 - 0.35 in M2.

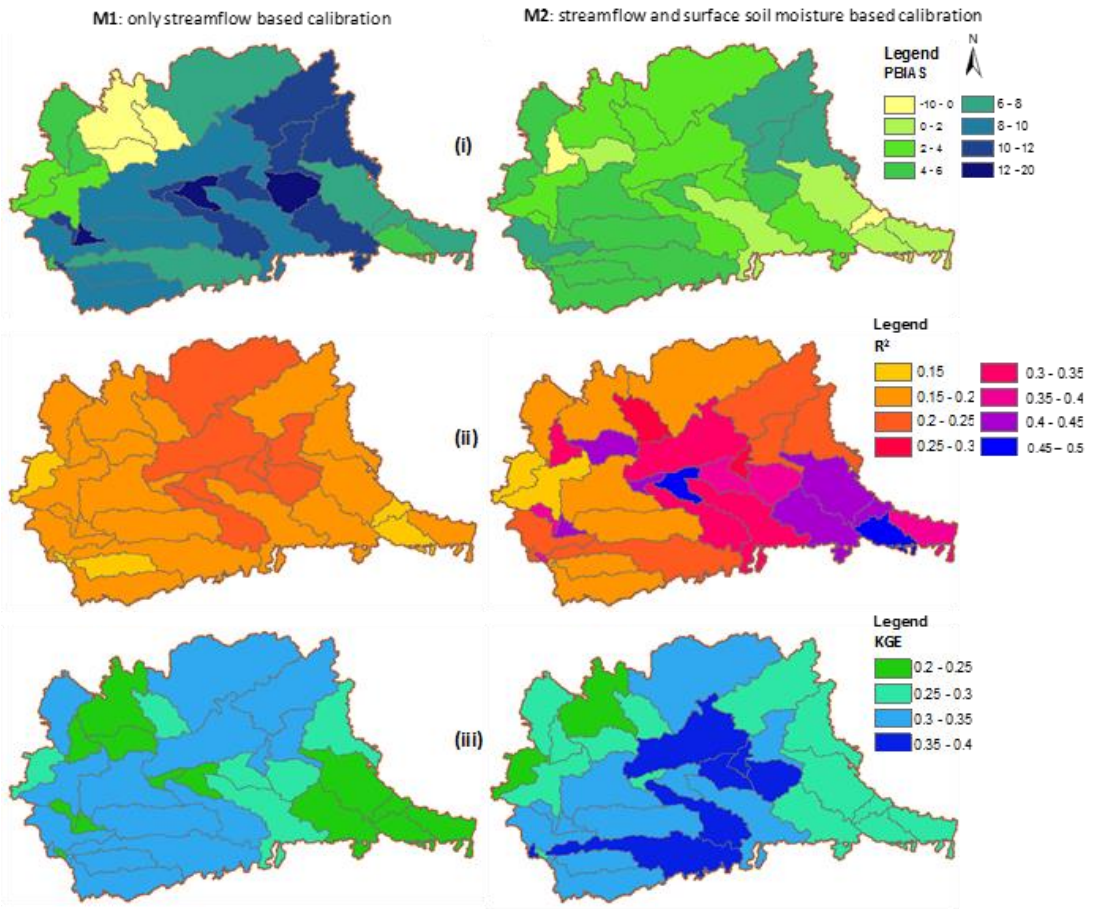

Figure 2. 2 Spatial distribution of (i) PBIAS, (ii) R^2 and (iii) KGE between the simulated surface soil moisture (PAW) and AMSR-E estimates in the Upper Wabash watershed: M1 (left), M2 (right). Shapes in the figure correspond to individual sub-basins. Statistics are calculated for the entire calibration-validation period.

Figure 2.4 shows the temporal comparison of simulated surface soil moisture with AMSR-E estimates in the Upper Wabash watershed. Regardless of M1 or M2, there is a resemblance in temporal dynamics of AMSR-E estimates with that of the model simulation which validates the ability of SWAT model in subsurface characterization. However, extensive disagreement in their absolute values is visible in case of M1. Especially, SWAT simulated moisture for M1 is seen to have reached wilting point (PAW≈0) at numerous occasions both during calibration and validation. Calibration with M2 setting enhances model simulation, but disagreement between the absolute values of model simulation and AMSR-E estimates still persists. Literature supports

similar findings in other modeling studies that used remotely sensed surface soil moisture in calibration (e.g. SWAT (Milzow et al., 2011), LISFLOOD (Wanders et al., 2014)). Considering that the surface layer is the most interactive and hence very "noisy", the improvement in the temporal dynamics of SWAT simulated daily surface soil moisture obtained in this study, as evident in Figure 2.2-2.4, is quite convincing.

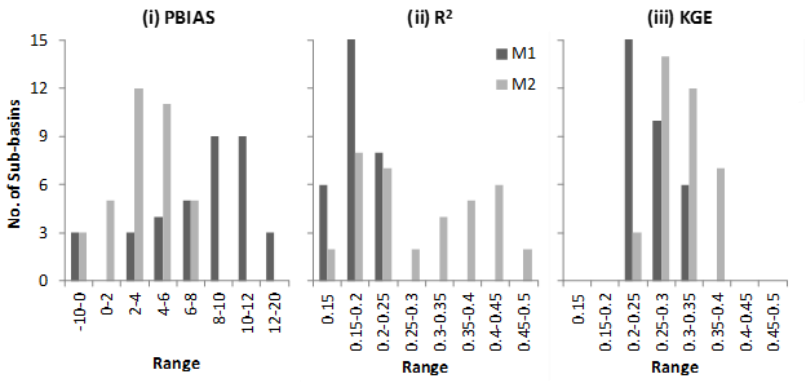

Figure 2. 3 Frequency distribution of sub-basin scale PBIAS, R^2 and KGE between simulated surface soil moisture (PAW) and AMSR-E estimates in the Upper Wabash watershed. Horizontal axis indicates the ranges of corresponding fit scores, where values in vertical axis mean the number of sub-basins within a particular range.

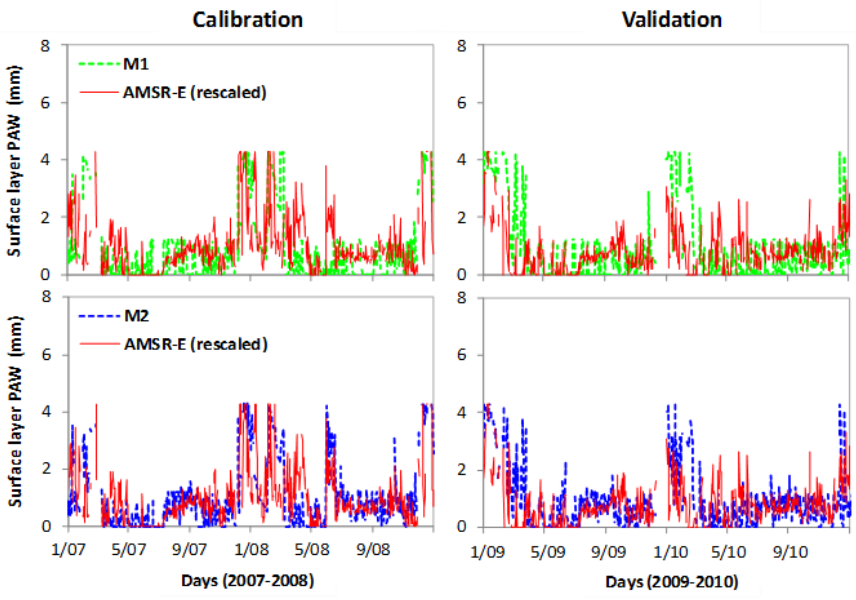

Figure 2. 4 Comparison of watershed-average simulated surface soil moisture (PAW) with AMSR-E estimates in the Upper Wabash watershed: M1 (top), M2 (bottom).

In order to further ascertain the ability of surface moisture in regulating deeper layer soil moisture content through model calibration, the in-situ total root zone moisture (top 60cm soil profile) content in the AS1 location of Cedar Creek watershed is plotted with corresponding SWAT simulations resulted from the M2 configurations when the model was calibrated with AMSR-E (top 1 cm) and in-situ (top 5 cm) surface moisture estimates (Figure 2.5). In either case, there is no noticeable improvement in root zone soil moisture. On the contrary, considerable improvement in model simulation is observed when root zone moisture (60 cm) is employed in the multi-objective calibration (Figure 2.6). Parajka et al. (2006) and Silvestro et al. (2015) reported similar findings with more consistent root zone soil moisture simulation. Large offsets in M1 simulations from the field estimates are evident; the deviation, as seen from the error plots, can be more than 25 mm on a day which is quite significant considering the average daily precipitation in the watershed. In comparison, the M2 configuration matches well with the field estimates invariably during the calibration and validation phase, except during the summer months.

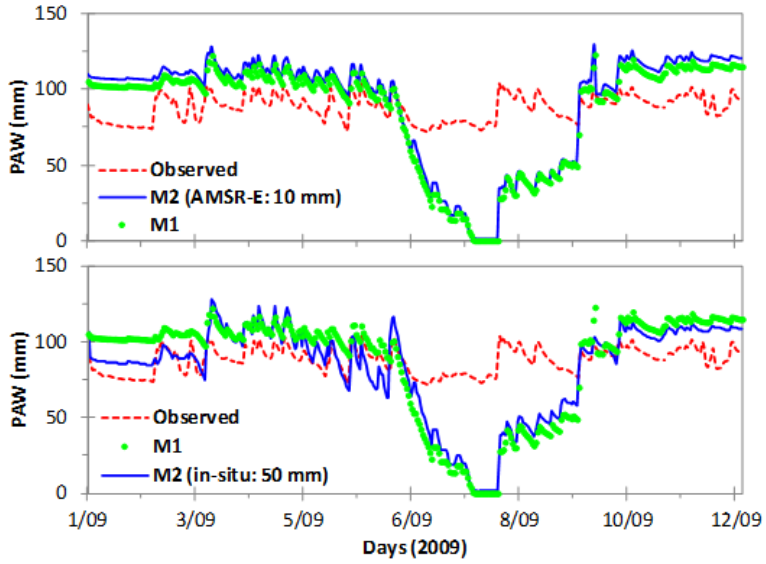

Figure 2. 5 Temporal comparison of simulated soil moisture (PAW) and field-sensor estimates of total root zone moisture in the top 60 cm of soil profile, when AMSR-E and in-situ surface moisture estimates are applied in model calibration (Cedar Creek; Table 2.2). The values correspond to the HRU where the AS1 sensor is located. Results for only one year of calibration are shown here. Calibration results for AME sensor is fairly similar (not shown here).

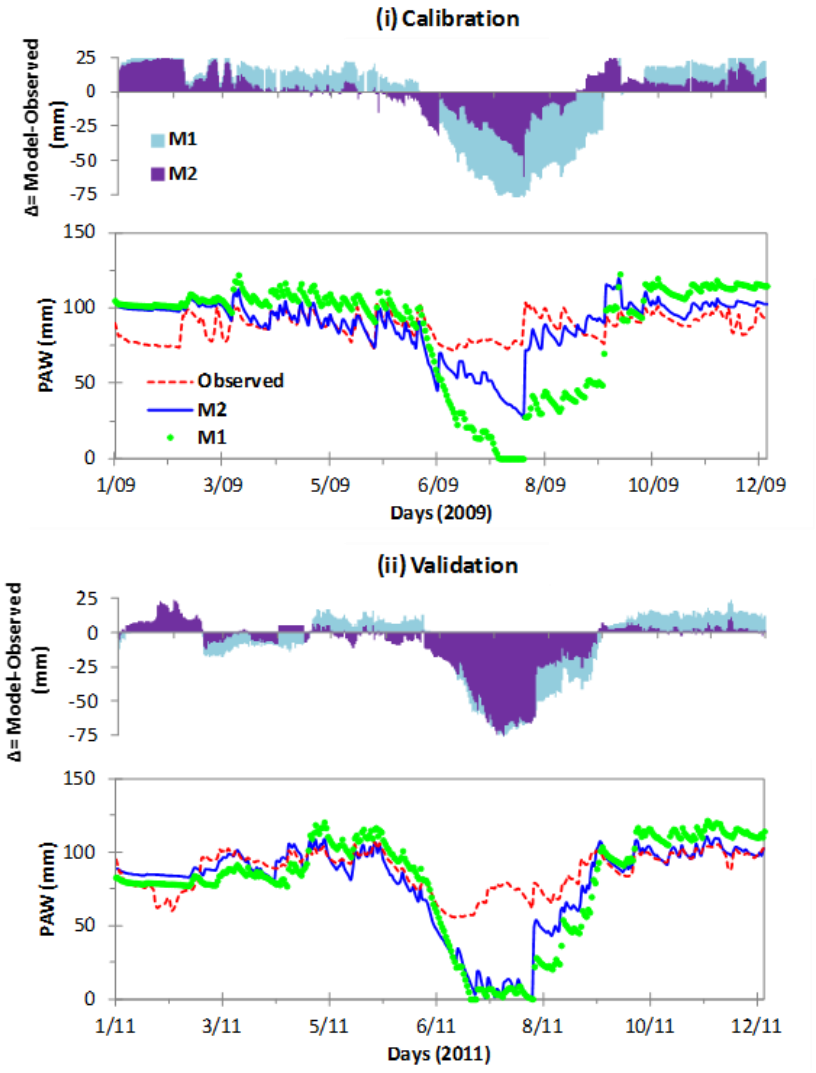

Figure 2. 6 Temporal comparison of simulated soil moisture (PAW) and field-sensor estimates, with corresponding simulation error (Error, Δ= Model-Observed) from the AS1 sensor in the Cedar Creek watershed: (i) calibration, (ii) validation. The values represent total PAW in the top 60 cm profile of the root zone of the corresponding HRU where the sensor is located. Results for only one year of the whole calibration/validation period are shown here for vivid comparison. The calibration/validation results for AME sensor is fairly similar (not shown here).

The error plot clearly indicates minimal or even zero residual of M2 simulations in the significant portion of the time-span, thereby attesting the greater utility of root zone soil moisture estimates toward improving model performance through calibration. The "summer deficiency" identified here is very much a model-specific issue and can be linked with the limitations in SWAT's ET depletion mechanism.

2.5.3 Potential model deficiency in ET mechanism

SWAT's ET mechanism uses an exponential depth distribution function for soil moisture depletion that tends to withdraw 95% of soil evaporative demand and 50% of plant transpiration uptake approximately from upper 6% (~10 cm) of the root zone (~150 cm in this case) (Neitsch et al., 2011). In reality, the upper portion of the root zone may not always hold enough moisture to satisfy this calculated demand. SWAT regulates ET depletion such that when the moisture depletes from one layer due to ET, moisture from another layer cannot be extracted to replenish the deficit. According to the availability of soil moisture in upper layers, the exponential depth distribution function can be adjusted through two empirical parameters ESCO and EPCO such that the lower layers can take part in meeting the actual evaporative demand. Either way, the upper layers tend to dry out (PAW≈0) even when sufficient moisture is still available in the deeper layers. This is a model structure issue rather than a parametric issue, hence cannot be resolved by model calibration even using soil moisture estimates. Therefore, regardless of the M1 or M2 configuration, significantly large error in model simulation is observed at the time of heavy ET demand during the peak of crop growing season in summer months (July-August). During this period, SWAT simulated soil moisture (PAW) in the top 60 cm stays around the wilting point over a persistently long period of time. This has caused the high negative PBIAS score in SWAT simulated root zone moisture (Table 2.4), even though M2 configuration produces substantial improvement in model performance by fairly imitating total amount of "observed" moisture in the top 60 cm throughout the rest of the year (Figure 2.6).

Although M2 configuration tends to match total moisture in the top 60 cm profile (Figure 2.6), SWAT may still unable to replicate actual vertical distribution of moisture content in individual soil layers. Figure 2.7 shows monthly simulated and observed average soil moisture values in the year 2009 at particular soil layers (0-20, 20-40 and 40-60 cm) at the AS1 sensor location of Cedar Creek watershed. Relative to the model simulations, average sensor values in a summer month (August 2009) are higher across the entire 60 cm depth being plotted here. Besides the structural

limitation in SWAT's ET mechanism, this can also be attributed with the actual agricultural management operations (e.g. spatial/temporal information on specific crop plantation and harvesting) which are not been considered in the model. Irrespective of that, relatively higher field estimates at around 15-35 cm depth compared to the model simulations (both M1 and M2) are persistent in other months along the year (e.g. May 2009 and November 2009), when growing crops and relevant management operations are not considerable issues. That indicates toward insufficient parameterization related to soil moisture and/or non-physical application of ESCO and EPCO, as well as the lack of vertical coupling strength among soil layers in SWAT's soil moisture accounting structure. From this standpoint, refurbishment of SWAT's ET mechanism would make the soil moisture based calibration even more efficient.

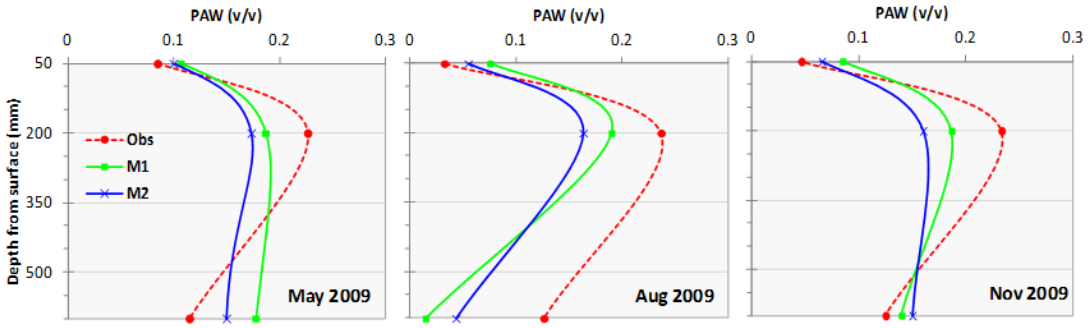

Figure 2. 7 Vertical distribution of simulated and field-sensor based soil moisture (PAW) content for Cedar Creek watershed. The distribution is derived from the corresponding values at 0-20, 20-40 and 40-60 cm layers of the root zone. Values correspond only to the HRU where AS1 sensor is located. The monthly-average values for May, August and November 2009 are considered representing a seasonal variation in soil moisture. Vertical distribution in case of AME sensor is fairly similar (not shown here).

2.5.4 Enhancement in streamflow simulation

Antecedent soil wetness condition is the major controlling factors for surface runoff generation. Therefore, it is expected that the extent of changes in the whole root zone moisture caused by the model calibration scheme will lead to possible changes in

streamflow hydrographs (Figure 2.8). Both runoff methods in SWAT (Curve Number and Green-Ampt) use moisture content (PAW) in the whole root zone for necessary parameterizations and subsequent calculations. Theoretically, the larger the change being imparted in the entire root zone moisture content, the higher will be the impact on SWAT simulated runoff volume and streamflow, following a storm event. In the case of Upper Wabash watershed, where only the surface soil moisture is improved, simulated hydrograph from M2 configuration does not suggest appreciable enhancement in streamflow prediction (Figure 2.8). This can be explained by the inability of surface moisture estimates in producing big changes in the deeper layer moisture contents through model calibration, as evident in the examples of Cedar Creek (Figure 2.5 and Table 2.4). This is quite analogous to the findings by Parajka et al. (2009) and Wanders et al. (2014). On the other hand, in the case of Cedar Creek, where the entire root zone moisture (60 cm) is included in the M2 configuration, simulated streamflow matches well with the observed hydrograph compared to M1. Brocca et al. (2012) assimilated a semi-empirical exponential filter-based root zone soil moisture product into a hydrologic model and showed similar significant improvement in streamflow simulation. Especially for high flow conditions in Cedar Creek, SWAT simulations from M2 configuration are quite precise, thereby addressing the long-standing limitation of SWAT in replicating watershed physics under extreme flow situations (e.g. Arnold and Allen, 1996; Arnold et al., 2000; Chu and Shirmohammadi, 2004; Vazquez-Amábile and Engel, 2005; Arabi et al., 2006; Bracmort et al., 2006; Larose et al., 2007; Wang et al., 2008; Kumar and Merwade, 2009; Oeurng et al., 2011; Rahman et al., 2012; Qiu and Wang, 2013; Rahman et al., 2014). Since a simple hydrograph comparison does not appear to be decisive enough for the Upper Wabash watershed (Figure 2.8), Figure 2.9 provides supplementary information in this regard. Figure 2.9 shows the Percentage Error (PE) in daily streamflow for all the individual data points over the entire duration of model simulation along with the average daily residual for specific flow regimes. Comparison of average daily residuals (observed *minus* simulated streamflow) indicates that simulations for high and low flow regimes are improved invariably for both watersheds, with slight exception for the moist flow condition. Considerable

degree of reduction in PE for Upper Wabash is evident as well, thereby validating the potential of remotely sensed data in enhancing streamflow prediction through a model calibration approach. In conjunction with the better fit between simulated and observed hydrographs for Cedar Creek watershed (Figure 2.8), much pronounced reduction of PE in Figure 2.9 further proves the comparatively efficient role of root zone moisture in model calibration.

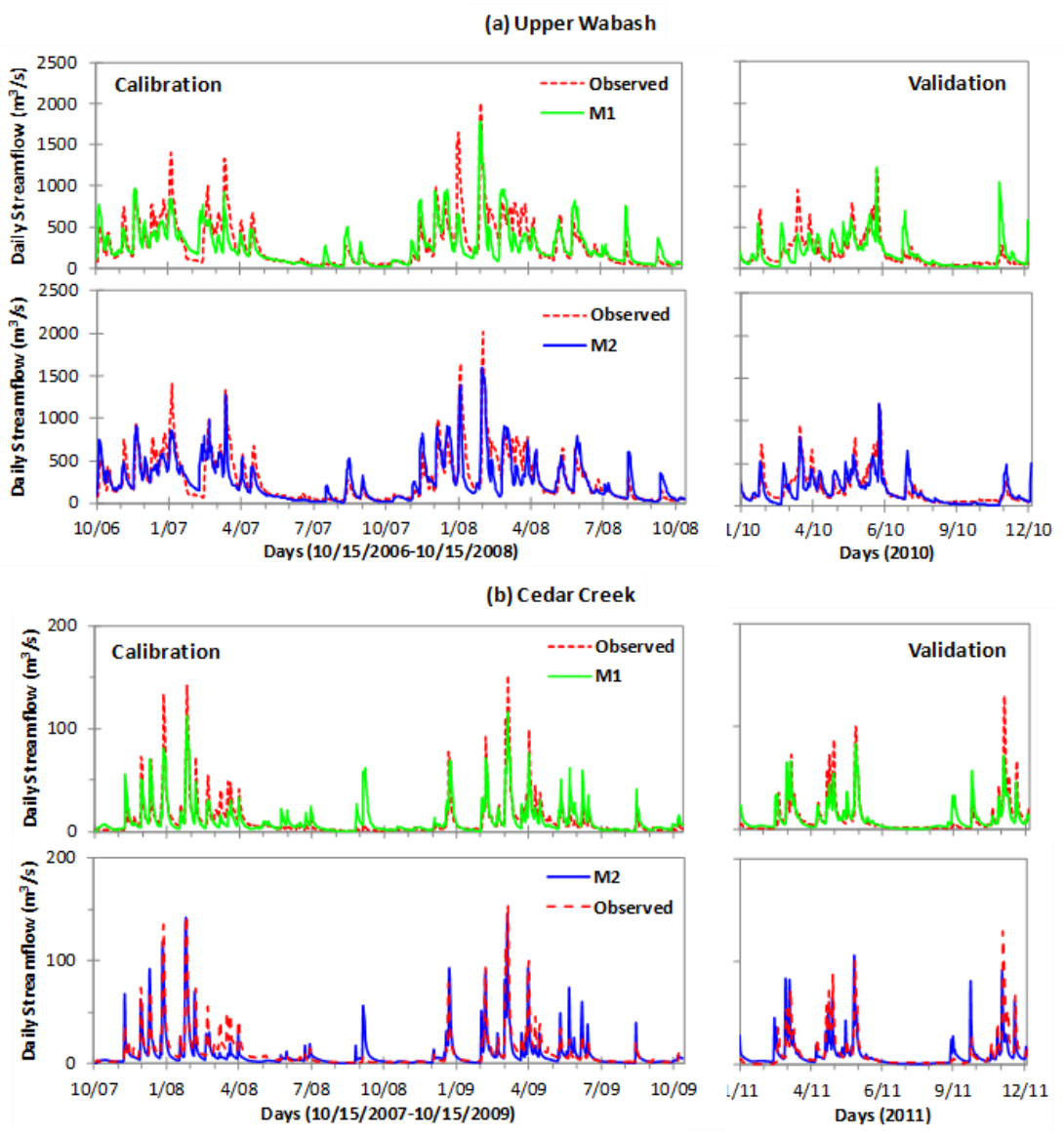

Figure 2. 8 Comparison of streamflow hydrographs. Only a representative segment from the whole simulation period is shown here: (a) Upper Wabash, (b) Cedar Creek.

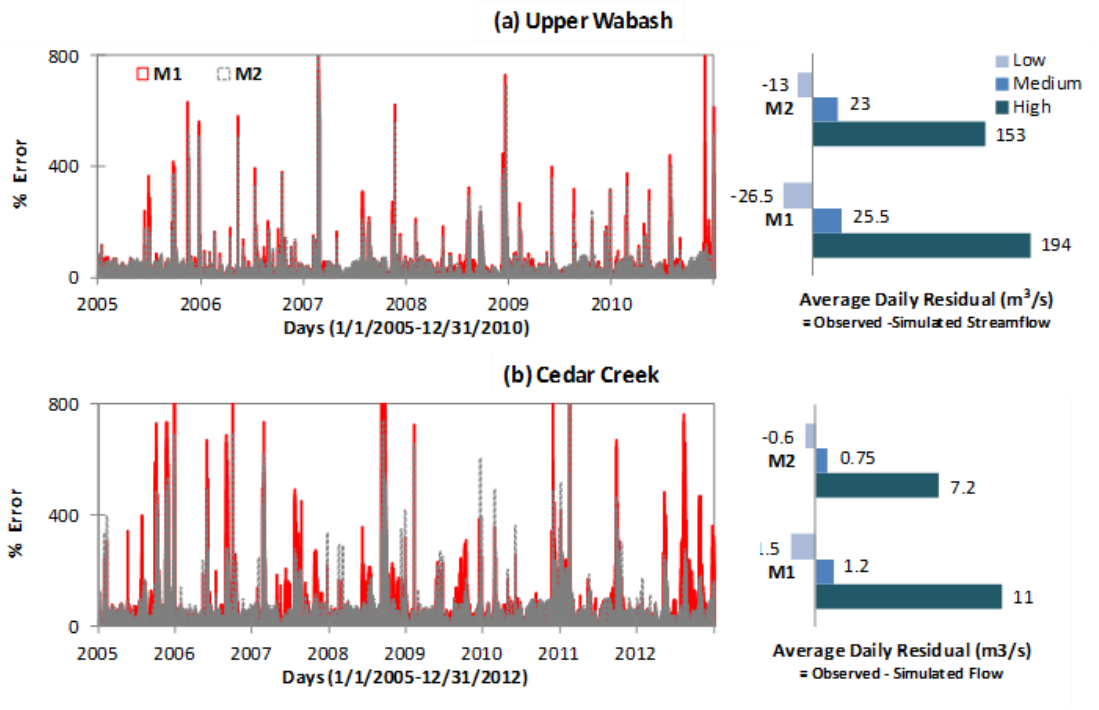

Figure 2. 9 (Left) Percentage Error (PE) in simulated streamflow during the entire calibration-validation period. PE = *Abs*[Model-Observed]/Observed x 100%. (Right) Average daily residual for three different flow regimes: (exceedance probability 0.0-0.1: high flow, 0.1-0.6: moist and mid flow, 0.6-1.0: dry and low flow).

2.5.5 Evaluation of relative parameter sensitivity

During a model calibration, the parameter space gets optimized, and the outcome is heavily dependent on the choice of objective variable (observation). Hence, relative sensitivity of parameters in a calibration only with observed streamflow will be different from a calibration involving both streamflow and soil moisture. Figure 2.10 compares the relative ranking of sensitive parameters between the two configurations based on p-value measurements. Obtained from the global sensitivity analysis of parameters during a set of calibration iterations, p-value determines the significance of the sensitivity, where a value closer to zero indicates more significance. The important feature from Figure 2.10 is that some of the parameters related to sub-

surface processes such as GWQMN, ESCO, ALPHA_BF in Upper Wabash, and SOL_AWC, ESCO, EPCO, SOL_K in Cedar Creek become more sensitive in the M2 configuration. In streamflow based calibration (M1), these subsurface related parameters do not get an appropriate constraint in their own spatial scale of variation (observations/estimates on soil moisture and ET in HRU/sub-basin scale) based on which they can be optimized, as such they play a less effective role in the calibration process. This is likely to be the cause for which the M1 configuration in this study suffers from imprecise soil moisture accounting even having well-predicted streamflow results with high goodness of fit scores. This shows that streamflow based calibration leads to parameter equifinality (Beven, 1993) and higher degree of uncertainty.

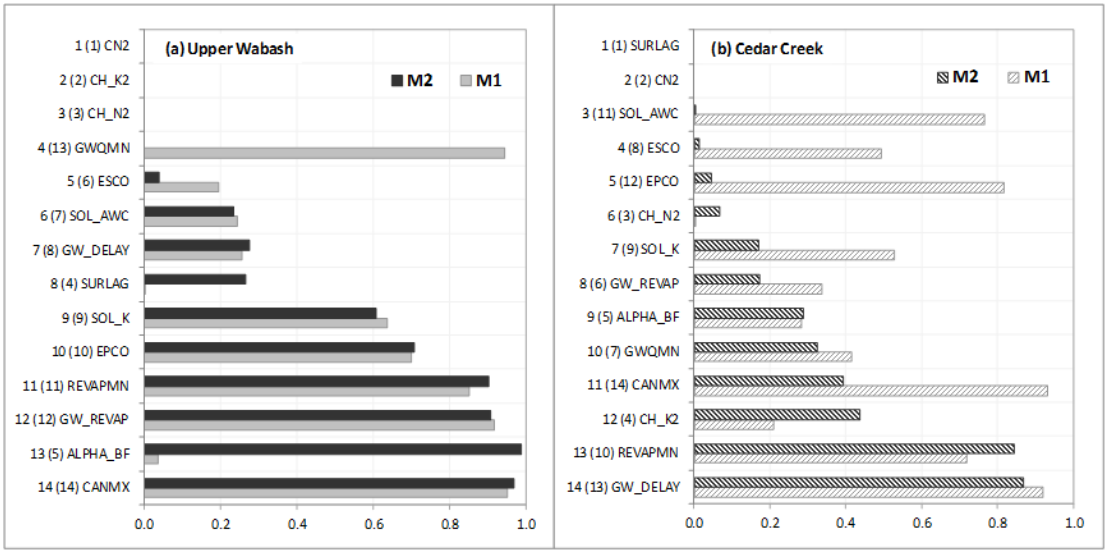

Figure 2. 10 Relative sensitivity of parameters. The numbers on the vertical axis indicate sensitivity ranking based on p-value; within parentheses are the values corresponding to M1 configuration. Results shown here are based on the Global Sensitivity Analysis being run after the 2nd set of 500 iterations in all the cases.

2.5.6 Reduction of parameter uncertainty

The calibrated parameter values for all the four modeling cases are listed in Table 2.5. Although Table 2.5 denotes the best estimate on how the parameters should be

changed in order to best fit the simulated outputs with the observations, it does not help measuring the reduction in parameter uncertainty that might have happened with the application of soil moisture in model calibration. Reduction in equifinality and associated degree of uncertainty can be evaluated in terms of the "behavioral range" of parameters. Hence, the narrower the behavioral range, the lower is the extent of equifinality or uncertainty (Price et al., 2014).

Table 2. 5 Calibrated parameter ranges [a,b]

Parameter [c]	Best parameter value			
	Upper Wabash		Cedar Creek	
	M1	M2	M1	M2
CN2	-0.002	0.009	0.09	0.04
CH_K2	64	60	38	74
CH_N2	0.15	0.13	0.02	0.02
CANMX	21.4	25	18.5	7.7
SURLAG	14.8	14.5	1.1	3.45
ESCO	0.97	0.91	0.93	0.86
EPCO	0.54	0.32	0.77	0.31
SOL_AWC	0.09	0.04	0.01	-0.08
SOL_K	-0.01	0.03	0.14	0.11
ALPHA_BF	0.77	0.65	0.73	0.45
REVAPMN	500	391	500	361
GW_DELAY	10	1.83	3.7	-1.9
GWQMN	81	14.7	1222	1135
GW_REVAP	0.15	0.15	0.2	0.2

[a] After equal number of SUFI-2 iterations (1500) in all the cases

[b] M1: calibration only against streamflow; M2: calibration against both streamflow and soil moisture

[c] Initial parameter ranges and the basis of adjustment are shown in Table 2.3

The range of uncertainty in parameters produced by M1 and M2 is tested by applying equation (2.4), which converts each behavioral parameter value into a normalized uncertainty score (Figure 2.11). For Upper Wabash watershed, two major parameters related to subsurface hydrology, GWQMN and ESCO, show prominent decrease in their uncertainty range in the M2 configuration compared to M1. Applying remotely

sensed surface soil moisture in calibration of LISFLOOD, Wanders et al. (2014) obtained similar results related to parameter uncertainty. However, the output from M2 in the case of Cedar Creek watershed is more remarkable as it is showing significant decrease in the uncertainty for all the parameters involved. This proves the stronger effect of root zone soil moisture in reducing equifinality when employed in model calibration.

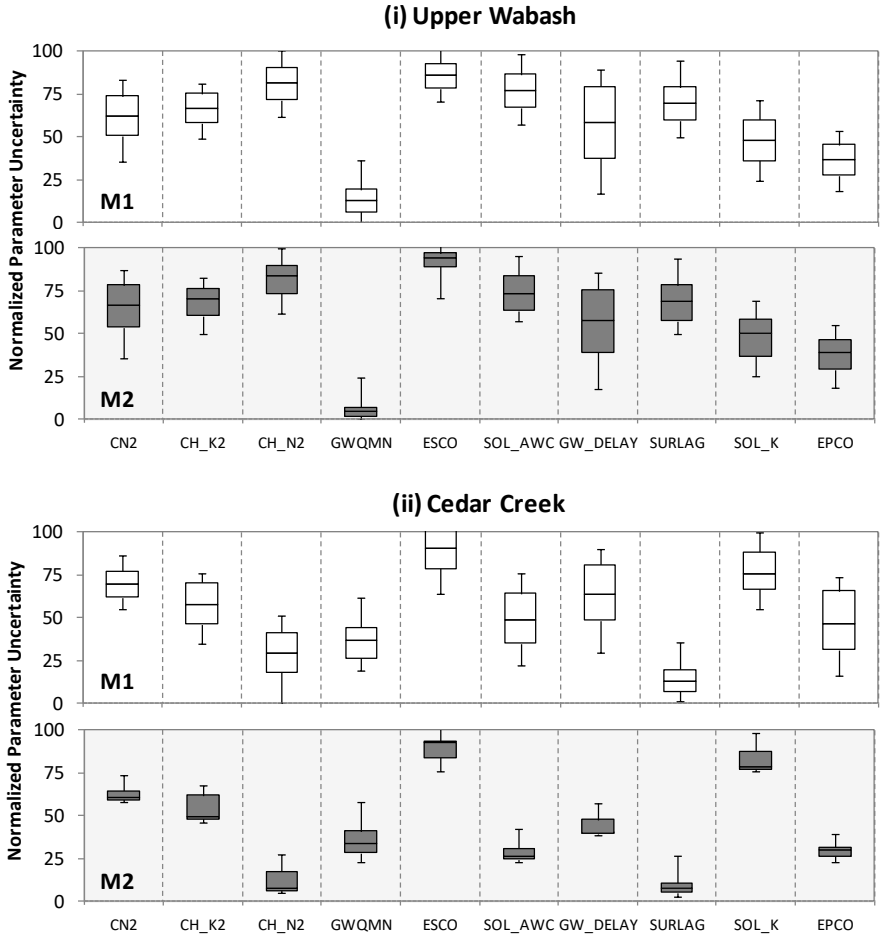

Figure 2. 11 Normalized uncertainty of parameters. Out of total 14 parameters, 10 most sensitive parameters are selected for this plot.

2.6 Conclusion

Good correspondence of observed and simulated streamflow cannot be sufficient as a criterion for evaluating physically based hydrologic models. Being derived from such notion, this study employs remotely sensed AMSR-E surface soil moisture (~ 1 cm top soil) estimates in calibrating SWAT model simultaneously at individual sub-basins, along with observed streamflow data at particular stream location. In order to validate the stronger role of root zone moisture over the surface moisture estimates in model calibration, similar approach is followed involving AMSR-E surface moisture (~1 cm), in-situ surface moisture (5 cm) and in-situ total root zone moisture (60 cm) contents in HRU scale calibration under three different settings. These cases are tested over two different agriculture-dominated watersheds in Indiana, USA (Upper Wabash and Cedar Creek, respectively) and compared with calibration results based on streamflow only. Following conclusions are drawn:

1. Acceptable streamflow simulation can be obtained without using any soil moisture information in model calibration. However, considerable amount of bias is still noticed in soil moisture outputs, indicating significant room for model uncertainty/equifinality. Using sub-basin scale AMSR-E data in calibration improves model simulated surface soil moisture all over the Upper Wabash watershed.
2. Such improvement is more prominent when root zone soil moisture data are employed in the calibration process as the PBIAS in root zone moisture (~60 cm) decreases from -19.1 to -8.7 with corresponding increase in KGE and R^2 from 0.13 to 0.35 and 0.18 to 0.23, respectively. Regardless of these low performance scores which may give an impression that SWAT is still under-performing even with the multi-objective calibration scheme, improvement achieved in the temporal dynamics of root zone soil moisture simulation is quite considerable.
3. Even though root zone moisture based calibration produces minimal or zero residual (simulation *minus* observed) in fairly large portion of the simulation time-span invariably during the calibration and validation periods, significant

negative PBIAS (model underestimation) is detected in the peak of summer growing season along with the inability of the model to replicate vertical distribution of moisture content throughout the year. This is likely to be influenced by SWAT's structural limitation regarding ET mechanism which cannot be resolved by calibration even with soil moisture information.

4. Use of either AMSR-E or field sensor estimates of surface moisture in calibrating the Cedar Creek model does not change the total moisture content of the top 60 cm soil profile. Thus, using surface estimates in model calibration can improve the simulation of surface moisture itself but that may exert minimal effect on the deeper layer moisture contents. Greater effect of using root zone soil moisture estimate in model calibration compared to that of surface layer is further validated in terms of enhancement in streamflow prediction. Especially for high flow conditions, SWAT simulation from the root zone moisture based calibration is found fairly matching with the observed data. In contrast, potential of surface estimates in improving streamflow simulation is still noticeable in terms of the reduced Percentage Error (PE) and residual of different flow conditions; however, those improvements may not be considered as substantial as in the earlier case.
5. Besides producing better water budget, the proposed approach shows reduced uncertainty of parameters. Also, the parameters specifically related to sub-surface hydrologic processes have been found more influential in this proposed scheme in contrast to the streamflow based calibration, thereby producing a less equifinal optimization.

Prior to the application of the distributed multi-objective calibration, this study also shows application of an automatic tool that helps to address the long-standing problem of extracting remotely sensed data in desired spatio-temporal resolution of SWAT model. While the tool is tested only on SWAT model framework through this study, it has a flexible design to be adopted for any hydrologic/land surface model’s geo-spatial structure.

Although the results from this study are promising, vigorous experiments are necessary to endorse the proposed approach across different scales, geographic and

hydro-climatic settings. Increasing the number of streamflow gauge stations in calibration along with the spatially distributed soil moisture estimates might result into improved watershed average streamflow simulations, however, that would complicate the optimization problem with too many objective variables involved. Another point of attention is the availability of remotely sensed ET data. ET, being a major driver of controlling the vadose zone and atmospheric interaction, inclusion of ET estimates in model calibration can also be considered as a potential avenue for increasing the efficiency of the proposed approach. The enhanced prediction skills and reduced equifinality from SWAT simulations, as shown here, can significantly contribute in studies related to long-term climate and land use impacts, flood forecasting, as well as nutrient transport, crop yield and agricultural management practices.

CHAPTER 3. IMPROVING SOIL MOISTURE ACCOUNTING AND STREAMFLOW PREDICTION IN SWAT BY INCORPORATING A MODIFIED TIME-DEPENDENT CN METHOD

3.1 Abstract

The objective of this study is to incorporate a time-dependent Soil Moisture Accounting (SMA) based Curve Number method (SMA_CN) in Soil and Water Assessment Tool (SWAT) and compare its performance with the existing CN method in SWAT by simulating the hydrology of two agricultural watersheds in Indiana, USA. Results show that fusion of the SMA_CN method causes decrease in runoff volume and increase in profile soil moisture content, associated with larger groundwater contribution to the streamflow. In addition, the higher amount of moisture in the soil profile slightly elevates the actual evapotranspiration. The SMA-based SWAT configuration consistently produces improved goodness-of-fit scores and less uncertain outputs with respect to streamflow during both calibration and validation. The SMA_CN method exhibits a better match with the observed data for all flow regimes, thereby addressing issues related to peak and low flow predictions by SWAT in many past studies. Comparison of the calibrated model outputs with field-scale soil moisture observations reveals that the SMA overhauling enables SWAT to represent soil moisture condition more accurately, with better response to the incident rainfall dynamics. While the results from the modification of the CN method in SWAT are promising, more studies including watersheds with various physical and climatic settings are needed to validate the proposed approach.

3.2 Introduction

Simulation of soil moisture content through a physically-based continuous-simulation distributed hydrologic model is largely dependent on simulation of runoff generation

process (Neitsch et al., 2011; Han et al., 2012b). Numerous models of varying complexity use the Soil Conservation Service Curve Number (SCS-CN) method for computing rainfall excess [e.g. EPIC (USDA, 1990); HELP (Schroeder et al., 1994); L-THIA (Harbor, 1994); PRZM (Carsel et al., 1997); APEX (Williams et al. 2000); SWIM (Krysanova et al., 2000); CELTHYM (Choi et al., 2002); SWAT(Neitsch et al., 2011)]. The versatility of CN method lies on its simplicity and capacity of accounting runoff producing watershed characteristics, such as land cover, soil type and antecedent moisture condition (Ponce and Hawkins, 1996; Geetha et al., 2007; Chung et al., 2010). However, the CN method is empirical in nature and its use has been extended beyond its intended purpose of estimating cumulative runoff depth and peak flow rate (White et al., 2009; Collick et al., 2014). Many of the practical limitations associated with CN method are discussed by Hawkins et al. (2009). In addition, the CN method suffers from several structural inconsistencies and lack of theoretical foundation which need to be addressed to enable better soil moisture accounting in a continuous simulation model.

Within a continuous model structure, the inherent SMA perception of the CN method is left unutilized mainly because of following two limitations. First, the runoff equations within the CN method compute surface runoff without incorporating any information of how much water is currently stored in the soil profile. The role of soil moisture content is rather implicit within the retention parameter and the initial abstraction, keeping the method independent of the infiltration excess or saturation excess phenomenon (Schneiderman et al., 2007; Lee and Huang, 2013) . Secondly, SCS-CN was originally designed as an event-based method without incorporating time in its equation, which is essential for its application in a continuous hydrologic model. Accordingly, there have been limited attempts to incorporate SMA procedure into the CN methodology. Among the noteworthy, Williams and LaSeur (1976) were perhaps the first to attempt an SMA conceptualization by computing rainfall excess using the antecedent 5-day rainfall-dependent CN values. An arbitrary fixation of maximum soil profile storage to 20 inches was the major weakness of that modified model (Mishra and Singh, 2004; Williams et al. 2012). Hawkins (1978) tried to

overcome this limitation by relating evapotranspiration (ET) with CN and varying storage from *0* to ∞, with a notion that soil profile never depletes fully out of moisture. Mishra et al. (2003) differentiated between static and dynamic infiltration, and incorporated the static part into the runoff equation as a loss factor along with the antecedent soil moisture amount. Williams et al. (2000) related retention parameter *S* with soil moisture depletion rather than available storage; later this was tested in Soil and Water Assessment Tool (SWAT) both by Kannan et al. (2008) and Williams et al. (2012). Kim and Lee (2008) pointed out the inconsistency associated with the updating process of *S* based on daily root zone soil moisture in a continuous simulation model such as SWAT. Need for a refurbishment of CN methodology within the existing SWAT structure has also been discussed in Gassman et al. (2007), Borah et al. (2007) and Bryant et al. (2006). Easton et al. (2008, 2010), White et al. (2009) and Collick et al. (2014) integrated the concept of Variable Source Area (VSA) hydrology with CN equations (Steenhuis et al., 1995; Lyon et al., 2004) inside the SWAT model with a view to better represent saturation excess runoff from VSAs. Jain et al. (2006) proposed a non-linear power functional relationship between the initial abstraction, incident rainfall and soil moisture retention parameter, and this was implemented within SWAT by Wang et al. (2008) in a slightly modified form.

Among the proposed CN modifications, the hypothesis proposed by Michel et al. (2005) is considered to be the most consistent from SMA standpoint because it counteracted both the aforesaid limitations. The SMA procedure adopted by Michel et al. (2005) assumes that the fraction of rainfall to be converted into runoff is directly proportional to the current moisture store level. Also, the runoff equations are re-derived as a function of time, validating CN to be applicable in a continuous model not only at the end of a storm but also at any instant during the storm. The objective of this study is to incorporate the time-dependent SMA-based CN hypothesis by Michel et al. (2005) within the existing structure of SWAT, which is a semi-distributed hydrologic model, and then test the modified SWAT model for improved simulation of streamflow regimes and soil moisture in different layers of the soil profile.

3.3 Conceptual Background on the SMA-based CN Equation

The original CN method (equation (3.1)) calculates accumulated runoff *Q* corresponding to an accumulated rainfall *P* at the end of a single rainfall event and hence, it is time-independent.

$$Q = \frac{(P - I_a)^2}{P - I_a + S} \; if \; P > Ia \; or \; 0 \text{ otherwise} \quad \ldots\ldots\ldots (3.1)$$

Here, I_a is the initial abstraction, which is computed as $I_a=0.2S$. *S* is the maximum potential retention or the maximum infiltration capacity after the runoff begins ($P>I_a$) (USDA-NRCS, 1999; USDA-NRCS, 2004).

$$S = \frac{25400}{CN} - 254 \quad \ldots\ldots\ldots (3.2), \text{ where } S \text{ is in mm}$$

In the original CN methodology, *S* is computed using equation (3.2) for a given rainfall event based on antecedent moisture condition and the curve number, thus making both *S* and I_a constant for the entire event.

In a continuous model, a storm event can get separated into several simulation time-steps depending on whether the chosen time-step is shorter or longer than the actual duration of the storm. For use in a continuous model, the CN method should be time-dependent and hence, cannot be restricted to accumulated depths. From this perspective, the proposed re-conceptualization considers rainfall and runoff within one particular simulation time-step as 'rate' in terms of rainfall intensity (*dP/dt*) and runoff rate (*dQ/dt*) respectively, *t* being the time. Differentiating equation [1] with respect to time (*t*) gives the following:

$$\frac{dQ}{dt} = \frac{dP}{dt}\frac{(P - I_a)(P - I_a + 2S)}{(P - I_a + S)^2} \quad \ldots\ldots\ldots (3.3)$$

In Equation (3.3), *S* and I_a are updated at the beginning of each simulation time-step in response to rainfall amount, simulated surface runoff, evapotranspiration from the soil profile and resultant soil moisture at the previous time step. Such updating of *S* and I_a enables the use of CN method in a continuous model (SWAT in this case),

without violating the integrity of its basic assumptions.

Despite of the regular updating at each time-step, the 'lumped' insertion of *S* and *Ia* in calculating runoff (equations (3.1) and (3.2)) does not allow the method to account for the variation of soil moisture during an event and over a continuous period of time. This lacking can be addressed by incorporating direct contribution of current soil moisture amount into equation (3.3). From the SMA perspective, a soil profile store would ideally absorb that part of the rainfall which is not transformed into runoff *(P-Q)*. This can be attributed to a notion that higher the moisture store level or moisture content, higher the fraction of rainfall that is converted into runoff. If the moisture store level is full, that is, for a saturated soil, all the incident rainfall will turn into runoff. On the basis of this hypothesis, following equation can be conceptualized:

$$V - V_0 = P - Q \quad \ldots\ldots\ldots (3.4)$$

where V_0 = soil moisture store level at the beginning of simulation time-step of a continuous model, also taken as the current soil moisture amount and V = soil moisture store level at the end of time-step when the accumulated rainfall is equal to P.

Combining equations (3.1, 3.3 and 3.4) gives the following equation (3.5), where $V'= (V_0+I_a)$

$$\frac{dQ}{dt} = \frac{dP}{dt}\frac{V - V'}{S}\left[2 - \frac{V - V'}{S}\right] \text{ if } V > V' \ldots\ldots\ldots (3.5)$$

$$\frac{dQ}{dt} = 0 \text{ otherwise}$$

Hence, V' is obtained as a threshold for runoff to occur. Therefore, the condition $P>I_a$ can be transformed as $(V_0+P)>(V_0+I_a)$ or, $(V_0+P)>V'$, in which difference between (V_0+P) and V' means the moisture deficit or surplus beyond this new threshold value V'. Hence, the incident rainfall will initially get utilized to bring the store level upto V'. To be precise, when P is not large enough such that (V_0+P) is smaller than V', there will be no runoff. Together *(Vo+Ia)* is not a portion of *S*; and *Ia* is independent of V_0

too (USDA-NRCS, 1999; USDA-NRCS, 2004). Thus, V' is conceptually different from *S*.

Michel et al. (2005) assumed V' to be a fraction of S such that $V'(t) = \alpha S(t)$, where α is determined through model calibration. Similar approach is followed by Sahu et al. (2007), Durbude et al. (2011) and Jain et al. (2012). This makes V' a model parameter, thus affecting its physical meaning. By the definition provided in this study, V' is equal to $(V_0 + Ia)$, where V_0 denotes the current moisture content which the soil profile has gained from the previous time-step and *Ia* is the amount to be intercepted in the current time-step. V' in the present study is updated at the beginning of each modeling time-step using the information of *S*, *Ia* and V_0 from the previous time-step, thereby eliminating the need to determine it through model calibration. This makes the new soil moisture-based runoff threshold internally consistent within the regular updating process of the continuous simulation structure of the SWAT model from one time-step to another (Neitsch et al., 2011), yet staying within the basic assumptions and formulations (equations (3.1) and (3.2)] based on which the CN method was originally formed.

Now, taking the time derivative of equation (3.4) and then combining with equation (3.5) will give equation (3.6):

$$\frac{dV}{\left[\frac{V - S - V'}{S}\right]^2} = \frac{dP}{dt}dt \quad \ldots\ldots\ldots (3.6)$$

Integration of equation (3.6) produces,

$$\frac{1}{S + V' - V} - \frac{1}{S + V' - V_0} = \frac{P}{S^2} \quad \ldots\ldots\ldots (3.7)$$

The detail steps of these derivations are shown in Appendix A. Replacing *V* by its expression from equation (3.4) into equation (3.7), a new expression of *Q* can be obtained as

$$Q = P\left[1 - \left[\frac{(S + V' - V_0)^2}{S^2 + P(S + V' - V_0)}\right]\right] \quad \ldots\ldots\ldots (3.8)$$

A full storage implies *dV/dt=0*, which means all the rainfall become rainfall excess or surface runoff to yield *dQ/dt=dP/dt*. According to equation (3.8), this state is mathematically achieved only if V_0 becomes equal to *(S+V')*, representing a full storage. The condition $Vo = (S + V')$ can be re-written as $Vo = (S + Vo + Ia)$. Cancelling *Vo* from both sides, we get *0=Ia+S*. According to USDA-NRCS (2004), this (*Ia+S*) is the total actual loss or retention. Now, from physical perspective, a saturation condition is achieved when soil storage does not have any room to hold moisture, needless to say *Ia* demand has already been filled beforehand. So, physically this state can be referred to as *S ≈0* and *Ia ≈0*, meaning there is no loss when the soil is saturated.

Equation (3.8) is valid not only when $V' < (V_0 + P) < (S + V')$, rather it is valid all through when $(V_0 + P) > V'$. Moreover, two concurrently possible extreme scenarios [$Vo = (S + V')$ and $(Vo + P) \gg (S + V')$] can now be satisfied with the runoff equation, if the condition is re-written as $(V_0 + P) > V'$. Thus, the original CN method can be re-conceptualized and transformed into a time-dependent approach, which will include the available moisture content of the soil profile directly inside the runoff equation. The derivation, being presented here in the light of Michel et al. (2005), can be summarized by the following set of equations and their relevant conditions:

$$i)\ If\ (V_0 + P) \le V',\ then\ Q = 0 \ldots\ldots\ldots (3.9)$$

$$ii)\ If\ (V_0 + P) > V',\ then\ Q = P\left[1 - \left[\frac{(S + V' - V_0)^2}{S^2 + P(S + V' - V_0)}\right]\right] \ldots\ldots\ldots (3.10)$$

3.4 Study Area and Data

The proposed SMA-based CN routine is analyzed by creating SWAT models for two watersheds in Indiana, USA (Figure 3.1). Both watersheds, Cedar Creek and White River, have United States Geological Survey's (USGS) streamflow gauging station at

their outlet (USGS station 04180000 and 03353000 respectively). The land use based on the NLCD 2006 data (USGS-NLCD, 2013) in both watersheds is mostly agricultural, although significant difference exists in the forest and developed portion. Table 3.1 presents a summary of their geospatial and hydro-climatic characteristics.

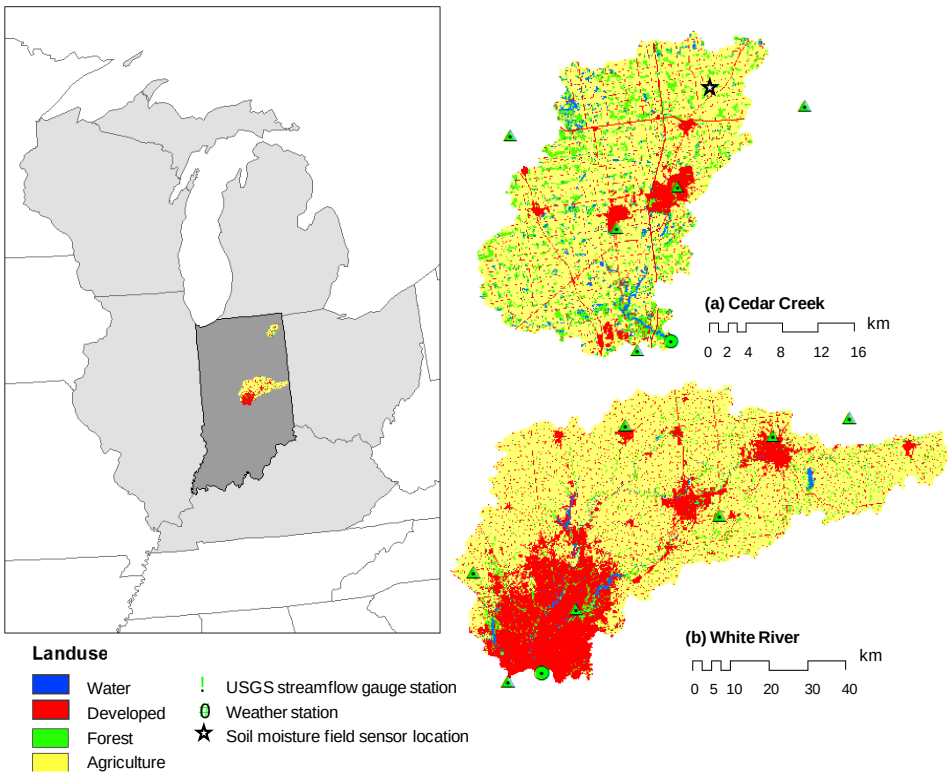

Figure 3. 1 Study areas: (a) Cedar Creek and (b) White River watershed with corresponding NLCD 2006 land use, Indiana, USA.

Creation of the SWAT models in ArcSWAT requires topography, soil texture, land use and climate data. The sources/resolution of these input data are the same as described in section 2.3. Soil moisture observations at 5, 20, 40 and 60 cm depths are obtained from one of the permanent field sensors (AS1) at Cedar Creek (Figure 3.1). The STATSGO database is modified while preparing the ArcSWAT model for Cedar Creek so that a uniform stratification of soil profile depth all over the watershed can be maintained (0-5, 5-20, 20-40, 40-60 cm, 60 cm to the maximum plant root depth). This modification is necessary to make SWAT simulated soil moisture values at different layers compatible with field measurements. Observed daily streamflow time

series for model calibration and validation are obtained from the USGS stations located at each watershed's outlet.

Table 3. 1 Watershed characteristics

	Cedar Creek	White River
Drainage area, km^2	700	4,235
No. of Sub-basins (1% threshold)	57	67
No. of HRUs (10% threshold)	253	365
Average Annual Rainfall during 2004-2012, mm	993	1,136
Maximum daily streamflow at the watershed outlet till December 31, 2014, m^3/s	163	1982
Landuse as per NLCD 2006 (%)		
Agricultural	71	67
Developed	11	26
Forest	14	6
Wetland/Open Water	4	1

3.5 Methodology

3.5.1 Modification of runoff sub-routine in SWAT

The current version of SWAT computes runoff by using either the CN or the Green-Ampt method. In the CN methodology, *S* is derived as a function of soil profile water content excluding the water held at wilting point, potential maximum retention, soil's field capacity and saturation, and the antecedent moisture conditions (Neitsch et al., 2011; Williams et al., 1984, 2012). The SMA re-conceptualization is incorporated by replacing equation (3.1) with equations (3.9-3.10) in the sub-routine that performs runoff volume estimation in SWAT. The proposed modification does not involve defining any new parameters. The sub-routine that computes retention parameter at

individual time-steps and updates CN based on the antecedent moisture conditions is kept unaltered. The edited sub-routine is then compiled with the SWAT 2009 version source code (revision no. 481) to get a new executable file. This modified version of CN approach in SWAT is referred to as SMA_CN; whereas the original implementation is referred to as CN.

3.5.2 Watershed discretization and modeling

To represent spatial heterogeneity, the study watersheds are first divided into sub-basins using 1% flow accumulation area threshold and then all sub-basins are further discretized into Hydrologic Response Units (HRUs) (Geza and McCray, 2008) using a threshold of 10% for land use, soil and slope. Table 3.1 lists the number of resultant sub-basins and HRUs for each study watershed.

In this study, the SWAT models for both watersheds are calibrated against daily streamflow records by using the existing CN method and the modified CN method (SMA_CN), thus creating a total of four calibrated models. A split-sample approach is followed for the calibration-validation study (Klemes, 1986), where a continuous 9-year daily simulation period is divided into two consecutive non-overlapping phases of calibration from 2004-2010 and validation from 2011-2012. The year 2004 is used as warm-up period.

Before starting the calibration process, 18 parameters involving surface, subsurface and channel hydrologic responses are used in the One-Factor-at-a-Time sensitivity analysis scheme (Morris, 1991) within ArcSWAT, separately for CN and SMA_CN configurations. This produced a common subset of 12 most sensitive parameters (Table 3.2) because both configurations are run with the same objective variable (i.e. streamflow). However, the difference in relative ranking of these sensitive parameters is determined through a global sensitivity analysis during the calibration phase. With a pre-defined initial range of these sensitive parameters, calibration is conducted in the SWAT Calibration and Uncertainty Program (SWAT-CUP) interface using

Sequential Uncertainty Fitting alogorithm-version 2 (SUFI-2) (Abbaspour et al., 2007; Yang et al., 2008; Abbaspour, 2015). Initial ranges of parameter value are defined based on the suggestions from model developers (Neitsch et al., 2011), existing literature and prior knowledge of the study area (Larose et al., 2007; Kumar and Merwade, 2009; Han et al., 2012b).

In SWAT-CUP, the efficiency or performance of an ongoing batch of iteration is quantified by 'P-factor' and 'R-factor'. The P-factor denotes the percentage of observed data bracketed within the 95 Percent Prediction Uncertainty (95PPU) of simulation results; whereas the R-factor denotes the average thickness of that 95PPU band divided by the standard deviation of the observed data (Abbaspour et al., 2007). Theoretically, a P-factor of 1 and R-factor of 0 is a simulation corresponding exactly to the observed data. As SUFI-2 is a sequential semi-automated procedure, more iterations can always be performed leading to a smaller 95PPU at the expense of more observation points falling out of the prediction band (Yang et al., 2008). Therefore, a stopping rule is imposed in this study following Price et al. (2014) with a view to avoid over-restricting the parameter space. Batch iterations are continued until the following two conditions are satisfied: P-factor > 0.75 and R-factor <1, with a maximum of four batches (i.e. 2001+1000+1000+1000 = 5001 total simulations). For each of the batch, coefficient of determination (R^2) is also calculated to assess the goodness of fit between the observed streamflow data and the best simulation having maximum objective function value (Nash Sutcliffe efficiency, NSE in this case).

3.5.3 Global sensitivity analysis in SWAT-CUP

A relative sensitivity ranking of parameters is obtained by the global sensitivity analysis technique in SWAT-CUP after executing the first batch of calibration iterations. The global sensitivity analysis in SWAT-CUP measures the 'relative' effect of parameters while they are getting optimized, thus reflecting the average changes in objective function values due to the changes in one parameter while all other parameters are also simultaneously changing (Abbaspour, 2015). Accordingly,

the measure of relative sensitivity among the parameters involved in optimization is translated through t-stat and p-values, providing respectively the extent and the significance of the sensitivity measured. Since the relative sensitivity of one parameter depends on the ranges of the others, this global sensitivity scheme is executed after first 2001 iterations when parameters are having a bigger control space and the deviation of the simulated streamflow from the observed data is still considerably large. Running this scheme for the later batches with narrower parameter space would have simply altered the relative sensitivity rankings.

Table 3. 2 SWAT calibration parameters

No.	Parameter	Description[a]	Adjustment [b]	Initial Rage
1	CN2	SCS Curve Number, moisture condition II	x	-0.2 – 0.2
2	CH_K2	Channel Hydraulic Conductivity, mm/hr	=	5.0 – 100.0
3	CH_N2	Main Channel Manning's n	=	0.02 – 0.15
4	CANMX	Maximum Canopy Storage, mm	=	0.0 – 25.0
5	ESCO	Soil Evaporation Compensation Factor	=	0.01 – 1.0
6	SURLAG	Surface Runoff Lag Coefficient, days	=	0.05 – 24.0
7	SOL_AWC	Available Soil Water Capacity, mm/mm	x	-0.15 – 0.15
8	ALPHA_BF	Baseflow Recession Constant, days	=	– 1.0
9	REVAPMN	Re-evaporation Threshold, mm	=	0.01 – 500.0
10	GW_DELAY	Groundwater Delay, days	+	0.02 -10.0 – 10.0
11	GWQMN	Threshold Groundwater Depth for Return Flow, mm	=	0.01 – 5000.0
12	SOL_K	Soil Hydraulic Conductivity, mm/hr	x	-0.15 – 0.15

[a] Source: Neitsch et al. (2011); [b] See Table 2.3 for necessary explanations of the symbols

3.5.4 Model validation

The optimized parameter ranges are further used in SUFI-2 to generate a new set of 2001 simulations for the 2011-2012 validation period. Model performance for streamflow simulation during the validation period is also evaluated through P-factor and R-factor values. Comparing the model output against observed streamflow is the conventional approach in validating a hydrologic model, but to test the effectiveness of soil moisture accounting, model simulated soil moisture output also needs to be compared with observed data. Hence, after calibrating the models for observed streamflow data, daily soil moisture in a particular Cedar Creek sub-basin is matched with the AS1 field sensor values (see Figure 3.1) during an average rainfall year 2007. However, prior assumptions and processing are essential to make field measurements comparable with SWAT simulations. Following the same methodology described in section 2.4.5, AS1 point measurements taken at 5, 20, 40 and 60 cm depths are made approximately comparable with the moisture contents simulated respectively at 0-5, 5-20, 20-40 and 40-60 cm layers in the particular sub-basin where AS1 is located.

3.6 Results and Discussion

This section presents the comparison of SWAT performance by looking at various flow fluxes over the study watersheds using the two model configurations (CN and SMA_CN). First, un-calibrated results are presented because calibrated outputs will be influenced by parameter optimization process and associated parameter equifinality (Beven, 1993). The un-calibrated outputs are obtained by running both model configurations with the same parameter values. After comparing the un-calibrated outputs, the models are calibrated to get the goodness of fit for simulated streamflow at respective watershed outlets. Finally, the root zone soil moisture in a single sub-basin of Cedar Creek is evaluated with respect to corresponding observed data.

Table 3.3 presents an overall view of the average annual differences in surface runoff, plant-available water, evapotranspiration, baseflow and water yield in the whole watershed scale. Here, 'difference' refers to the change in amount (mm) obtained by subtracting the output of the original SWAT model (CN) from the corresponding output of the modified SWAT model (SMA_CN).

Table 3. 3 Calculated change in water fluxes for a dry and wet year[1, 2]

Watershed	Year	PREC(mm)	ΔSURQ (mm)	ΔPAW (mm)	ΔET (mm)	ΔGWQ (mm)	ΔWYLD (mm)
Cedar Creek	Dry	812.5	-9.8	5.6	1.5	12.5	3.2
	Wet	1107.4	-13.6	0.2	2.5	23.7	10.8
White River	Dry	1007.6	-13.4	2.0	3.7	16.1	3.3
	Wet	1303.1	-21.9	0.2	1.4	24.8	4.2

[1]PREC = Total annual precipitation, SURQ = surface runoff, PAW = plant-available water content in soil profile, ET= evapotranspiration, GWQ = groundwater contribution to streamflow, WYLD = water yield = SURQ + GWQ + lateral flow – losses.

[2]Difference, Δ= SMA_CN – CN

Entries in Table 3.3 are separately listed for a dry (2010) and a wet (2006) year, having respectively the least and the most amount of total incident annual rainfall during the simulation period. The water fluxes in Table 3.3 show a specific pattern of change for both watersheds. Specifically, the SMA_CN method leads to decrease in the surface runoff and increase in profile soil moisture content, which in turn leads to larger contribution of groundwater to the streamflow (e.g. Kannan et al., 2008). Increase in profile/root zone soil moisture content also elevates the model evapotranspiration. All these changes result in overall increase in the water yield. The differences in various components are discussed in detail in the following sections.

3.6.1 Surface runoff

Figure 3.2 shows the difference in average daily CN and surface runoff in a typical

agricultural sub-basin in the study watersheds. It is difficult to relate the temporal change in CN value caused by the SMA-based method to the change in runoff (Figure 3.2) because of the incident precipitation amount and use of a threshold (*Ia* and *V'*). Moreover, the PAW in the whole root zone is not an instantaneous result of the weather on a particular day; rather, it is influenced by the antecedent weather of preceding many days or weeks (Wagner et al., 1999). SWAT's existing formulation uses the total root zone PAW at the end of previous day's simulation to update *S* and CN, and then the total precipitation of the current day is used to compute the runoff. Thus, correlating the variations among CN, runoff and/or soil moisture values becomes even more ambiguous (Kim and Lee, 2008; Qiu et al., 2012), regardless of the incorporation of SMA_CN method.

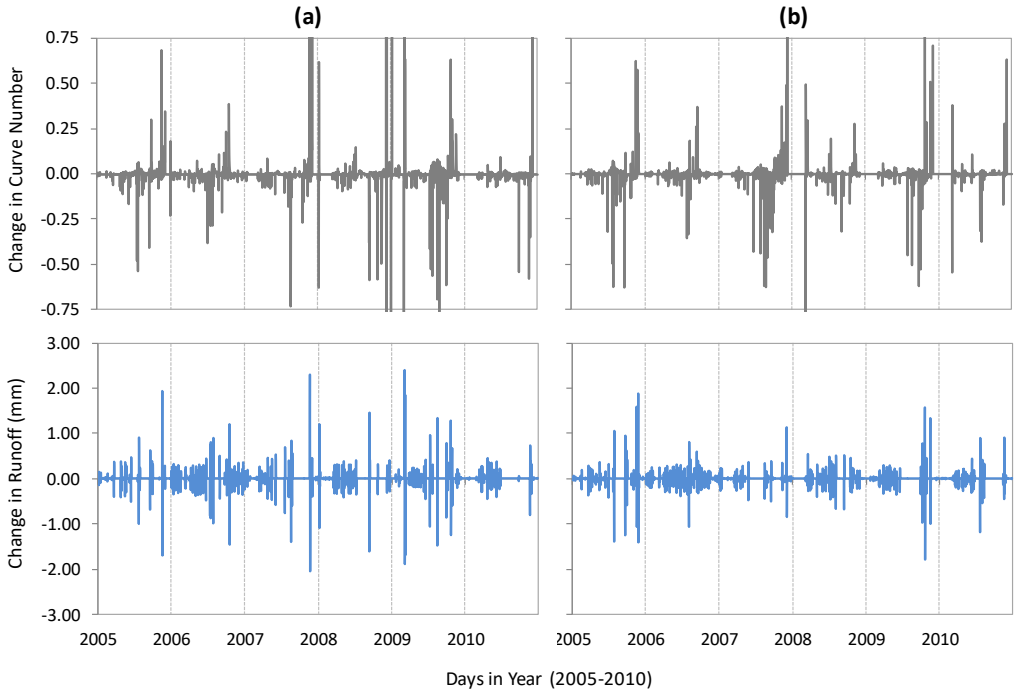

Figure 3. 2 Difference (SMA_CN – CN) in daily average CN and surface runoff volume in a typical agricultural sub-basin; (a) Cedar Creek, (b) White River. Values correspond to un-calibrated model output.

Many past studies report SWAT's inaccurate representation of overland flow processes. For example, Kannan et al. (2008), Neitsch et al. (2011) and Williams et al. (2012) pointed out the weaknesses of SWAT's original CN method for shallow soil

regions. Moreover, in humid well-vegetated regions, which is likely the case for the current study watersheds, SWAT does not capture the spatial distribution as well as the volumetric magnitude of the runoff (Easton et al. 2008, 2010). Similarly, many other studies have reported the shortcomings of the modeling of overland flow in SWAT across various regions, even after model calibration (e.g. Di Luzio et al., 2005; Kang et al., 2006; Tripathi et al., 2006; Borah et al., 2007; Wang et al., 2008; Santhi et al., 2009; White et al., 2009; Licciardello et al., 2011; Qiu et al., 2012; Collick et al., 2014). In this regard, the overall lowering of surface runoff volume as shown in Table 3.3 based on the SMA-based SWAT model delivers a positive notion. However, these results need to be validated against field observations under various geographic and climate conditions

3.6.2 Moisture content at different soil layers

SWAT conceptualizes the soil profile as the topmost portion of the vadose zone having thickness equal to the maximum plant root depth (approximately 150 cm for this study). To visualize the effect of change in surface runoff volume as induced by the SMA-based method, temporal variations in PAW content at different depths are analyzed for different land use conditions. Figures 3.3 shows the PAW simulated by the original CN method, as well as the calculated difference between the two configurations, at three consecutive layers from the surface (0-40, 40-60 and 60-150 cm) and the whole root zone (0-150 cm) for agricultural land use. The frequent fluctuations in moisture in the topmost layer (0-40 cm) show that this layer is readily active in response to the incident rainfall amount as well as the change in runoff resulting from the SMA_CN method. But the change in overland runoff volume does not have an immediate effect on the moisture content in underlying deeper layers due to the use of saturation flow phenomenon and associated exponential storage routing methodology in SWAT. SWAT's current moisture depletion mechanism can potentially remove all the available moisture (i.e. PAW) from the top layers till 60 cm because of increased plant uptake and elevated surface temperature during the

summer growing season (Milzow et al., 2011). On the contrary, the SMA_CN method, which reduces the surface runoff, allows more water to enter the soil profile; as a result, the moisture content in all layers stays above the wilting point.

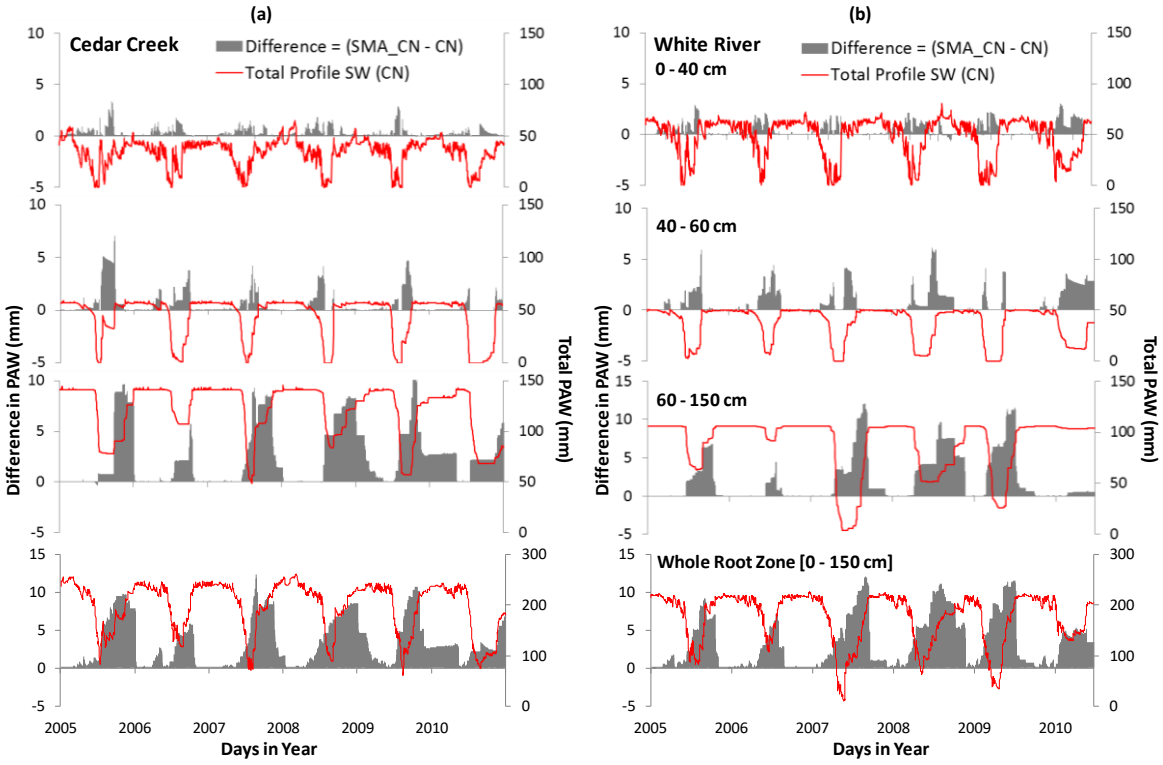

Figure 3. 3 Un-calibrated model outputs for plant-available water (PAW) content and the calculated difference (SMA_CN - CN) at different soil layers: (a) Cedar Creek, (b) White River. Values correspond to HRU-averages aggregated for agricultural land use.

Thus, the overall increase in the soil moisture as simulated by the SMA_CN model is more prominent particularly in summer months. Total increase in the whole profile moisture content has been found to be as high as 25 mm on a given day in one agricultural HRU, if considered separately. Such extent of change is quite significant considering the amount of daily average rainfall the watersheds usually receive.

In case of developed land use as in Figure 3.4, the middle and bottom layers (40 – 150 cm) maintain nearly a constant soil storage level due to less plant root density and hence less ET depletion.

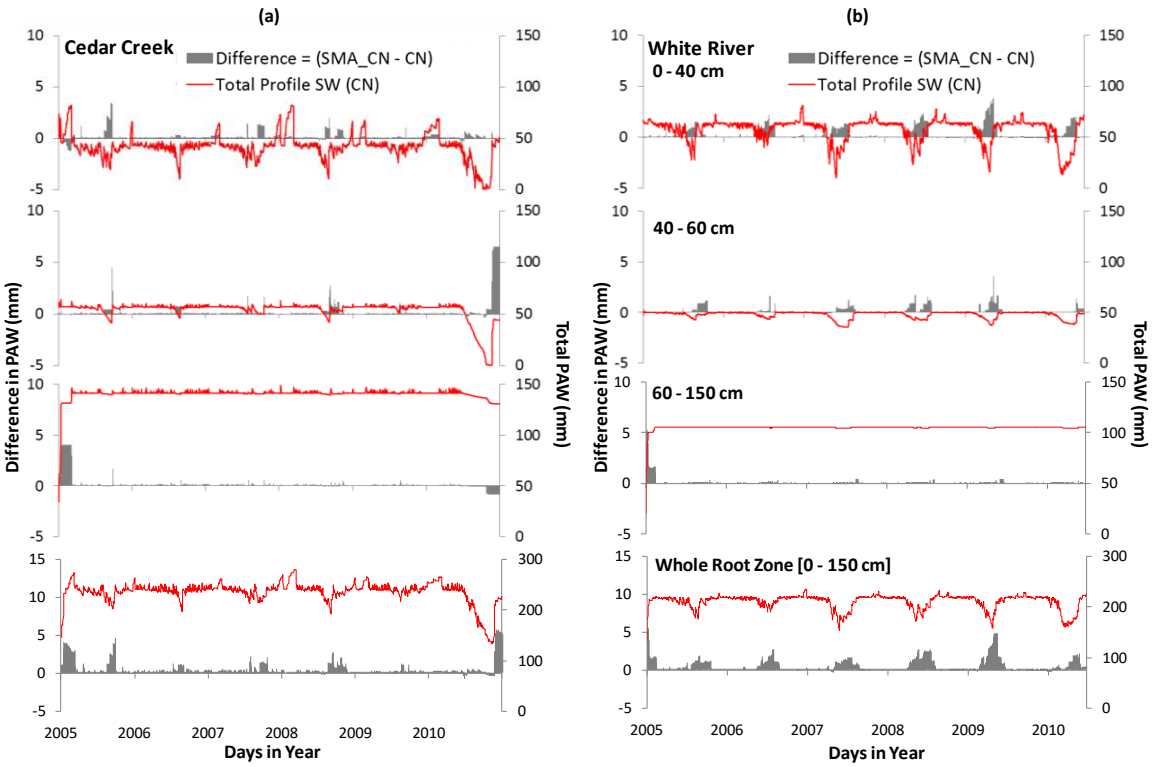

Figure 3. 4 Un-calibrated model outputs for plant-available water (PAW) content and the calculated difference (SMA_CN - CN) at different soil layers: (a) Cedar Creek, (b) White River. Values correspond to HRU-averages aggregated for developed land use.

3.6.3 Partitioning of soil and plant ET

Figure 3.5 shows the calculated difference (SMA_CN - CN) in actual soil evaporation and plant transpiration across the entire soil profile. SWAT partitions evapotranspiration into its soil and plant components primarily as a function of aboveground biomass and leaf area index, respectively (Neitsch et al., 2011). The partitioning mechanism in SWAT maintains a balance between the two ET components such that amount of soil evaporation gets adjusted during the period of high plant water use and vice versa. SWAT allocates the demand for both the ET components into different layers of the soil profile using a depth distribution function (discussed in section 3.6.7 with examples).

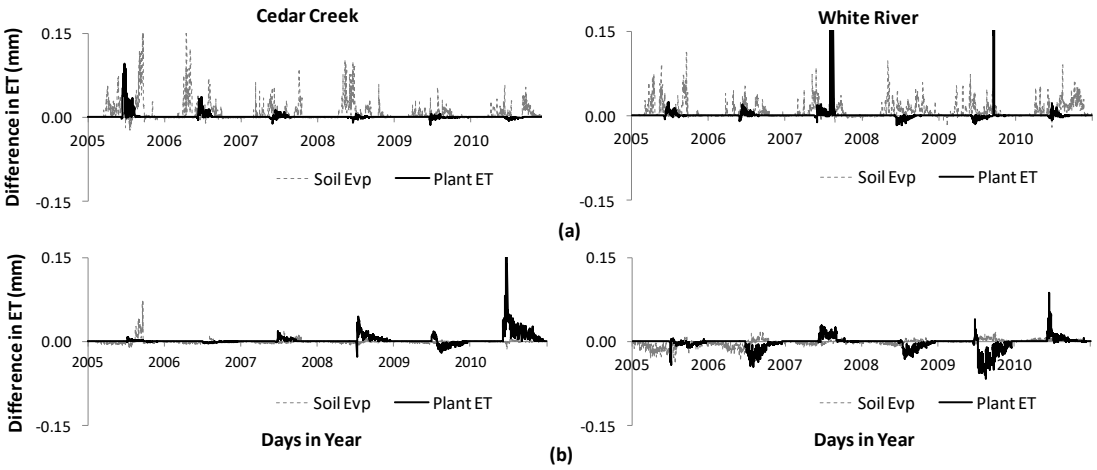

Figure 3. 5 Calculated differences (SMA_CN - CN) in HRU-average ET components: (a) agricultural landuse, (b) developed landuse. Values correspond to the un-calibrated ET outputs from the entire 150 cm soil profile.

From Figure 3.5, it is evident that the increased soil moisture content induced by the SMA_CN method is likely to alter both ET components irrespective of land use types. Calculations on the watershed-scale reveal a net increase in total ET amounts (Table 3.3), staying within the same PET limit, which is empirically calculated using the Penman-Monteith method. However, these potential differences in ET as detected from the SMA_CN model can be significant in applications related to irrigation and plant growth.

3.6.4 Spatial pattern of changes in profile soil moisture

Corresponding to the temporal variation in PAW between the two model configurations in different layers of the soil profile (Figures 3.3 and 3.4), Figure 3.6 shows the spatial maps of the difference across the entire soil profile (~ 150 cm) for two extreme wetness conditions in a given year for both watersheds. Figure 3.6(a) shows the spatial map for Cedar Creek for Julian days 245 and 264 from year 2008. Julian day 245 represents a dry day after at least 7 dry days; whereas day 264 represents a wet day immediately after the end of a wet period. Similarly, spatial map

for White River is shown in Figure 3.6(b) for Julian days 256 and 273 from year 2005. Clearly, on a given day, difference in PAW across the whole soil profile caused by the SMA_CN method has been found to be as high as 16 mm after a continuous rainfall event subsides. Most importantly, even after a consecutive number of dry days, there can be 6-10 mm difference in significant portion of the area.

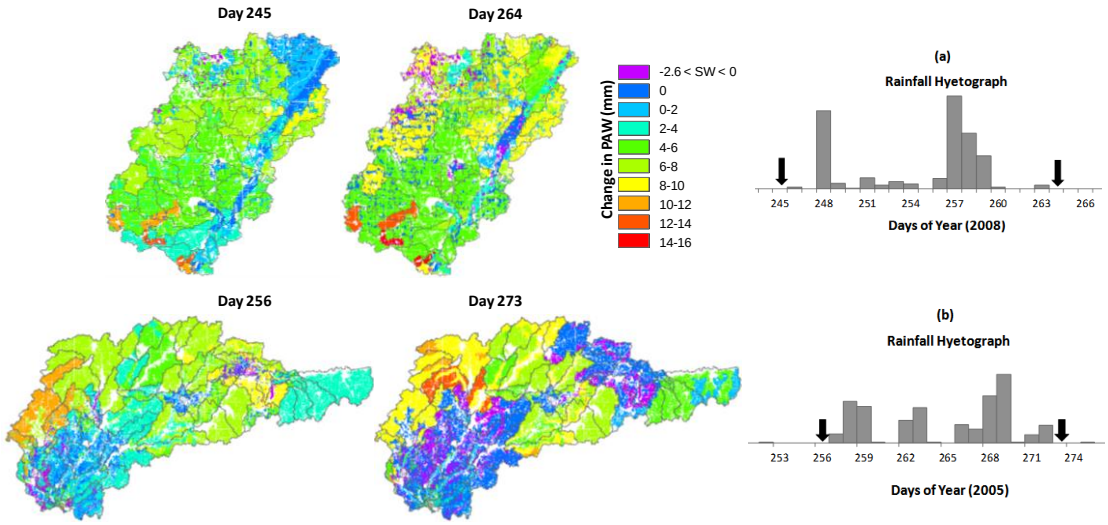

Figure 3. 6 Spatial pattern of calculated difference (SMA_CN - CN) in plant-available water (PAW) across the whole soil profile (~ 150 cm) at two opposite wetness conditions: (a) Cedar Creek, (b) White River.

With correspondence to the land use map from Figure 3.1, the difference in soil moisture levels between the original CN and the SMA_CN configurations are not observed in urban areas, thus validating the fact that the SMA-based approach does uniformly affect soil moisture over the entire watershed. Furthermore, the SMA_CN method tends to produce negative difference in soil moisture during or just after a storm event only in case of denser vegetative cover (forest and perennial grassland) along with soils of higher infiltration capacity (hydrologic group B), under a condition when HRUs of this category receives nearly equal amount of precipitation. Therefore, the magnitude and spatial pattern of the difference in soil moisture between these two model configurations are largely dependent on land use and soil drainage characteristics, besides being affected by the incident precipitation intensity

and its spatial distribution. Further analysis is required in order to ascertain the causal effect of these watershed characteristics over the changes in soil moisture content caused by the SMA_CN method under different geographical contexts.

3.6.5 Streamflow calibration and validation

Streamflow prediction skills metrics from calibration and validation periods are presented in Table 3.4. Table 3.4 indiactes that the SMA_CN method produces consistently higher P-factor at the end of the calibration- validation phase relative to the original CN method. In addition, the R-factor shows a desired value of less than 1 in all cases. Both P-and R-factors form a conjugate and need to be assessed together. Higher P-factor is achievable through higher R-factor values. However, a balance between these two measures needs to be drawn, which essentially produces an 'optimized' set of model parameters including most of the observed data within 95PPU as well as the narrowest possible uncertainty band.

Validation of Cedar Creek exemplifies a critical scenario in this aspect. As reported in Table 3.4, the CN and the SMA_CN models have nearly the same P-factor (84% and 85%, respectively) in the validation stage. But the SMA_CN model has R-factor equal to 0.75, which is 0.82 for the original CN model. Thus, in case of Cedar Creek the SMA-based technique brackets almost the same amount of the observed streamflow data within its 95PPU band as in the conventional method, yet producing a narrower output uncertainty width. In addition, the fit scores (NSE and R^2) are relatively higher for the SMA-based model, except for a single case of Cedar Creek's validation.

Values obtained in all the four modeling cases are acceptable according to the evaluation guidelines by Moriasi et al. (2015). The calibrated parameter ranges (holding the best estimates) are shown in Table 3.5.

Table 3. 4 Goodness of fit statistics for streamflow[a]

	Cedar Creek		White River	
	CN	SMA_CN	CN	SMA_CN
Goodness of fit [b, c]				
NSE	0.67 (0.69)	0.69 (0.66)	0.60 (0.72)	0.66 (0.73)
R^2	0.68 (0.70)	0.70 (0.77)	0.65 (0.70)	0.66 (0.73)
Calibration and validation efficiency [b]				
P-factor	0.81 (0.84)	0.86 (0.85)	0.87 (0.75)	0.89 (0.81)
R-factor	0.99 (0.82)	0.99 (0.75)	0.97 (0.68)	0.99 (0.84)

[a] Single objective calibration/validation with respect to the streamflow at watershed outlet; [b] Within parentheses are the values from model validation; [c] Only for best simulation

Table 3. 5 Calibrated Parameter Ranges obtained from SUFI-2 iterations

Parameter	Calibrated parameter range			
	Cedar Creek		White River	
	CN	SMA_CN	CN	SMA_CN
CN_2	0.03 – 0.19	-0.07 – 0.11	0.04 – 0.12	0.04 – 0.14
CH_K2	70.0 – 100.0	34.0 – 78.0	62.0 – 84.5	40.0 – 74.0
CH_N2	0.02 – 0.06	0.02 – 0.06	0.02 – 0.05	0.02 – 0.05
CANMX	4.4 – 13.17	5.6 – 16.8	8.6 – 19.2	17.6 – 22.5
ESCO	0.31 – 0.91	0.66 – 1.0	0.39 – 0.75	0.55 – 0.85
SURLAG	0.05 – 6.7	0.05 – 6.8	0.05 – 3.8	0.05 – 3.7
SOL_AWC	-0.12 – -0.03	-0.15 – -0.02	-0.02 – 0.06	-0.12 – -0.05
ALPHA_BF	0.5 – 0.97	0.6 – 0.95	0.76 – 1.0	0.68 – 0.96
REVAPMN	127.0 – 280.0	296.0 – 500.0	0.01 – 227.5	213.0 – 288.0
GW_DELAY	-10.0 – -3.4	2.6 – 9.2	-3.4 – 4.8	-2.4 – 5.0
GWQMN	1267 – 3340	0.01 – 1440	2859 – 4288	1665 – 3086
SOL_K	-0.07 – 0.02	0.03 – 0.15	-0.05 – 0.05	-0.07 – 0.04
Number of runs required in SUFI-2[a]	2001+1000 (2001)	2001+1000 (2001)	2001+1000+ 1000 (2001)	2001+1000+ 1000 (2001)

[a] Numbers within parentheses refer to model validation;

[c] Initial parameter ranges and the basis of adjustment are shown in Table 3

Figure 3.7 shows the comparison of calibrated streamflow hydrographs for three discrete time segments from the entire calibration-validation period (2005-2012). The time segments are chosen such that they individually represent dry, moist and high flow phenomenon. A better match between the SMA_CN hydrographs and observed data is clearly visible in Figure 3.7. With few deviations, the rising and falling limbs of the SMA_CN hydrographs tend to match with observed data, thereby validating that SMA-based SWAT model can reproduce watershed physics more accurately in response to rainfall dynamics. Specifically, SMA_CN uses the current soil moisture amount directly inside the CN equation, thus enabling better representation of the actual wetness condition of the watershed before and during a rainfall event. As a result, the limbs of these simulated event-based hydrographs tend to match well with the observed data.

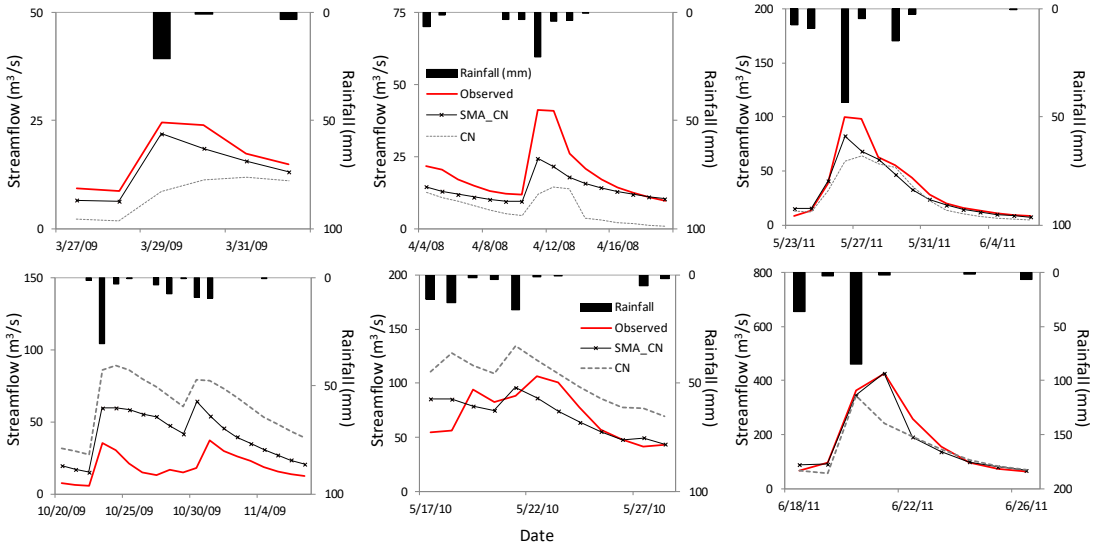

Figure 3. 7 Comparison of calibrated streamflow hydrographs for shorter time segments: Cedar Creek (top), White River (bottom). Time segments represent dry, moist and high flow conditions respectively (left to right).

The calibrated models are also compared over the period 2004-2010 at three different flow regimes using flow duration curve (FDC) analysis (Figure 3.8). These regimes

consist of high flow, moist and mid flow, dry and low flow, respectively having 0.0-0.1, 0.1-0.6 and 0.6-1.0 exceedance probability. FDCs from SMA_CN method provides a better match with observed data compared to the CN method for all flow regimes. This addresses the long-standing concern of SWAT not precisely representing the high and low flow conditions in many past studies (e.g. Arnold and Allen, 1996; Arnold et al., 2000; Chu and Shirmohammadi, 2004; Vazquez-Amábile and Engel, 2005; Arabi et al., 2006; Bracmort et al., 2006; Larose et al., 2007; Wang et al., 2008; Kumar and Merwade, 2009; Oeurng et al., 2011; Rahman et al., 2012; Qiu and Wang, 2013; Rahman et al., 2014).

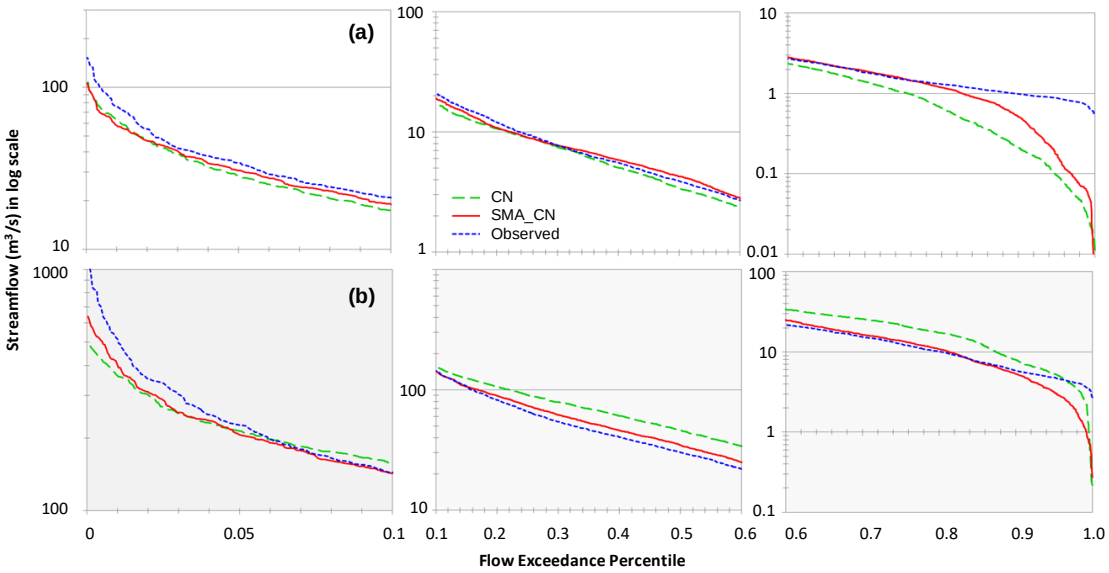

Figure 3. 8 Flow duration curve comparison of calibrated streamflow at three different flow regimes (0.0-0.1: high flow, 0.1-0.6: moist and mid flow, 0.6-1.0: dry and low flow): (a) Cedar Creek, (b) White River.

3.6.6 Measure of relative parameter sensitivity

Figure 3.9 compares p-value and t-stat measurements between the two model configurations for the study watersheds, resulted from the global sensitivity analysis of parameters. The p-value determines the significance of the sensitivity, where a value closer to zero means more significance. In addition, t-stat provides the extent of

sensitivity, where larger t-stat absolute value for a particular parameter means it is more sensitive relative to others. Larger t-stat is associated with smaller p-values.

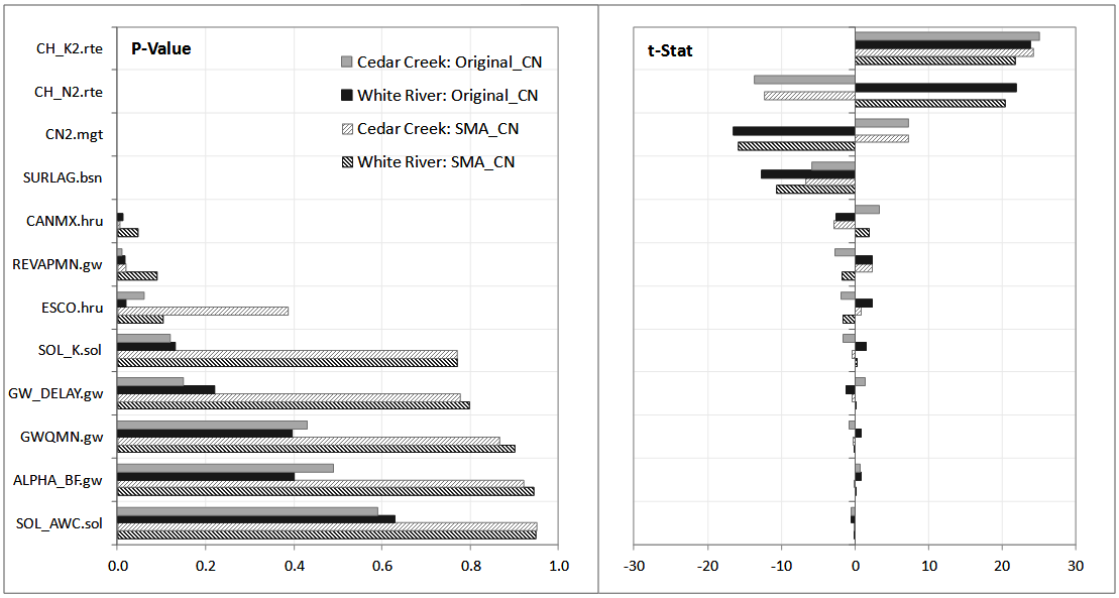

Figure 3. 9 Relative sensitivity results: p-value and t-stat measurements.

As presented in Figure 3.9, CH_K2, CH_N2, CN2 and SURLAG are the four most sensitive parameters having very high t-stat with p-values close to zero for both watersheds and model configurations. All other parameters show a large variation in the p-value between the CN and SMA_CN models. Another important feature is the opposite t-stat signs between the two models for some of the less significant parameters (lower t-stat with higher p-value). For example, in case of CANMX, REVAPMN and ESCO, t-stat between the two models show opposite signs even for the same watershed, signifying reversal in the directionality of effect of the same parameter on streamflow. To ascertain the opposite trend of relationships of these parameters with streamflow, a set of 25 iterations are run separately in SWAT-CUP for each of the four model cases using SUFI-2, employing all the 12 parameters with their initial ranges. Figure 3.10 (a) and (b) compare the trend of change in resultant objective function values (NSE) relative to each 25 iterated values of ESCO and REVAPMN respectively for Cedar Creek and White River, while the other parameters are also simultaneously changing. Clearly, the trends of NSE with these

two parameter values are simply the opposite for the SMA_CN configuration. Because parameters such as REVAPMN and ESCO can affect the simulation of storage, fate and transport of nutrients and contaminants through root zone, their different behavior in the SMA-based model may have substantial influence in case of multi-variable optimization involving both hydrologic and water quality parameters together.

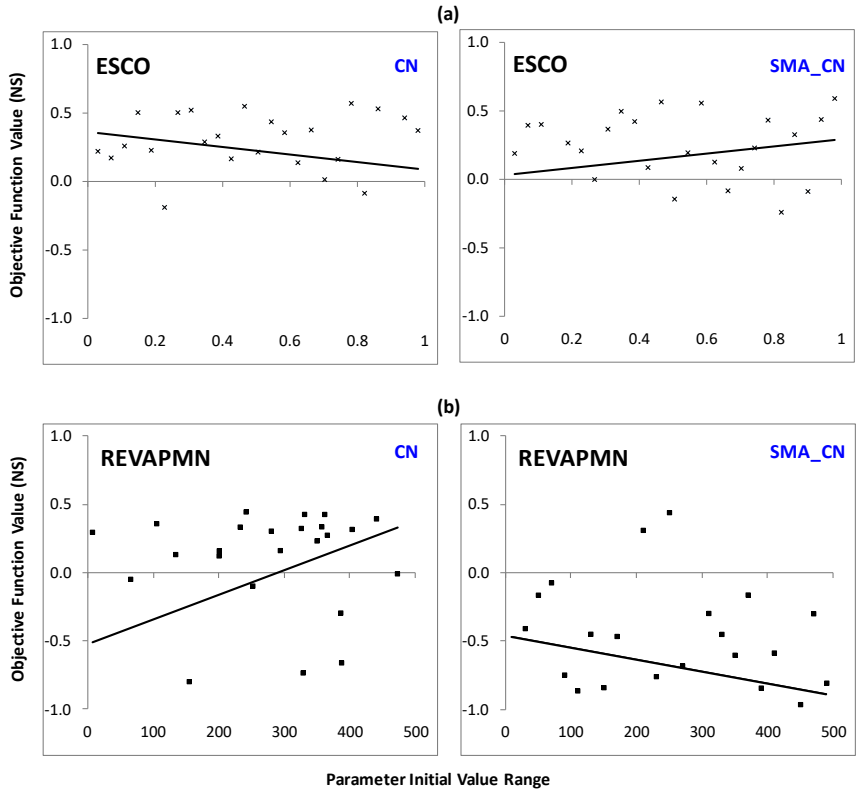

Figure 3. 10 Change in objective function with parameter values from a sample SUFI-2 iterations of 25 runs using initial parameter ranges: (a) Cedar Creek, (b) White River.

3.6.7 Validation using observed soil moisture data

In this section, model simulated soil moisture from both model configurations is compared with field observations (Figure 3.11). The simulated values presented in the figure represent the average moisture content for the soil layers at 5-20, 20-40 and 40-

60 cm depth spacing, in the particular sub-basin where AS1 sensor is located. Clearly, soil moisture at different layers of the soil profile is poorly captured by the original model with respect to in-situ data.

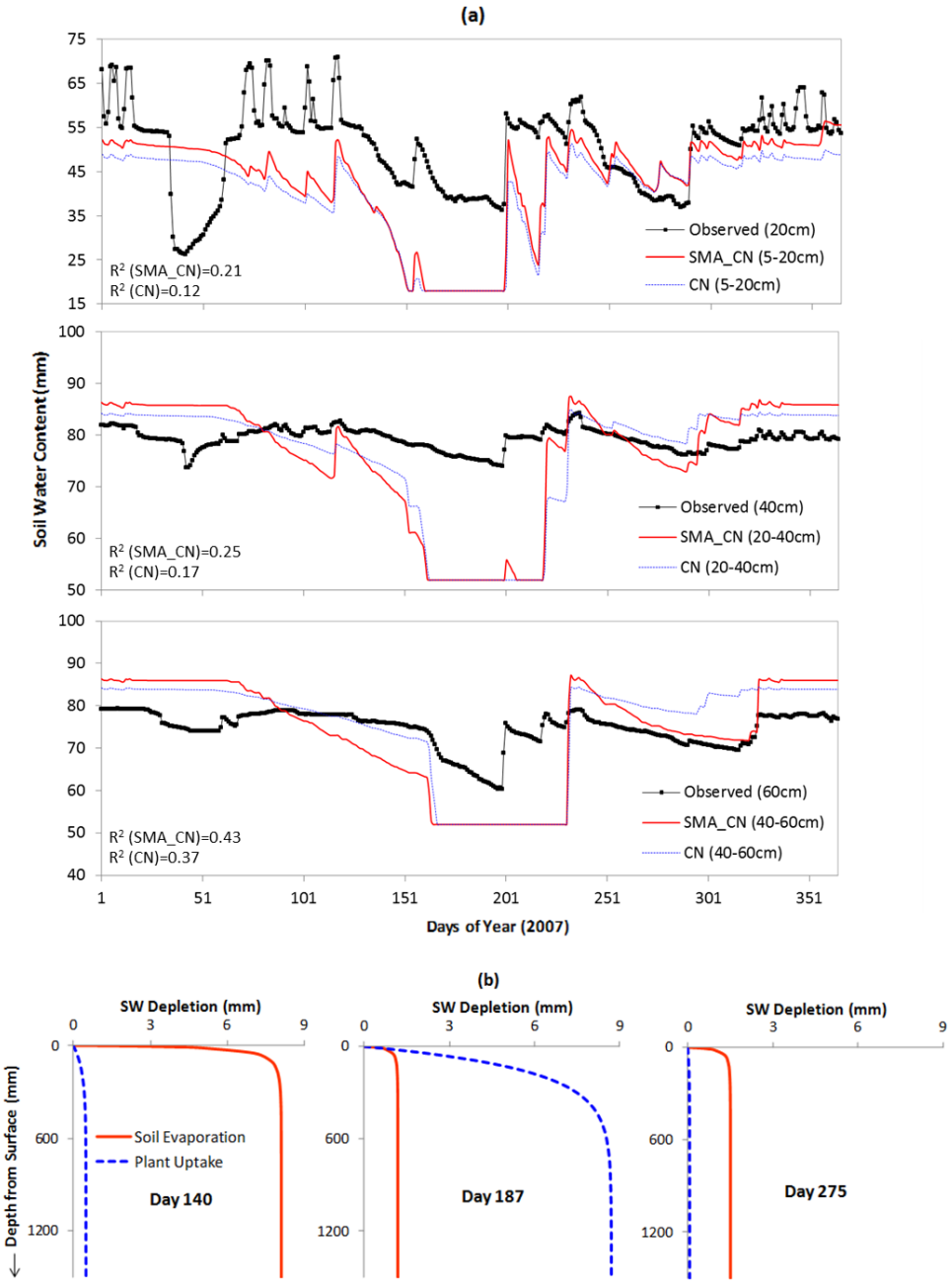

Figure 3. 11 (a) Model validation with observed soil moisture data, (b) soil moisture depletion in three separate days following SWAT's depth distribution function (Neitsch et al., 2011).

Although the general temporal variation between the two configurations are quite identical, soil moisture simulated by the new SMA_CN model is relatively closer to the field condition in terms of higher R^2 value in all layers. Furthermore, Figure 3.11(b) shows summer moisture depletion as exhibited by both model configurations, which is largely attributed to the model conceptualization of ET removal. Here, using the depth distribution functions described by Neitsch et al.(2011), maximum water demand for soil evaporation and plant uptake is calculated at three different days (140, 187 and 275) at different depths across the root zone. It is found that the model conceptualization causes nearly 100% of the demands to get exerted within first 40 cm from the surface. This means, that the top layers (up to 60 cm) may not have sufficient water to meet this 'calculated' demand, causing moisture content to get fully depleted as seen in Figure 3.11(a). This is an issue which cannot be overcome by a better soil moisture accounting approach; rather it needs to be addressed by looking at the formulation of the two ET components in the SWAT model. It is also a valid concern that the two model configurations in this study are calibrated with respect to streamflow only; therefore, comparing the two models for soil moisture would have been more legitimate if the models were put under multi-variable calibration with respect to observed soil moisture data as well.

3.7 Conclusion

This study proposes a modified soil moisture accounting (SMA) based modification to the existing CN methodology in the SWAT model. The proposed SMA_CN method is then compared with the CN method by applying the SWAT model to two watersheds in Indiana, USA. The following conclusions are drawn:

1. The calibration and validation of SMA based model produce relatively higher fitness and efficiency statistics compared to the original model. The flow duration curve analysis shows that the SMA_CN method produces better match with the observed data for all flow regimes. These results address SWAT's long-standing

difficulty in exact representation of flood and dry conditions. Moreover, the rising and falling limbs of the SMA_CN hydrographs tend to match with those of the observed data, thereby validating that the newly configured SMA-based SWAT model can more accurately capture watershed behavior in response to rainfall dynamics.

2. The SMA_CN method produces elevated soil moisture store level compared to the CN method. This increased soil moisture can support additional plant uptake and soil evaporation without totally removing the available moisture from the top 60 cm, which is a prominent phenomenon in the current SWAT model. The spatial distribution of this soil moisture variation even in dry condition is found to be consistent with the results obtained through time series. Specifically, the total profile moisture content as simulated by the modified model remain 6-10 mm higher than that of the original model in significant parts of the watersheds even after seven consecutive dry days with zero rainfall.
3. Besides providing better water budget, the calibration of SMA based model produces narrower parameter band compared to the original model for the same number of calibration iterations.
4. Finally, as part of a model validation with respect to the observed soil moisture data, the SMA-based model is found to produce soil moisture that is closer to observations compared to the soil moisture estimates from the original model in terms of R^2 values.

Overall, the major focus of the current study is to modify the soil moisture accounting in SWAT in order to improve the model physics and predictability. The results obtained herein are quite supportive of this attempt. While the proposed time-dependent CN method can be potentially used with any time-step, the current study used only daily time-step to avoid the major overhaul of all the sub-routines in the program, which is beyond the expertise of the authors. Even with the daily time-step, results from this study showed that the proposed method is able to improve the soil moisture predictability and consequently the streamflow hydrograph output. Although the results from this study are promising, vigorous experimentations are necessary for

validating the modified SWAT model under heterogeneous scenarios, including diverse land use types, soil characteristics, geographic locations and climate settings. Similarly, in addition to the hydrologic perspective discussed in this study, research looking at how nutrient transport and plant growth get affected from the proposed SMA method can be of immense interest.

CHAPTER 4. RATIONALE AND EFFICIACY OF DIRECTLY INGESTING REMOTELY SENSED POTENTIAL EVAPOTRANSPIRATION IN A HYDROLOGIC MODEL

4.1 Abstract

Source-attribution of evapotranspiration uncertainty in a hydrologic model and evaluation of a remote sensing based solution are the two main aspects of this study. Using Soil and Water Assessment Tool (SWAT) for three US watersheds in different geophysical settings, this study first addresses the effects of parameter equifinality, energy related weather input-uncertainty and lack of geo-spatial representation on evapotranspiration simulation. In every case, remotely sensed 8-day total actual evapotranspiration (AET) estimate from Moderate Resolution Imaging Spectroradiometer (MODIS) is used as the reference to evaluate model outcome. Results from these assessments indicate the likelihood of a pseudo-accurate model that invariably shows high streamflow prediction skills despite having severely erroneous spatio-temporal dynamics of AET. As a remedial measure, a hybrid daily PET estimate, derived from MODIS and the North American Land Data Assimilation System phase 2 (NLDAS-2), is directly ingested at each Hydrologic Response Units (HRUs) of the SWAT model to create a new configuration called SWAT-PET. Noticeably increased accuracy of three water balance components (soil moisture, AET and streamflow) in SWAT-PET, being evaluated against completely independent sources of observations/reference estimates (i.e. field sensor, satellite and gauge stations), proves the efficacy of the proposed approach towards improving physical consistency of hydrologic modeling. A key contribution of this study is the development of a modified SWAT source code to execute SWAT-PET that is fully integrated with an automatic remote sensing data processor. While the proposed approach is evaluated for a past period, the main motivation here is to serve the purpose of hydrologic forecasting once near real-time PET estimates become available.

4.2 Introduction

Evapotranspiration, the largest outgoing component in the hydrologic cycle, regulates Soil Moisture Accounting (SMA) (Long et al., 2014; Wang and Dickinson, 2012), which in turn affects the accuracy of surface/sub-surface runoff simulation in a hydrologic model (Rajib and Merwade, 2016). Precipitation input is the "supply of water" from atmosphere to the land surface, whereas, potential evapotranspiration (PET) is an index of "available energy" required by the model to drive the water back to the atmosphere. Inaccuracy in calculated PET induced from relevant weather inputs propagates into the simulation of actual evapotranspiration (AET) and other hydrologic processes (Yin et al., 2016). Moreover, many of the poorly understood land-to-atmosphere feedback mechanisms that affect AET are described in semi-empirical ways in otherwise physics-based hydrologic models (Beven, 2012; Lin et al., 2017). Precision of geo-spatial heterogeneity (e.g. topography, land use, soil texture, anthropogenic management practices) also has serious implications; however, their explicit effects on AET have hardly been examined. Despite using more reliable precipitation input which typically shows enhanced model performance (e.g. Fuka et al., 2014; Golden et al., 2010; Looper et al., 2012; Price et al., 2014; Strauch et al., 2012), the above-indicated factors can persistently induce wrong spatio-temporal dynamics in the simulated water balance. Traditional practice is to perform parameter calibration that supposedly encounters "all forms of uncertainty" in a model (Abbaspour et al., 2015; Daggupati et al., 2015; Her and Chaubey, 2015). However, an apparently well-calibrated model can still be a pseudo-accurate, equifinal model giving right answers for wrong reasons (Beven, 2012; Favis-Mortlock, 2004). Therefore, reliance only on the best precipitation input or a rigorous model calibration is not the panacea. In such context, it is timely to explore how to advance the representation of PET/AET such that overall consistency and predictability of a hydrologic model can also be improved.

The general objectives of this study include the source-attribution of inaccuracies in SWAT's AET simulation, and accordingly, proposing an effective solution. The

specific tasks include separately analyzing the effects of parameter equifinality, energy related weather input-uncertainty and model's physical deficiency on the prediction accuracy of AET. Ultimately, spatially-distributed direct ingestion of remotely sensed daily PET is introduced as a corrective measure towards enhancing the overall hydrologic response of the model including streamflow, root zone soil moisture and AET. The notion of ingestion (direct insertion assimilation, *DI* or "nudging") refers to the replacement of model-calculated PET with corresponding remotely sensed data at each simulation time-step. Integration of remote sensing and hydrologic modeling also requires hydroinformatics for data management purposes. Complex binary formats, large volume of data, and most importantly, inconsistency with the conventional hydrologic models in spatial resolution and geo-structure (e.g. grid versus sub-basin) have turned remote sensing application into a "big data" problem. This is likely the reason why remote sensing integrated hydrologic modeling is not yet full-fledged despite availability of data in public domain across the globe. To meet the level of interoperability required in spatially-distributed continuous hydrologic simulation, this study shows the application of a new, adaptive tool that can perform rapid extraction and processing of remotely sensed PET/AET time-series at user-defined spatial resolution.

SWAT (Arnold et al., 2012; Neitsch et al., 2011) is chosen for this study because it is a semi-distributed, physics-based, integrated hydrology-water quality model that has been extensively tested in different geographic/hydro-climatic settings (e.g. Abbaspour et al., 2015; Daggupati et al., 2016; Schuol et al., 2008; Zang et al., 2012). Considering the wide-ranging applications of SWAT on water availability, flood prediction, sediment/nutrient transport and crop yield, positive outcomes of the proposed approach would be beneficial to a large scientific community worldwide. The model is undergoing continuous development in its geo-spatial structure, with a view to represent physical characteristics of a landscape as realistically as possible (e.g. Bieger et al., 2016; Rathjens et al., 2015). A replicable way to integrate remote sensing data resources, as shown in this study, is a valuable contribution to the ongoing developments of the SWAT model.

Three US watersheds, Upper Wabash and Cedar Creek in Indiana and the Saline River in Arkansas (Figure 4.1) are selected here as the test beds. Upper Wabash watershed (18,500 km^2), because of its larger size, is suitable to capture the effects of parameter equifinality and energy related weather input-uncertainty on AET. Cedar Creek (700 km^2), is a test site for the National Soil Erosion Research Laboratory's (NSERL) environmental monitoring network, having well-maintained database on agricultural management practices and in-situ root zone soil moisture observations (Boles et al., 2015; Han et al., 2012a,b; Heathman et al., 2012). It is possible to create a robust SWAT model for Cedar Creek incorporating "known" watershed characteristics such that the model is physically realistic, hence, can be used as a reference to evaluate the effects of model's physical deficiency on AET. Both Upper Wabash and Cedar Creek watersheds are predominantly agricultural, whereas Saline River watershed (5,500 km^2) in Arkansas has a forested land use and a much drier climatic condition compared to Indiana. Therefore, directly ingesting remotely sensed PET in Cedar Creek and Saline River watersheds enables testing the efficacy of the proposed approach in two different geo-physical settings.

4.3 Related Works

There have been attempts to improve SMA (thereby, AET) via re-conceptualizing the model physics on infiltration mechanisms (e.g. Grimaldi et al., 2013; Kannan et al., 2007; Michel et al., 2005; Rajib and Merwade, 2016). These modifications cannot overcome model's physical deficiency to represent bio-geochemical cycles/vegetation growth or the uncertainties in energy related weather inputs. Mediating model SMA with remotely sensed estimates has emerged as an alternative solution in recent times. Applications of remote sensing in hydrologic modeling have long been confined on assimilating surface ("skin") moisture estimates (e.g. Alvarez-Garreton et al., 2015; Crow and Van den Berg, 2010; Parajka et al., 2006; Reichle and Koster, 2005; Renzullo et al., 2014). Depending on the model structure, using surface moisture may

have minimal effects on the simulation of total root zone soil moisture, AET and streamflow (e.g. Chen et al., 2011; Han et al., 2012). Considering such limitation, recent studies (e.g. Brocca et al., 2012; Rajib et al., 2016a; Silvestro et al., 2015) have recommended constraining models with estimate(s) that represents the entire/most part of the root zone, not necessarily using only soil moisture. Remotely sensed PET and/or AET estimates can be useful resources from these perspectives.

While there are several methods to estimate evapotranspiration (either evaporation, transpiration or both) using remotely sensed soil temperature, radiation (*albedo*), land use and vegetation indices (Bastiaanssen et al., 1998; Cleugh and Dunin, 1995; Mu et al., 2007, 2011; Nishida et al., 2003a,b; Su, 2002; Zhang et al., 2008; Zhang and Wegehenkel, 2006), use of these evapotranspiration data to improve hydrologic models is still very limited. Kunnath-Poovakka et al. (2016) applied MODIS (Moderate Resolution Imaging Spectroradiometer) AET (Guerschman et al., 2009) to calibrate the AWRA-L (Australian Water Resource Assessment – Landscape) model at daily time-step, proving AET to be more influential than surface moisture in parameter identification. Immerzeel and Droogers (2008) used SEBAL (Surface Energy Balance Algorithm for Land) monthly AET data (Bastiaanssen et al., 1998) to calibrate SWAT (Soil and Water Assessment Tool) model. Besides calibration, another approach is to assimilate remotely sensed AET into the model using techniques such as the Ensemble Kalman Filter (e.g. Pan et al., 2008; Yin et al., 2016). However, given the highly non-linear relations between the parameter(s) and respective hydrologic component(s) as well as the unknown degree of intra-parameter correlations, feeding the "extra water" (i.e. difference between modeled and remotely sensed AET, Δw) back to the water balance is not simple. Pan et al. (2008) could not show any favorable outcome after assimilating SEBS (Surface Energy Balance System) AET data (Su et al., 2005) into the Variable Infiltration Capacity (VIC) model. This is because AET in many models, including VIC and SWAT, is a non-state variable as such the assimilation effect cannot be fed back to update other hydrologic processes. Yin et al. (2016) assimilated limited amount of Landsat daily AET data into the Distributed Time Variant Gain (DTVG) model; it is viable in this

particular case because AET in DTVG model is regarded as a state-variable in terms of soil moisture recurrence relations. Which layer of the root zone would receive Δw is another pivotal factor regardless of the assimilation technique, because simulation of infiltration, surface runoff, plant uptake and soil evaporation can intrinsically depend on the vertical stratification of the soil moisture profile (e.g. SWAT; Chen et al., 2011; Rajib et al., 2016a). Hence, assimilation of AET is conceptually complex and prone to implementation error depending on model structure; in comparison, use of PET offers a universally effective solution. Direct ingestion is an appropriate method to input remotely sensed PET; several studies have previously applied this technique in a variety of models to assimilate snow cover, leaf-area index (*LAI*) and surface moisture data (e.g. Arsenault et al., 2013; Fletcher et al., 2012; Heathman et al., 2003; Meng et al., 2013; Zhang et al., 2009).

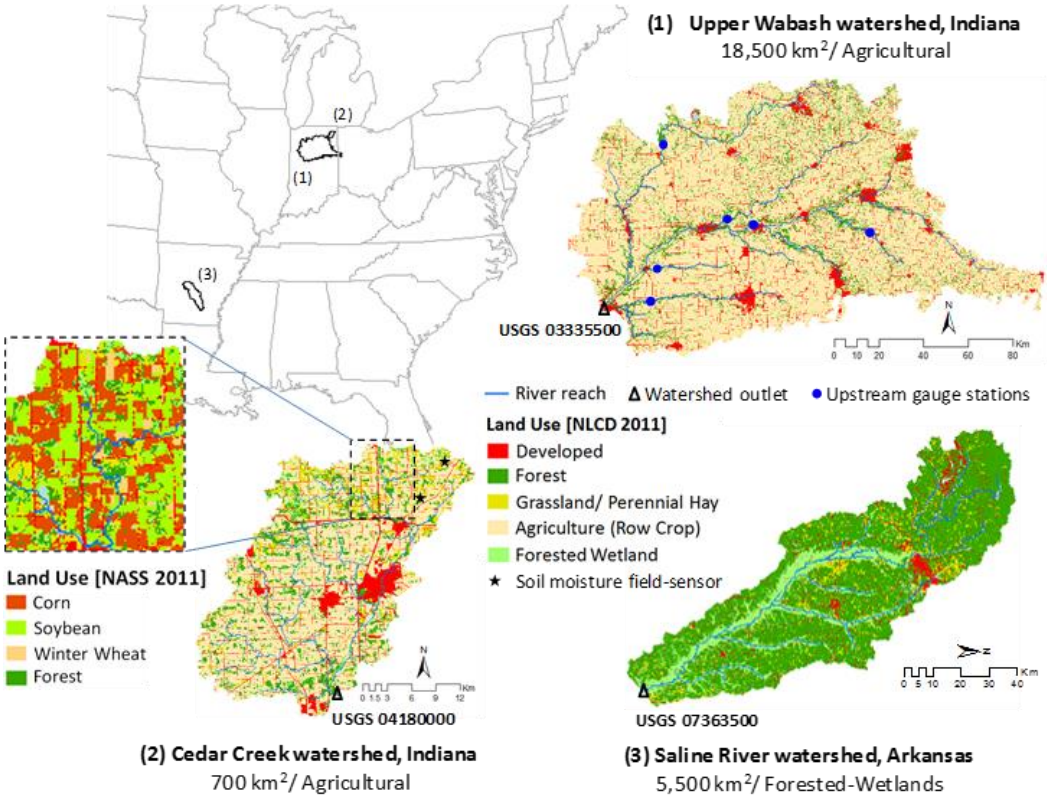

Figure 4. 1 Study watersheds with corresponding 2011 land use. Streamflow gauge stations used in model calibration are shown here. Map of Cedar Creek also shows the location for soil moisture field-sensors being used in this study.

4.4 Methodology and Data Sources

This study involves four modeling experiments (Table 4.1). SWAT model(s) under each experiment is created in the ArcSWAT GIS interface using respective topography, land use, soil texture and weather input data as listed in Table 4.2. In every case, remotely sensed AET estimate from MODIS (Mu et al., 2011, 2013) is used as the reference to evaluate the inaccuracy in SWAT simulations.

Table 4. 1 Modeling experiments with respective SWAT simulation periods

Experiment	**Assessment purpose(s)**	**Watershed(s)**	**Simulation period (years)**
1	Effect of multi-site streamflow calibration on the spatial accuracy of AET simulation	Upper Wabash	Initialization: 2005-2006 Calibration: 2007-2010
2	Effect of energy related weather input-uncertainty on simulated AET and streamflow		
3	- Level of accuracy in AET simulated by a "fully realistic" SWAT model; - cross-validation of remotely-sensed estimate	Cedar Creek [a]	Initialization: 2006-2007 Calibration: 2008-2010
4	Efficacy of directly ingesting remotely sensed PET	Cedar Creek, Saline River [b]	Saline River: Initialization: 2005-2006 Calibration: 2007-2010 Cedar Creek: Same as in (3)

[a] (3) involves creation of two configurations for the same watershed: SWAT and SWAT-Process

[b] (4) involves creation of two configurations for each watershed: SWAT and SWAT-PET.

Table 4. 2 Data used in SWAT model creation [a]

Data	Source	Spatial/temporal resolution
Digital elevation model (DEM)	National Elevation Dataset (USGS-NED, 2016)	30m b
Land use	2011 National Land Cover Database (USGS-NLCD, 2016) b	30m
Soil type/texture/class	State Soil Geographic (STATSGO) data included in SWAT 2012 database b	1:250,000
Total precipitation	National Oceanic and Atmospheric Administration, temporally interpolated by the US Department of Agriculture (USDA, 2016)	Daily; no. of gauge stations used: 23 (UW), 12 (SR), 5 (CC)
Average maximum and minimum temperature, solar radiation, wind speed, relative humidity	National Centers for Environmental Prediction - Climate Forecast System Reanalysis (NCEP-CFSR) (NCAR-RDA, 2016) c	~ 38 km x 38 km; daily; no. of grid points used: 19 (UW), 11 (SR), 2 (CC)
	Statistical weather generator (WGN) included in SWAT 2012 database (developed on the basis of Matalas, 1967; Nicks et al., 1995; Richardson and Wright, 1984) c	Daily; assigned to each sub-basin
Average streamflow	US Geological Survey (https://waterdata.usgs.gov/nwis/sw)	Daily; gauge data for selected locations (Figure 1)
Remotely sensed PET and AET	Moderate Resolution Imaging Spectroradiometer 8-day total estimates - MOD16 A2 (http://www.ntsg.umt.edu/project/mod16; Mu et al., 2011, 2013)	~ 1km, spatially re-scaled to HRU level; 8-day total estimates
Root zone soil moisture d	Permanent field-sensors of the National Soil Erosion Research Laboratory (http://amarillo.nserl.purdue.edu/ceap/; Rajib et al., 2016a)	Sensors in 5, 20, 40 and 60 cm depths at two locations (Figure 1); daily average
Agricultural management operations e	Adopted from Boles (2013) and Boles et al. (2015)	

[a] UW: Upper Wabash, SR: Saline River, CC: Cedar Creek; [b] 10m NED, 30m - 2011 National Agricultural Statistics Service – Cropland Data Layer (NASS-CDL, 2016) and 1:12,000 Soil Survey Geographic (SSURGO) database (Soil Survey Staff, 2016) are used to create the SWAT-Process configuration for CC (modeling experiment 3; Table 4.1); [c] CFSR and WGN inputs are separately used in the Upper Wabash model (modeling experiment 2; Table 4.1); [d] available only for CC; [e] used in SWAT-Process configuration for CC

A “Hybrid” PET estimate generated from MODIS (Mu et al., 2011, 2013) and the North American Land Data Assimilation System phase 2 (NLDAS-2; Rui and Mocko, 2014) is directly ingested in the Cedar Creek and Saline River watersheds. To enable compatibility with MODIS/NLDAS-2 estimates, all SWAT models being created in this study use Penman–Monteith (P-M) equation (Neitsch et al., 2011) for evapotranspiration related computations. Simulations are performed in daily time-step using Curve Number (CN) method for surface runoff and Variable Storage method for channel routing computations (Neitsch et al., 2011).

4.4.1 Spatial rescaling of MODIS data and creation of daily time-series

In this study, the original ~1 km gridded MODIS data (both PET and AET) are geo-referenced, spatially re-scaled and aggregated into each of the HRUs using an automatic python-based tool (Figure 4.2). The newly developed tool dynamically accounts for the heterogeneity in size, shape and locations of any number of HRUs within any watershed. For a given temporal extent in the form of start and end date, and geographic extent in the form of GIS shapefile, the tool assigns an area-weighted average value of 8-day total PET and AET (in mm H_20) from encompassing and/or intersecting MODIS grids onto each Hydrologic Response Units (HRUs – the spatial unit of SWAT simulation). Creating HRU-scale MODIS PET or AET data for each 8-day span in case of a watershed with 200 HRUs takes about 1.5 minutes in a Windows Intel core i7 2.4 GHz computer. The output is stored in a database that can be linked with the SWAT model by respective HRU IDs.

The same tool is applied to extract daily NLDAS-2 PET at sub-basin level due to a much coarser spatial resolution (~ 12 km). MODIS 8-day total PET for an HRU is temporally disaggregated (equation 4.1) using the daily NLDAS-2 estimate for the corresponding sub-basin where that particular HRU is actually located:

$$PET_{i(M)} = PET_{T(M)} \text{x } [\frac{PET_{i(N)}}{PET_{T(N)}}] \ldots\ldots \text{(4.1)}$$

where M and N represent values from MODIS and NLDAS-2 respectively; T refers to the total 8-day value; the index i denotes a particular day within that 8-day segment (T). NLDAS-2 PET is derived from the North American Regional Reanalysis (NARR) climate modeling, whereas MODIS is based on satellite remote sensing. Possible differences between MODIS and NLDAS-2 in the absolute values of PET might impart nominal bias in $PET_{i(M)}$. This is because the use of NLDAS-2 in equation (4.1) is limited only as a temporal scaling factor which does not alter the total amount of PET estimated by MODIS in each 8-day span ($PET_{T(M)}$). Therefore, it is justified to refer the MODIS-NLDAS hybrid estimate ($PET_{i(M)}$) simply as daily MODIS PET.

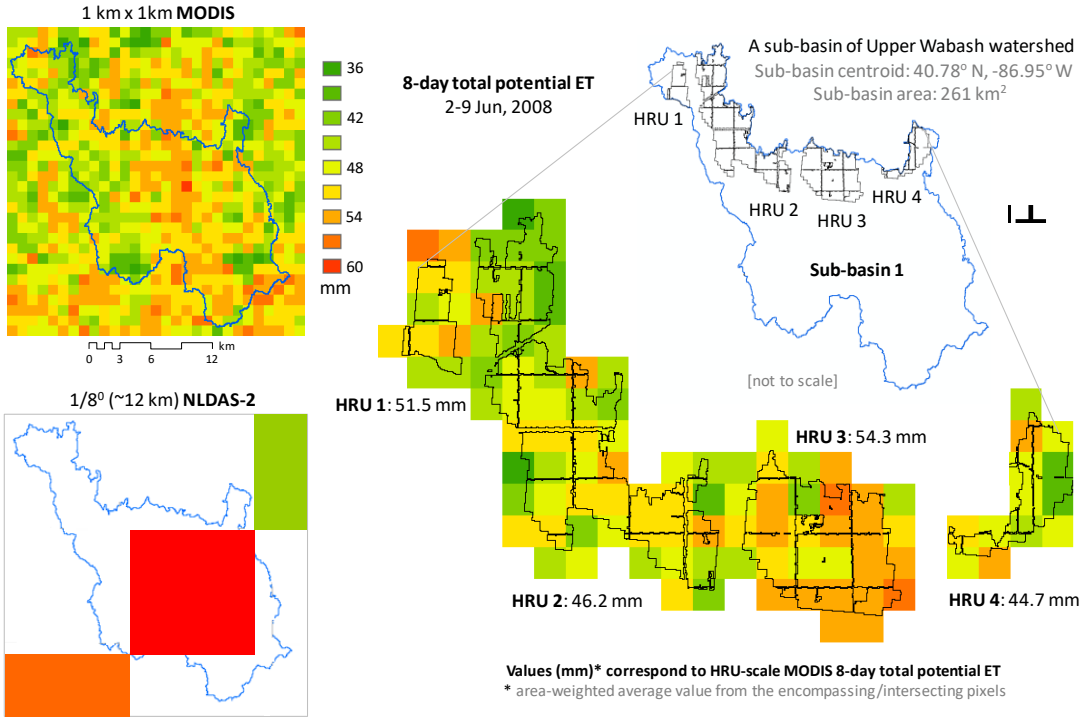

Figure 4. 2 Comparison of MODIS and NLDAS-2 8-day total PET for a sub-basin in the Upper Wabash watershed. HRU-level aggregation of gridded remote sensing estimates using an automatic data processor tool is also demonstrated here.

An older prototype version of the "processor tool" was used in evaluating the accuracy of WRF-Hydro (Lin et al., 2017), by extracting MODIS 8-day AET time-series for each of the 269 x 314 model grid-cells at 5 km resolution. Rajib et al. (2016a) also showed the application of a different version by preparing Advanced

Microwave Scanning Radiometer - Earth Observing System (AMSR-E) soil moisture time-series for sub-basin level calibration of SWAT models. Thus, the processor tool has a flexible architecture that can be universally applied to any model framework with any structure of spatial representation, which can also be improvised to interact with different sources/formats of remotely sensed data. Pertinent to such value, an important contribution of this study is the "tight-coupling" of the processor tool with a new version of SWAT source code.

4.4.2 Development of new SWAT source code

The default version of SWAT model does not allow direct ingestion of alien PET data at a user-defined spatial scale (each HRU in this case). A new sub-routine is developed in SWAT's FORTRAN source code (version 2012 - revision 629) that calls the daily MODIS PET from the newly developed python-based data processor (Figures 4.3) and directly ingests in respective HRUs. It would also allow sub-basin level ingestion of monthly total PET, especially in large scale SWAT models that are often created without HRU discretization (e.g. Abbaspour et al., 2015; Faramarzi et al., 2017). For HRUs/sub-basins where MODIS data is not available (e.g. highly urbanized areas, large water bodies), the sub-routine will reinstate SWAT's default P-M based PET (Neitsch et al., 2011). The new sub-routine is compiled with the rest of the source code to get a new executable file which is compatible both in Windows and Linux based computer operating systems, along with other supporting software services such as SWAT-CUP (Abbaspour, 2015) or high-performance cyberinfrastructures such as SWATShare (Rajib et al., 2016b). However, the simulation time for the new executable file is slightly longer relative to the default version.

As a whole, dynamic coupling of an automatic earth observation processor with the modified SWAT exemplifies a unique case of scale/space-independent, user-friendly interoperability between open-source "big data" resources and complex hydrology-water quality models. While the coupling framework is evaluated in this study in

simulation mode over a past period, the main motivation here is to serve the purpose of hydrologic forecasting once near real-time PET estimates become available (e.g. Tang et al., 2009).

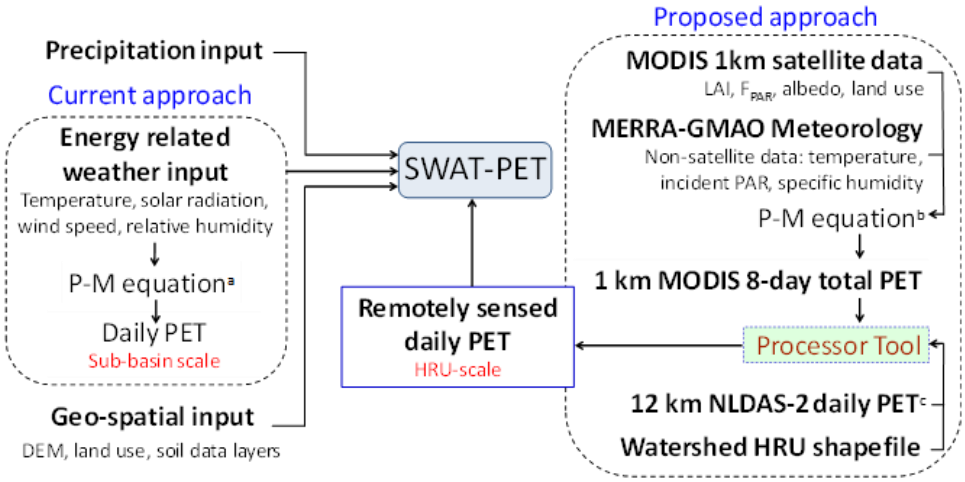

Figure 4. 3 Schematic representation of an integrated SWAT modeling framework with the option of directly ingesting MODIS PET (hereafter, SWAT-PET). Use of NLDAS-2 data is limited only to temporally disaggregate MODIS PET from 8-day total to daily estimates. The new source code for SWAT-PET executes the current approach to calculate PET in highly urbanized HRUs where MODIS data is not available. ([a]Neitsch et al., 2011; [b]Mu et al., 2011, 2013; [c]Rui and Mocko, 2014; P-M: Penman–Monteith; LAI: Leaf-Area Index; PAR: Photosynthetically Active Radiation; MERRA-GMAO: Modern Era Retrospective analysis for Research and Applications – Global Modeling and Assimilation Office)

4.4.3 Modeling experiment 1: parameter equifinality

In the first modeling experiment, effect of parameter equifinality on model simulated AET is evaluated for the Upper Wabash watershed. The Upper Wabash model is created using 30 m Digital Elevation Model (DEM), 2011 National Land Cover database (NLCD) and State Soil Geographic (STATSGO) data (Table 4.2). The model has 209 HRUs, being discretized using a 10% area aggregation threshold. Gauge records are used for precipitation forcing while the weather data related to PET calculation, specifically referred here as the "energy related weather inputs" (surface temperature, solar radiation, wind speed and relative humidity), are obtained

from Climate Forecast System Reanalysis (CFSR). Effect of parameterization is captured by separately calibrating the model first by using average daily streamflow observations only at the watershed outlet and then simultaneously at seven gauge stations across the watershed (denoted as the outlet only and multi-site calibration, respectively).

A common set of 19 parameters involving surface, subsurface, channel routing and snow-melt processes are used in the calibrations (Table 4.3). Selection of parameters and their initial ranges are based on the prior knowledge of the study area (Kumar and Merwade, 2009; Larose et al., 2007; Rajib et al., 2016a) and suggestions from the SWAT developers (Abbaspour, 2015; Neitsch et al., 2011). Calibrations are conducted by using the Sequential Uncertainty Fitting algorithm-version 2 (SUFI-2) which is a semi-automated inverse modeling procedure available inside SWAT-CUP. Kling-Gupta Efficiency (KGE) (Gupta et al., 2009; Kling et al., 2012) is used as an objective function to measure the agreement between simulated and observed data. With the addition of multiple streamflow gauge stations as objective variables, KGE is modified to a weighted mean value, KGE′ following the approach shown by Abbaspour et al. (2015):

$$KGE' = \sum_{i=1}^{n_f} w_{f_i}(KGE_{f_i}) \ldots \ldots (4.2)$$

where *n* and *w* are the number of objective variables (observational datasets) involved and the weight assigned to each of them, respectively. The index *f* stands for streamflow and *i* denotes the respective gauge stations brought under calibration. Equal weights are assigned in this study for calculating KGE′, however, the choice is subjective. For an even comparison, models are evaluated after equal number of SUFI-2 iterations. Coefficient of Determination (R^2), Percent Bias (PBIAS) and Nash-Sutcliffe Efficiency (NSE) are also calculated to evaluate the goodness of fit between observed streamflow and the best simulation having the highest objective function value (KGE or KGE′).

Table 4. 3 Parameters used in SWAT calibrations

No.	Parameter [a]	Definition [b]	Initial range
1	v_ALPHA_BF	Baseflow recession constant (days)	0.01 - 1
2	v_CANMX	Maximum canopy storage (mm H_2O)	0.01 - 25
3	v_SURLAG	Surface runoff lag coefficient (days)	0.05 - 24
4	v_CH_K2	Main channel hydraulic conductivity (mm/hr)	5 - 100
5	v_CH_N2	Main channel Manning's *n*	0.01 - 0.15
6	r_CN2	Curve number (moisture condition II)	-0.2 – 0.2
7	v_EPCO	Plant uptake compensation factor	0 - 1
8	v_ESCO	Soil evaporation compensation factor	0 - 1
9	a_GW_DELAY	Groundwater delay (days)	-10 - 10
10	v_GW_REVAP	Groundwater "revap" coefficient	0.01 - 0.2
11	v_GWQMN	Threshold depth for return flow (mm H_2O)	0.01 - 5000
12	v_REVAPMN	Re-evaporation threshold (mm H_2O)	0.01 - 500
13	r_SOL_K	Soil saturated hydraulic conductivity (mm/hr)	-0.15 – 0.15
14	r_SOL_AWC	Available soil water capacity (mm/mm)	-0.15 – 0.15
15	v_SFTMP [c]	Snowfall temperature (^oC)	0 - 5
16	v_SMFMN [c]	Melt factor for snow on December 21 (mm H_2O/ ^oC-day)	0 - 10
17	v_SMFMX [c]	Melt factor for snow on June 21 (mm H_2O/ ^oC-day)	0 - 10
18	v_SMTMP [c]	Snow melt base temperature (^oC)	-2 - 5
19	v_TIMP [c]	Snow pack temperature lag factor	0 - 1

[a] The indices shown with the parameter names denote the type of change to be applied over the existing parameter value: 'v_' means the original value is to be replaced by a value from the range, 'a_' means a value from the range is added to the original value, 'r_' means the original value is multiplied by the adjustment factor (1+ given value within the range); [b] Source: Neitsch et al. (2011); [c] Snow related parameters are not included in the calibrations of the Saline River models

4.4.4 Modeling experiment 2: energy imbalance

Inaccurate PET in the model indicates energy imbalance, which can affect AET simulation despite having the best precipitation forcing and rigorous parameter calibration process. In order to evaluate the role of energy input (i.e. PET) on model's

hydrologic responses, the second modeling experiment involves a separate setup of the Upper Wabash model using surface temperature, solar radiation, wind speed and relative humidity data from SWAT's weather generator (WGN; Neitsch et al., 2011; Table 4.2). WGN creates daily weather inputs for any watershed in the continental US from monthly average statistics summarized over a number of years (1960-2010 for this study). The WGN-based model is calibrated with the same multi-site approach as in the first modeling experiment. Since the precipitation forcing (gauge data), method to calculate PET (P-M equation) and calibration tactic are kept unaltered, differences in model outputs in this case come solely from the different sources of energy related weather inputs (i.e. CFSR versus WGN).

4.4.5 Modeling experiment 3: process uncertainty

The third modeling experiment involves creation of two configurations (SWAT and SWAT-Process) for the Cedar Creek watershed. The objective of this particular experiment is to test whether a model having the best available weather inputs, precise geo-spatial representation, anthropogenic management practices, better model physics, as well as the least-equifinal parameter set can produce AET that is near to reality. Similar to the first modeling experiment, gauged precipitation and CFSR weather inputs are used for both configurations. SWAT configuration includes 30 m DEM, NLCD land use and STATSGO soil data; whereas, SWAT-Process is built upon 10 m DEM, spatially-explicit Cropland Data Layer (CDL) and a much finer resolution Soil Survey Geographic (SSURGO) data. Most importantly, SWAT-Process configuration also incorporates agricultural management operations, being adopted from Boles (2013) and Boles et al. (2015) (Table 4.2). These management data include annual crop rotation, dates of plantation and crop harvest/kill operations, tillage and manuring practices, sub-surface (tile) drainage, as well as the timing/type/rate of fertilizer and pesticide applications. CDL and agricultural operations impart a conjugate effect, because together they enable crop-specific growth-cycles and biome-properties to be used in model simulation; otherwise, the

model would just assume some lumped conjectures giving way to inaccurate AET. While the SWAT configuration has only 217 HRUs due to the 10% area aggregation threshold being used, SWAT-Process has 10,252 HRUs (0% threshold) with no loss of spatial heterogeneity in the landscape. Another difference between these configurations lies in the model physics as the SMA in SWAT-Process follows a modified time-dependent CN method (Rajib and Merwade, 2016). SWAT configuration is calibrated only with streamfow data at the watershed outlet. SWAT-Process intends to have least equifinality through a multi-objective calibration (e.g. Rajib et al., 2016a) including streamfow data at the watershed outlet and root zone soil moisture data (~top 60 cm of the soil profile) from two permanent field-sensors (Figure 4.1). Both calibrations are performed using the same parameters and their initial ranges as in experiment 1. KGE″ (equation 4.3) is used as the objective function for the multi-objective calibration with equal weights assigned to each variable:

$$KGE'' = \sum_{i=1}^{n_f} w_{f_i}(KGE_{f_i}) + \sum_{j=1}^{n_s} w_{s_j}(KGE_{s_j}) \ldots \ldots (4.3)$$

where the indices *f* and *s* stand for streamflow and soil moisture, respectively. Also, *i* denotes the streamflow gauge stations and *j* denotes sub-basins with soil moisture estimates. Certain assumptions and pre-processing are essential to enable compatibility of sub-basin average model output and the in-situ point estimates of soil moisture. Detail on these assumptions/processing steps are discussed by Rajib et al. (2016a).

Ideally, SWAT configuration represents the default model, standard data availability scenario and modeling practice. SWAT-Process, on the other hand, leverages all the "known" watershed information which may not be available in every case. That is why a model configuration similar to SWAT-Process could not be created for Upper Wabash and Saline River. Considering that the SWAT-Process configuration for Cedar Creek is robust, physically-realistic, and hence, supposedly accurate, the simulated AET from therein can be used to cross-validate remotely sensed estimates.

4.4.6 Modeling experiment 4: ingestion of MODIS PET

The last modeling experiment involves spatially-distributed direct ingestion of daily MODIS PET estimates into each of the HRUs. Figure 4.3 schematically shows the methodology in contrast to the default/current approach of SWAT modeling. The proposed methodology is implemented for Cedar Creek and Saline River watersheds by creating two configurations for each watershed: SWAT and SWAT-PET. SWAT configuration for Saline River is created using 30 m DEM, NLCD land use and STATSGO soil data as the geo-spatial inputs, with 10% area threshold resulting into 223 HRUs; precipitation is obtained from gauge stations while other weather inputs are obtained from CFSR. SWAT configuration for Cedar Creek in the third experiment has the same source of geo-spatial/weather input data and HRU discretization scheme, which makes it suitable to be reused here. However, execution of SWAT-PET requires using the new SWAT source code (section 4.4.2). SWAT-PET models are calibrated with average daily streamflow data at respective watershed outlets enabling even comparison with the models in SWAT configuration. Model calibrations for Saline River do not include snow parameters because of its location in a warmer climate region; initial ranges for other parameters are the same as in the case of Cedar Creek (Table 4.3).

4.5 Results and Discussion

The following discussion sequentially presents the outcomes of the four modeling experiments in separate sub-sections by addressing the effects of parameter equifinality, energy related weather input-uncertainty and lack of geo-spatial representation on the possible inaccuracies in SWAT's AET simulation. These assessments rationalize the adoption of a remedial measure. Accordingly, efficacy of the new approach involving spatially-distributed direct ingestion of MODIS PET is evaluated. Differences between SWAT and MODIS in their respective evapotranspiration algorithms are also presented here. Improvement in model's

overall hydrologic responses as a result of PET ingestion are shown by comparing AET, soil moisture and streamflow outputs with corresponding reference estimates/observations.

4.5.1 Effect of parameter equifinality on actual ET

Simultaneously using multiple streamflow gauge stations in model calibration can reduce parameter equifinality with improvement in streamflow simulation (e.g. Chiang et al., 2014; Her and Chaubey, 2015), however, the consequence on model's SMA have not been explored in previous studies. Figure 4.4 shows the effect of outlet-only and multi-site calibrations on simulated streamflow for an upstream location in the Upper Wabash watershed.

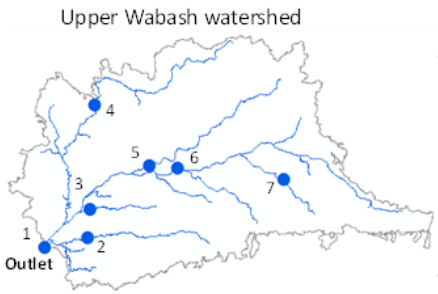

Streamflow Prediction Skills

		Outlet-only calibration				Multi-site calibration			
USGS Gauge ID		R^2	KGE	NSE	PBIAS	R^2	KGE	NSE	PBIAS
(1)	03335500	0.70	0.80	0.73	-5.5	0.67	0.75	0.65	-11
(2)	03334000	0.48	0.42	0.20	+41	0.54	0.70	0.42	+13
(3)	03329700	0.37	0.10	0.10	+45	0.51	0.44	0.24	+19
(4)	03331753	0.24	0.21	0.10	-37	0.55	0.66	0.34	-15
(5)	03328500	0.34	0.53	0.13	+23	0.30	0.53	0.14	-7
(6)	03327500	0.36	0.60	0.24	-26	0.55	0.55	0.50	+1
(7)	03324300	0.40	0.47	0.40	-25	0.56	0.42	0.50	+1.5

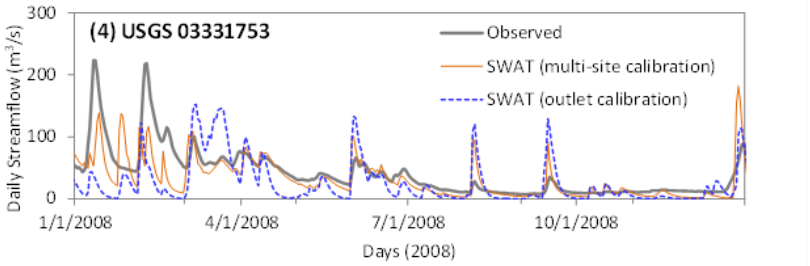

Figure 4. 4 Modeling experiment 1: comparison of outlet-only and multi-site streamflow calibration in the Upper Wabash watershed. Numbers in the watershed boundary map correspond to specific USGS gauge station IDs. Performance skills reported here represents the entire simulation periods of respective models (Table 4.1).

The multi-site calibration has invariably produced higher fit scores (R^2, KGE, NSE and PBIAS) across the watershed, especially with noticeably lower PBIAS (i.e.

increased accuracy in the water balance). Differences in the best parameter values (Table B1 in Appendix B) that have evolved from different arrangements of model calibration indicate equifinality. Because of the consistently higher accuracy in simulated streamflow regardless of the location, parameters in the multi-site calibrated model can be considered less equifinal.

Figure 4.5 shows the spatial pattern of bias in simulated AET (SWAT *minus* MODIS) in the Upper Wabash watershed, over an 8-day time period between two successive precipitation events. Despite showing very high fit scores (R^2 = 0.70, KGE = 0.80, NSE = 0.73 and PBIAS = -5.5; Figure 4.4), parameter equifinality/sub-optimality in the outlet-only calibration is still at large which makes the model produce erroneous AET. Bias larger than ±10mm (±1.25 mm/day) in the 8-day total AET in many of the sub-basins can be considered significant given the small amount of average daily precipitation the watersheds in the Midwestern US usually receives. A more rigorous streamflow calibration is found to have improved the accuracy of AET in almost all the sub-basins (bar plots in Figure 4.5), although the bias may persist in huge magnitudes. Figures 4.4 and 4.5 prove that parameter equifinality is not the main reason causing inaccurate AET simulation. The problem could be just the opposite; it might be the inaccurate AET consistently inducing inappropriate parameter values which is beyond the model's capacity to overcome via streamflow calibrations. Therefore, parameter calibration cannot be taken as the unique solution to enable better AET prediction by the model.

4.5.2 Effect of uncertainty in energy related weather inputs

Several studies have shown the differences in model outputs resulting from different methods of calculating PET (e.g. Aouissi et al., 2016; Kannan et al., 2007, Schneider et al., 2007; Wang et al., 2006), but none of these studies have examined the effect of energy related weather inputs that are the determinants of PET (and so, AET). The Upper Wabash model that uses SWAT's weather generator (WGN; Table 4.2) to obtain energy related weather inputs shows noticeably poor fit scores for streamflow,

even though the model is calibrated at multiple sites (Figure 4.6). Relying on WGN generally provides reasonable outputs where required data are discontinuous or sparsely available (Alighalehbabakhani et al., 2017; Evenson et al., 2016; Paul et al., 2017; Price et al., 2014). Accordingly, the WGN-based model for Upper Wabash, despite under-performing with R^2 = 0.56 and NSE = 0.5 in daily streamflow simulation, can be vetted acceptable based on the criteria suggested by SWAT developers (e.g. Moriasi et al., 2015). The model with CFSR data has a completely different state of optimized parameter space (Table B1 in Appendix B) with significantly higher fit scores in streamflow simulation, although precipitation forcing, watershed characteristics and calibration operation are the same as in the WGN-based model.

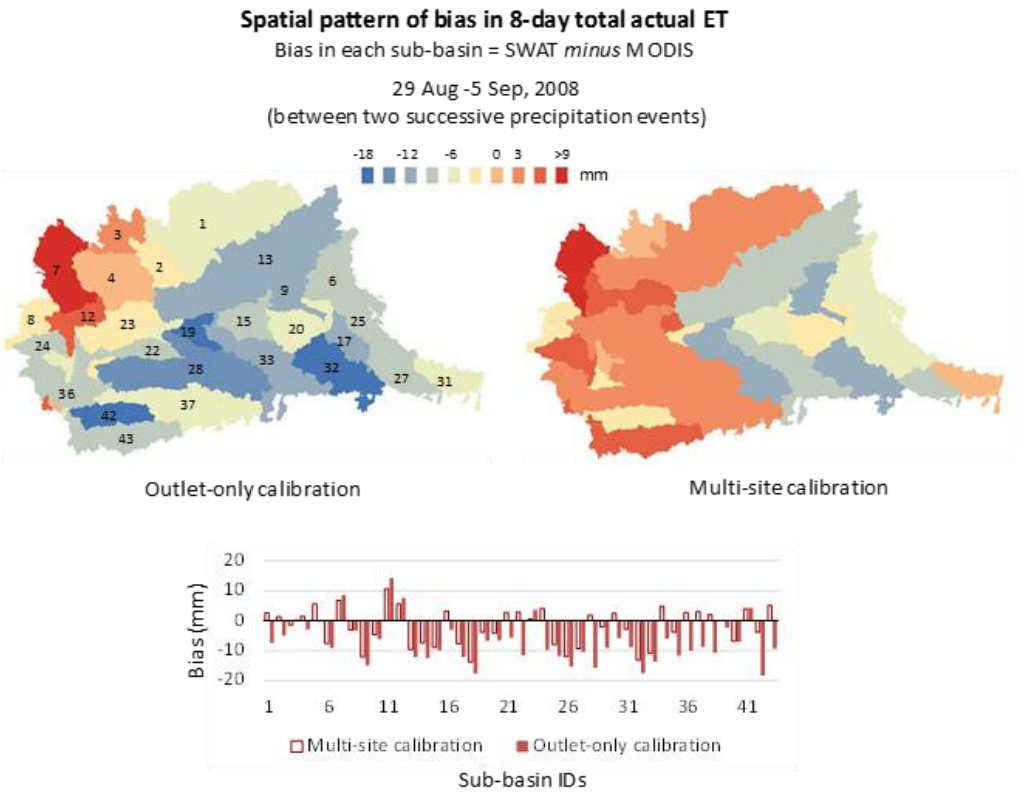

Figure 4. 5 Modeling experiment 1: effect of multi-site streamflow calibration on the spatial accuracy of simulated AET in the Upper Wabash watershed. Numbers on the watershed (top left) indicate sub-basin IDs to help relating the spatial maps with the bar diagram.

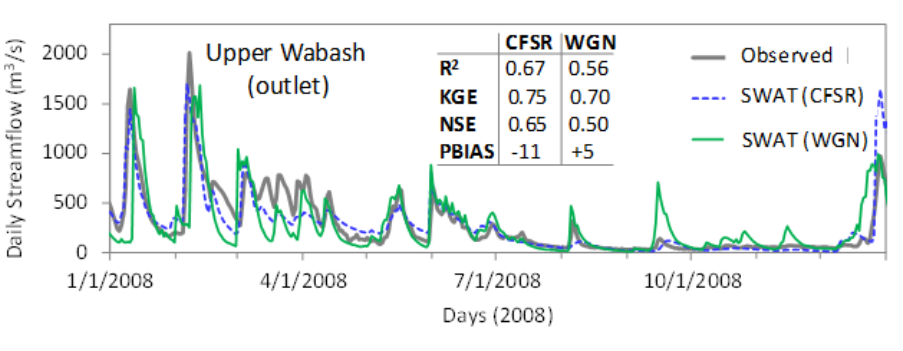

Figure 4. 6 Modeling experiment 2: effect of energy related weather input-uncertainty on streamflow simulation. CFSR and WGN refers to the SWAT model for which input of temperature, solar radiation, relative humidity and wind speed are obtained from Climate Forecast System Reanalysis and SWAT's default weather generator, respectively. Performance skills reported here represents the entire simulation periods of respective models (Table 4.1).

Figure 4.7 compares watershed-average MODIS AET in Upper Wabash with the corresponding output from both CFSR and WGN-based SWAT models over a 3-year period (2007-2009; Table 4.1). Although CFSR data is better in accuracy compared to WGN (Faramarzi et al., 2017; Fuka et al., 2014), it is not unlikely that the CFSR-based model would show high magnitude of bias in simulated AET. Assuming precipitation to be accurate, bias in AET in the CFSR-based model could be attributed to SWAT's process uncertainties. However, because of using the exact same model approximations, process uncertainties in this particular experiment have equal effects on both cases. Consequently, it must be the lesser uncertainty in energy related weather inputs (i.e. more accurate PET) that makes CFSR-based model mimic the temporal pattern of MODIS AET more closely. Temporal variability of AET in the WGN-based model is rather erratic and apparently unrealistic. Thus, results presented in Figures 4.6-4.7 shed light on an often disregarded aspect, that is, energy imbalance due to erroneous PET can significantly impact the simulation of water balance in a hydrologic model even if the model is forced with the best available precipitation or has relatively small equifinality extent in parameters.

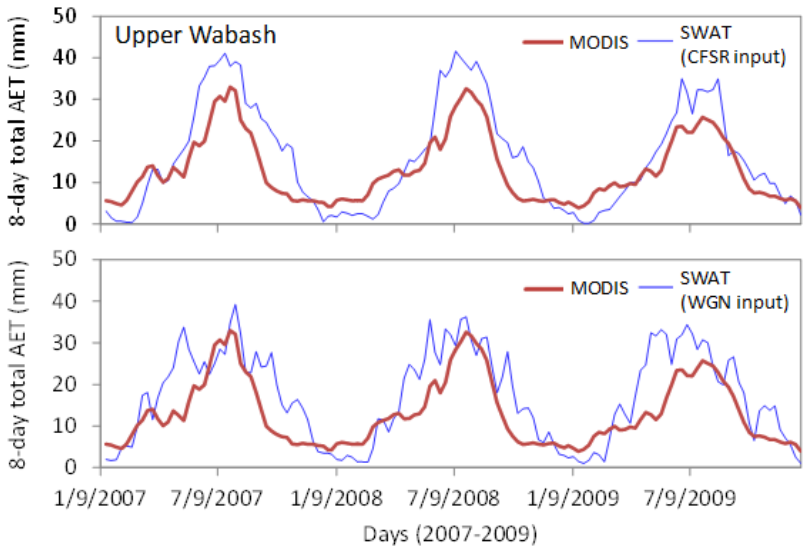

Figure 4. 7 Modeling experiment 2: effect of energy related weather input-uncertainty on AET simulation. Results indicate watershed-average values. Significance of CFSR and WGN weather input is explained in Figure 4.6.

4.5.3 Effect of geo-spatial representation in the model

A "physically realistic" model should have minimal bias in simulated AET (and other hydrologic fluxes). The notion of being physically realistic, though barely pragmatic, refers to a model that does not have any deficiency in representing actual watershed characteristics and physical processes; of course, it includes use of reliable precipitation and energy-related weather inputs in the model. A relevant key determinant is the model's bio-geochemical database (default biome properties/plant growth parameters) which is more functional if used with a detailed land use. User-specific modeling practices such as the lumping of land use/soil/slope in HRU discretization (e.g. Her et al., 2015) and multi-objective calibration (e.g. Rajib et al., 2016a) can also affect accuracy of AET. The SWAT-Process configuration for Cedar Creek is designed to have all these aspects in the model. As seen from the HRU-scale spatial map in Figure 4.8(b), the SWAT-Process model has nearly zero bias in 8-day total AET in the majority portion of the landscape, especially in the summer growing season. Its counterpart model configuration (SWAT), despite having nearly

equivalent streamflow accuracy (Figure 4.8(a)), exhibits large bias in AET (+12 mm i.e. +1.5 mm/day) during the same period of time (Figure 4.8(b)). Although Figure 4.8(b) shows one example, pattern of relative accuracy between the configurations (very high and very low, respectively in SWAT-Process and SWAT) is found to be the same in every growing season throughout the 3-year simulation period (2008-2010; Table 4.1). In the context of an agricultural watershed such as Cedar Creek, achieving minimal bias in model simulated AET is indeed significant because the land-atmosphere interaction through AET feedback and the root zone soil moisture dynamics are vibrant during the growing season, therefore, misrepresentation by the model is not unlikely. What is remarkable in this regard is that a hydrologic model like SWAT, regardless of its semi-empirical approximations on many physical processes, can "behave" realistically. Considering the degree of accuracy, simulated AET from SWAT-Process is further used in this study for HRU/sub-basin scale cross-validation of remotely sensed data. Table B1 in Appendix B lists the best parameter sets for the two configurations.

Despite its robustness, SWAT-Process could not get past through all the deficiencies in the model. Although SWAT-Process is fed with survey-based data on plant's growth cycle corresponding to the CDL land use, these inputs have effectively regulated AET simulation only where/when they are relevant (i.e. agricultural area/growing season). In the remaining portion of the landscape (e.g. forest, wetland) or the year (e.g. spring), AET from SWAT-Process may not be fully accurate. One vivid example of persistent AET bias in the SWAT-Process configuration lies with the riparian wetlands along the flood-plain (Figure 4.8(b)), where the difference (model *minus* MODIS) over an 8-day period of summer growing season is found as high as -18 mm (-2.25 mm/day). Such extensive bias is expected because the model is conceptually under-developed in representing wetland vegetation and fill-spill dynamics (Evenson et al., 2016) which control release of AET from depression areas; neither the CDL or the maximum heterogeneity of HRUs could provide any meaningful help to minimize this process deficiency in the model. Traces of similar magnitude of bias along the flood-plain wetlands are not evident in the SWAT

configuration. This is due to the 3 times coarser topography, a lumped land use and a 10% threshold of land use aggregation used is HRU discretization which have virtually removed wetlands form the landscape while reducing some computational burden.

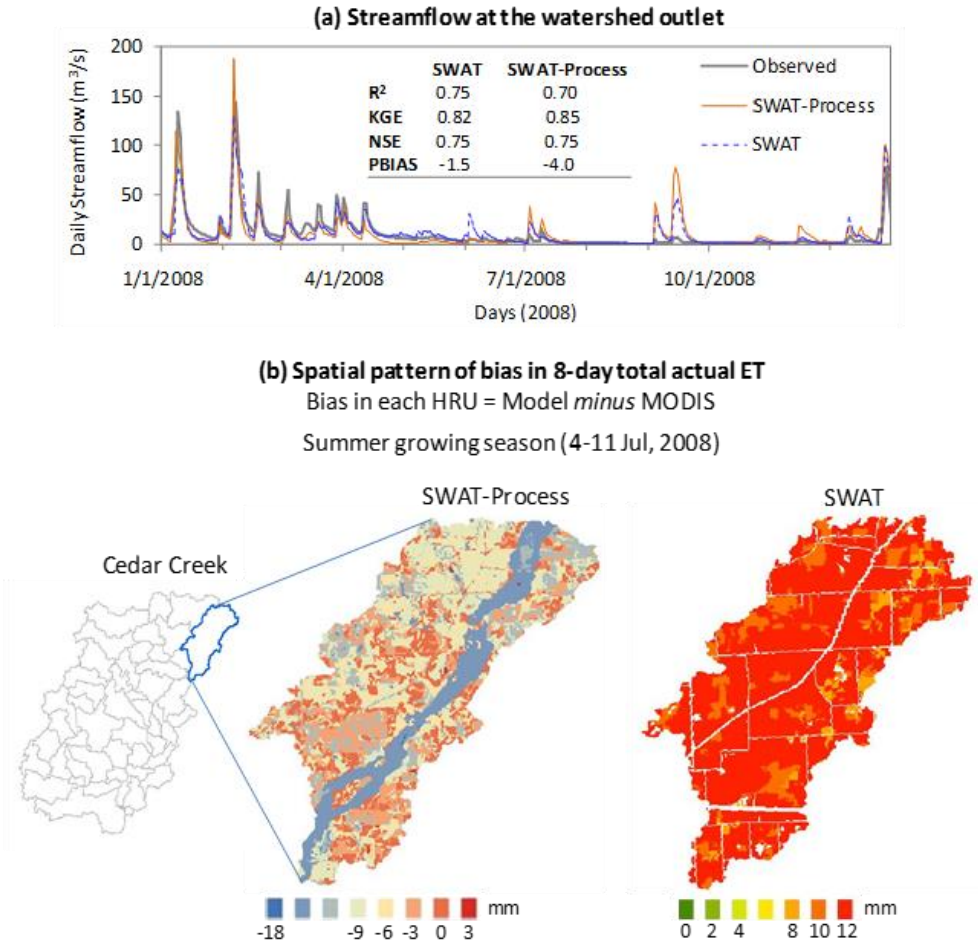

Figure 4. 8 Modeling experiment 3: performance evaluation of the default SWAT model and one of its "physically realistic" configurations (SWAT-Process). (a) Streamflow hydrographs and corresponding prediction skill metrics. Performance skills reported here represents the entire simulation periods of respective models (Table 1). (b) HRU-scale AET bias in one particular sub-basin in an 8-day period of summer growing season during 2008.

The three modeling experiments presented above prove the likelihood of getting pseudo-accurate water balance from an apparently well-calibrated model; such a model can show high streamflow prediction skills despite having severely erroneous

AET. On the positive side, overall soundness and physical consistency of the same model can be significantly improved (with some discrepancies) if that model is jointly driven with the best possible weather/geo-spatial inputs, model physics and parameters. Ironically, in this era of big data, high resolution precipitation, DEM, land use and soil inputs are still not available in the data-poor developing world. Even if they are available, using coarser DEM or lumped HRUs is not uncommon where computational resource is limited. Regardless, a major difficulty in making a realistic model remains in the proper acquisition of required "ground-truths" related to actual vegetation types and their characteristics across space and time, which play decisive role in predicting AET by mediating model physics (Long et al., 2014). Not to mention, the default bio-geochemical database even in the case of a well-developed model cannot have the perfect realization of nature let alone the semi-empirical process-approximations in so-called physics-based models. These blockades cannot be overcome by parameter calibration. Against these conceptual and practical complexities, an effective solution needs to be sought that could implicitly compensate model's inability to capture land surface processes without trading-off with the circumstantial dependency on coarse geo-spatial representation. In this regard, remotely sensed PET data as a model input might offer efficient solution by minimizing many of the uncertainties from the source.

4.5.4 Efficacy of directly ingesting remotely sensed potential ET

A closer look on the critical differences between SWAT and MODIS evapotranspiration algorithms (according to Neitsch et al. (2011) and Mu et al. (2013) respectively) would justify the causal effects of ingesting MODIS PET data towards improving hydrologic simulations. While calculating PET using the P–M equation, a major difference between SWAT and MODIS lies in the use of *albedo*. SWAT uses a constant *albedo* (= 0.23) for vegetation surface irrespective of crop/plant types to estimate net radiation; whereas, *albedo* for soil surface is a user-defined parameter (SOL_ALB) that is derived from soil database and often calibrated (e.g. Sellami et al.,

2014; Schierhorn et al., 2014). On the other hand, MODIS *albedo* (MCD43B2/B3) is a satellite product that has been evaluated for accuracy at selected locations using field estimates. SWAT also ignores *soil heat flux, G* assuming that the heat stored in soil during day time gets dissipated when temperature drops at night. To have more precision in PET, MODIS algorithm calculates *G* using a simplified version of the method proposed by Jacobsen and Hansen (1999). Canopy/surface and aerodynamic resistances in the P–M equation strongly regulates the rate at which water vapor gets released from soil, intercepted precipitation and plant tissue. Without considering the degree of spatial details in the user-defined land use, SWAT invariably assumes constant values of canopy height, h_c (= 40 cm) and *LAI* (= 4.1) to approximate these resistances for PET calculation. In comparison, resistance terms in the MODIS algorithm are calculated by applying calibrated biome-properties on the remotely sensed, time-varying 1km spatial grids of *LAI* and fraction of absorbed photosynthetically active radiation, F_{PAR} (MOD15A2; Myneni et al., 2002). All of the biome-properties, including the leaf resistance parameters (e.g. stomatal conductance, C_S) and the day/nighttime thresholds of vapor pressure deficit, *VPD* for stomata opening and closure (i.e. diurnal cycle of CO_2 fertilization), are spatially linked with a land use grid (MOD12Q1; Friedl et al., 2002) of 17 UMD (University of Maryland) classes.

Both PET and AET estimates in MODIS have the exact same representation of "observed" vegetation in their respective computations. Having detected the true state of vegetation on the ground in terms of remotely sensed LAI/F_{PAR}, MODIS algorithm calculates PET by assuming fully wet canopy and soil surface. MODIS AET is estimated for the actual fraction of wet surface for which the dry and wet surfaces are distinguished using relative humidity data (e.g. Fisher et al., 2008). In SWAT, the crudely estimated PET is taken as the maximum permissible limit to simulate evaporative demand (AET_d) separately for canopy and soil surface. AET_d depends on time-varying *LAI* and h_c that are simulated following a semi-empirical optimal leaf development curve with several user-defined biome-properties including maximum LAI for a plant, *BLAI* and maximum canopy height, h_{cmax}. SWAT also uses C_S and a

radiation-use efficiency constant, RU_e to imitate the role of *VPD* and F_{PAR} on vegetation growth (e.g. Stockle and Kiniry, 1990). Finally, AET_d is factorized by the actual amount of moisture present in different layers of the soil profile to produce AET.

Compared to SWAT's AET that relies on simulated *LAI* and root zone soil moisture, remotely sensed estimate is superior in capturing vegetation effects but less-informed about actual wetness conditions. Actually, no hydrologic model can simulate *LAI* and soil moisture with full congruence of reality, while remotely sensed PET/AET retain their value by implicitly capturing soil moisture through "observed" *LAI* (Long et al., 2014). Yet, there remains the dilemma whether such AET estimate should at all be used to mediate model's SMA via direct ingestion or other data assimilation approaches (Lin et al., 2017). Direct ingestion of MODIS PET seems to be the least-ambiguous avenue as it essentially means using a remotely sensed energy and vegetation constraint, at the same time, allowing the hydrologic model to apply its own SMA algorithm and bio-geochemical database for AET simulation.

Part of the remote sensing algorithm that depends on semi-empirical relationships to estimate PET/AET may not be too deviant from well-developed models (e.g. SWAT, VIC). From this perspective, use of h_{cmax}, C_S, *BLAI* and RU_e rather indicates a potential structural strength of the SWAT model. In fact, SWAT is equipped with a bio-geochemical database, containing biome-properties for 79 different crop/plant types, that has evolved from numerous experiments/field campaigns (e.g. Kiniry et al., 1989, 1991, 1995; Körner et al., 1979). However, depending on the available land use data for model construction, these parameters may or may not be active in AET simulation. For example, if NLCD (land use with generic classes) is used instead of CDL (spatially explicit crop/plant information), the model assumes only corn and oak trees respectively on the entire agricultural and forested landscapes. Accordingly, full functionality of the bio-geochemical database with respect to CDL might have helped SWAT-Process (Figure 4.8) to show minimal AET bias compared to the SWAT configuration. Since both PET and AET in MODIS are estimated considering the same satellite-derived radiation, land use and vegetation indices, direct ingestion of

PET time-series at each HRU of the SWAT configuration should work as a surrogate for a fully-functional bio-geochemical database despite having generic land classification (NLCD) in the model with no other exquisite geo-spatial attributes (finer resolution DEM/soil etc.). Of course, use of MODIS PET would also set a more accurate "available energy" in the model barring SWAT's crude assumptions and the probable weather uncertainties induced from limited user-inputs. Being driven by a realistic spatio-temporal distribution of PET, the model is likely to be forced to follow its pattern and better predict AET as well (e.g. Figure 4.7). Therefore, it is expected that remotely sensed PET is capable of enhancing the overall representativeness of a well-developed, semi-distributed model that has a more-or-less physics-based SMA and bio-geochemical architecture. Similarly, using this approach for a lumped model may produce limited improvements.

Figure 4.9 compares 8-day total AET simulated by the SWAT and SWAT-PET configurations with corresponding MODIS estimates for Cedar Creek and Saline River watersheds. The improved model outputs in SWAT-PET are entirely the effect of remotely sensed PET because other influential model attributes (e.g. SWAT-Process) do not exist in either of the configurations. AET from the SWAT-Process configuration (Cedar Creek) are also shown here with a two-fold objective: showing the accuracy of SWAT-PET configuration and cross-validation of MODIS algorithm. Even with the least-detailed geo-spatial inputs and the absence of a multi-objective parameter calibration, SWAT-PET in Cedar Creek closely replicates MODIS and SWAT-Process. In the case of Saline River, a configuration such as SWAT-Process cannot be created because of unavailable data. However, SWAT-PET is found to have captured a moderate-to-severe drought followed by a prolonged wet period that actually took place in the Saline River watershed during July-September, 2008 (US Drought Monitor, http://droughtmonitor.unl.edu/). These consecutive extreme events are evident from MODIS but completely misrepresented in the SWAT configuration. Overall, irrespective of the watersheds' geo-physical setting (size, location, topography, land use and soil type), ingestion of remotely sensed PET seems to produce more realistic simulation of AET.

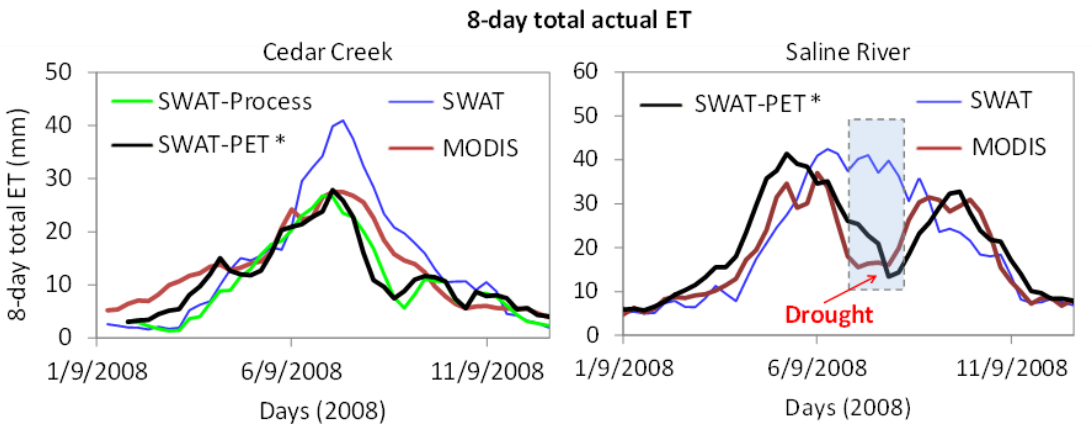

Figure 4. 9 Modeling experiment 4: effect of directly ingesting remotely sensed PET on model simulated AET (* MODIS PET is ingested/nudged in the SWAT configuration that produces SWAT-PET). Results shown here represent a subjectively chosen sub-basin within a watershed. AET simulated by the SWAT-Process (Cedar Creek) configuration is also shown here for cross-validation purposes.

As indicated earlier, MODIS AET data, like many other remote sensing product, are more of an estimation than actual observation. Although the biome-properties used in MODIS algorithm are extensively calibrated using in-situ AmeriFlux data (Mu et al., 2013), uncertainties in the calibrated data might still exist mostly because of satellite retrieval issues (Yang et al., 2006). It is also possible that the processor tool used in creating HRU-scale MODIS time-series (section 4.4.1; Figures 4.2 and 4.3) might have disturbed the spatial pattern of the actual gridded product. The fairly good correlation of AET between MODIS and SWAT-Process in Figure 4.9, both in terms of absolute values and overall temporal distribution, validates the accuracy of MODIS data while also proving the reliability of the processor tool. A pessimistic impression could arise assuming that some of the calibration sites are in close proximity to Cedar Creek and Saline River for which MODIS has the least uncertainty in these particular locations. In fact, the nearest AmeriFlux stations used in MODIS AET calibrations are approximately 200 km (Oak Openings, Ohio; latitude 41.6^{o}/longitude -83.8^{o}) and 680 km (Freeman Ranch, Texas; latitude 29.9^{o}/longitude -98.0^{o}) away from the center location of Cedar Creek and Saline River watersheds, respectively. Although the biome-property calibration has so far been conducted only over the North and South America, Mu et al. (2013) showed 85% accuracy of the current algorithm with

respect to quasi AET observations (e.g. Budyko, 1974; Donohue et al., 2007) across 232 global watersheds. Thus, use of MODIS data in SWAT modeling is expected to produce favorable results for watersheds outside the US as well.

Plant uptake and soil evaporation in SWAT are regulated by vertical stratification of root zone soil moisture using a pair of semi-empirical parameters (*esco* and *epco*; Neitsch et al., 2011). These parameters and the associated model conceptualizations do not allow consistent vertical coupling of soil moisture between adjacent soil layers (Chen et al., 2011; Rajib et al., 2016a). Accordingly, soil moisture simulated by SWAT can be closer to the wilting point in one particular layer while substantial volume can still exist in the bottom layers depending on the values of *esco* and *epco*. Since *esco* and *epco* are applied on residual PET (= PET – canopy evaporation) in their respective computations (Neitsch et al., 2011), relatively accurate PET in the SWAT-PET configuration might have indirectly influenced the model to obtain a reasonable value for these parameters (Table B2 in Appendix B). Accordingly, soil moisture profile might have become realistic while improving the plant uptake/soil evaporation and vice versa. Figure 4.10 shows the differences among the simulated (SWAT and SWAT-PET) and the in-situ daily average soil moisture (~60 cm of the root zone) throughout the year 2008, for a particular sub-basin of Cedar Creek where the permanent soil moisture sensors are located (Figure 4.1 shows the sensor locations). In order to correlate how increased accuracy in AET as a result of PET ingestion might have improved soil moisture, Figure 4.10 also draws an analogy of biases. For example, SWAT generally underestimates AET and overestimates soil moisture before the start of summer growing season (e.g. March). In the peak of growing season (e.g. July), SWAT severely overestimates AET which gets reflected into drastic depletion of soil moisture from the upper layers. In the SWAT-PET configuration, model's tendency to show such "conditional bias" is nearly eliminated as both the soil moisture and AET outputs match better with the corresponding reference estimates. Increased accuracy of two hydrologic components (soil moisture and AET), being evaluated against two completely independent sources of observations/reference estimates (i.e. field sensor and satellite), attests the worth of

the proposed approach towards improving overall soundness and predictability of the model.

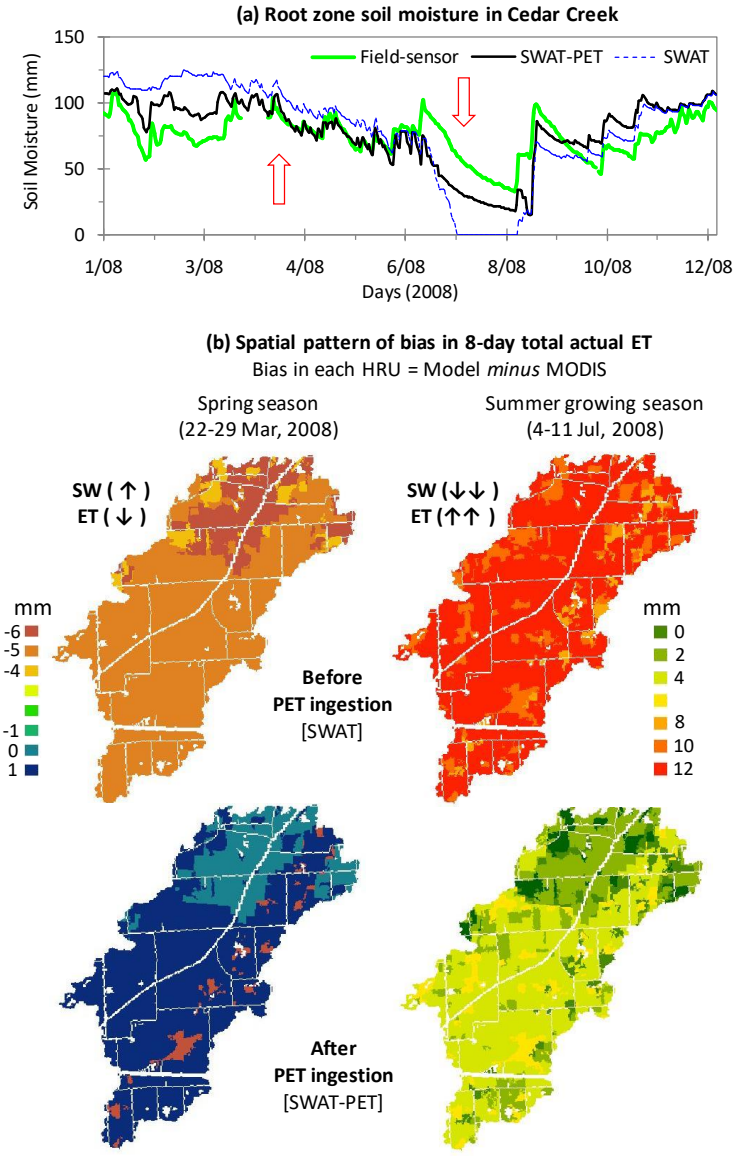

Figure 4. 10 Modeling experiment 4: (a) comparison of simulated root zone soil moisture (~ 60 cm) in the SWAT and SWAT-PET configurations with field sensor estimates, for the sub-basin where sensors are located (Figure 1). Moisture values reported here represent Plant Available Water (water content above the wilting point), being averaged for the two sensors. (b) Spatial maps of AET bias in the same sub-basin before/after PET ingestion. The "before-ingestion" (SWAT configuration) map for the summer season is replicated from Figure 8. (↑ indicates overestimation and ↑↑ indicates very high overestimation by the model while ↓ and ↓↓ indicate the opposite).

The effect of directly ingesting remotely sensed PET in simulated streamflow is demonstrated in Figure 4.11. SWAT-PET has comparatively higher fitness scores for streamflow in both Cedar Creek and Saline River watersheds. Especially, simulation of high-flow events is noticeably better in the SWAT-PET configuration irrespective of the watershed. Poor performance in the low-flow conditions is apparent in some cases which contradicts the general expectation that a better AET (and soil moisture) simulation by the SWAT-PET configuration should ideally produce relatively accurate baseflow. This leads to the likelihood that sub-optimal sub-surface parameters can persist despite the improvements shown in Figures 4.9 and 4.10. This is because SWAT's sub-surface parameters, even after ingesting remotely sensed PET, might remain insensitive to streamflow calibration. Although such limitation could be specific to SWAT, putting AET along with streamflow in a multi-objective calibration can render a more robust solution irrespective of the model being used (e.g. Kunnath-Poovakka et al., 2016). Specifically, a simultaneous ingestion-calibration approach using remotely sensed PET as the energy forcing and AET as the objective variable in parameter optimization should be explored in future studies.

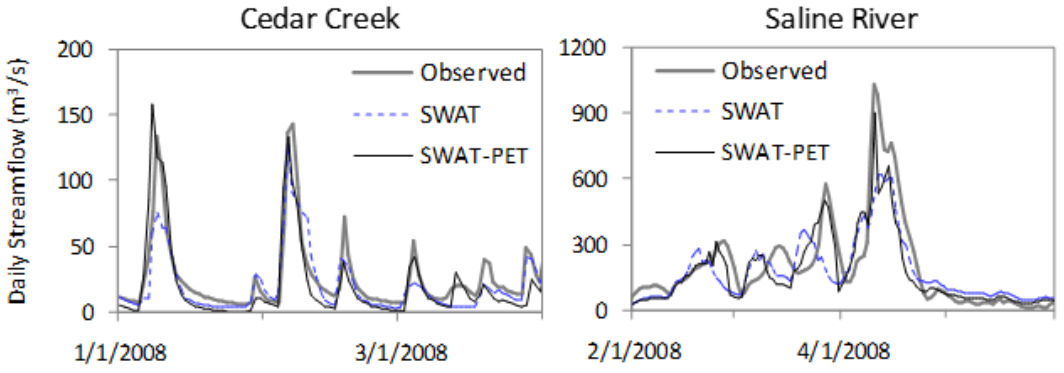

	SWAT	SWAT-PET
R^2	0.75	0.78
KGE	0.82	0.85
NSE	0.75	0.81
PBIAS	-1.5	+0.5

	SWAT	SWAT-PET
R^2	0.67	0.70
KGE	0.76	0.77
NSE	0.66	0.71
PBIAS	+3.5	+3.0

Figure 4. 11 Modeling experiment 4: effect of directly ingesting remotely sensed PET on model simulated streamflow. Performance skills reported here represents the entire simulation periods of respective models (Table 4.1).

4.6 Conclusion

This study features a two-fold aspect: first identifying the effects of parameter equifinality, energy related weather input-uncertainty and lack of geo-spatial representation on the simulation of actual evapotranspiration (AET), and then evaluating a remedial solution by directly ingesting daily MODIS potential evapotranspiration (PET). To accomplish these objectives, four modeling experiments are conducted using SWAT. In every experiment, 8-day total AET from MODIS and daily streamflow from USGS gauge stations are used as references to measure the degree of model accuracy, while one of the experiments also includes in-situ root zone soil moisture enabling a holistic assessment. Based on the outcome of these experiments, following conclusions can be drawn.

1. Inaccurate AET in a hydrologic model is not a parametric issue. Comparison of a single-site and multi-site streamflow calibration in a watershed proves the inability of rigorous parameter optimization to eliminate inaccuracy from simulated AET output, although some improvements might be possible.
2. Inaccurate PET in the model, due to the uncertainties in energy related weather inputs, significantly affects AET and streamflow even if the model is forced with the best available precipitation data and has relatively less parameter equifinality. This finding sheds light on an often disregarded aspect, that is, energy balance is as crucial as ensuring realistic water balance to achieve accurate prediction from a hydrologic model.
3. In the absence of detailed geo-spatial/process representation, results suggest the likelihood of a pseudo-accurate model that invariably shows high streamflow prediction skills despite having severely erroneous spatio-temporal dynamics of AET.
4. The new SWAT configuration, developed to allow direct ingestion of MODIS PET at each HRU (hereafter, SWAT-PET), shows increased accuracy in the simulation of root zone soil moisture, AET and streamflow. As an additional reference, a “physically realistic” SWAT setup is created incorporating high

resolution DEM and soil texture, detailed land use and crop-specific agricultural operations, better runoff estimation method, as well as a multi-objective calibration protocol with both streamflow and soil moisture. MODIS and SWAT-PET are cross-validated against this reference model, showing noticeably good agreements in AET for both cases. Where such a reference model cannot be created due to unavailable data, temporal variability of AET from the SWAT-PET model is found to have detected specific drought and wet periods as reported in the national database.

An alternative that could have been considered is to use remotely sensed AET instead of PET. However, that approach would be questionable if AET in the particular hydrologic model is not designated as a state variable. Since both PET and AET in MODIS have the exact same representation of LAI/F_{PAR} in their respective retrieval algorithms (only difference is how the wetness condition is approximated), the PET estimate is an equally capable surrogate as AET for conveying actual vegetation effects into a hydrologic model. Thus, spatially distributed direct ingestion of MODIS PET is the least-ambiguous, universally-applicable solution as it essentially means using a remotely sensed energy and vegetation constraint while allowing the model to apply its built-in SMA algorithm for AET simulation. Such data-model fusion is quite effective because the semi-empirical approximations used in the current generation land surface/ hydrologic models (e.g., SWAT, VIC) to estimate PET/AET are quite similar to those used in the remote sensing algorithms.

With the availability of real-time remotely sensed PET in near future, the proposed approach would help increasing the accuracy of hydrologic forecasting. Pertinent to the usefulness of the proposed approach for data-poor regions of the globe, a noteworthy factor is that SWAT-PET produces improved results despite having static/lumped land classification (e.g. NLCD) with no other exquisite geo-spatial attributes (e.g. finer resolution DEM, soil or the best quality solar radiation, humidity, wind speed data). This has significant implications even for the data-rich regions where modeling is often done using coarse geo-spatial inputs trading-off the prediction accuracy with available computational resource.

CHAPTER 5. SYNTHESIS

This dissertation resonates Klemes (1986) who wrote: "*For a good mathematical model it is not enough to work well. It must work well for the right reasons. It must reflect, even if only in a simplified form, the essential features of the physical prototype*". Because of its regulatory role on how closely a hydrologic model would reflect physical processes, Soil Moisture Accounting (SMA) needs considerable attention. Against all the circumstantial uncertainties associated with hydrologic modeling, a sound physically consistent SMA would supposedly enable better prediction.

5.1 Parameter Uncertainty

Traditional practice is to perform parameter calibration that supposedly encounters "all forms of uncertainty" in a model and provides "acceptable" outputs. However, several parameter combinations are possible for the same model that can produce equally reasonable results (equifinality). Not to mention, simulation of surface and sub-surface fluxes in a hydrologic model is strongly affected by the choice of objective variables used in calibration and the resultant parameter values adopted from therein. Therefore, the traditional approach of model calibration using observed streamflow data only at discrete locations might produce a model where several components of the watershed's hydrologic system remain virtually uncalibrated, consequently leading towards imprecise SMA and inaccurate predictions. The proposed approach of using remotely sensed surface moisture estimates in sub-basin/HRU level together with observed streamflow data at the watershed's outlet for model calibration could not noticeably effect streamflow and deeper layer moisture content. An extension of this approach to apply root zone soil moisture estimates from limited field sensor data showed considerable improvement of simulation for those cases. Difference in relative sensitivity of parameters and reduced extent of

uncertainty are also evident from the proposed method, especially for parameters related to the subsurface hydrologic processes.

5.2 Process Uncertainty

The process of rainfall-runoff partitioning in the continuous simulation structure of hydrologic models directly influences estimation of root zone soil moisture and vice versa. Effectively relating actual state of soil wetness condition with the infiltration mechanism can potentially increase the accuracy of SMA. From this perspective, a time-dependent, SMA based Curve Number method (SMA_CN) is incorporated within the existing structure of the Soil and Water Assessment Tool (SWAT). The main argument here is that CN method, though formulated for event-based cumulative rainfall-runoff simulation, should be modified for a continuous model such that it is valid not only at the end of a storm but also at any instant during the storm. At the same time, the fraction of rainfall to be converted into runoff should be directly proportional to the existing moisture store level. Based on daily simulation for a past period, rising and falling limbs of streamflow hydrographs simulated using the SMA_CN method tend to match with those of the observed data, thereby validating that the newly configured SMA-based SWAT model can more accurately capture watershed behavior in response to rainfall dynamics. The SMA-based model is also found to produce soil moisture that is closer to observations compared to the soil moisture estimates from the original model. These attributes have important implications for sub-daily hydrologic forecasting. Improved runoff mechanism such as SMA_CN can still be influenced by the uncertainties in other hydrologic processes. Hence, re-conceptualizing model physics is not the panacea; it can only address part of a bigger problem.

5.3 Input Uncertainty

While better parameterization or model physics can enable a relatively accurate state of water balance, energy balance in a hydrologic model is often disregarded even though it has considerable influence on SMA via evapotranspiration. Precipitation input is the "supply of water" from atmosphere to the land surface, whereas, potential evapotranspiration (PET) is an index of "available energy" required by the model to drive the water back to the atmosphere. Inaccuracy in calculated PET induced from relevant weather inputs propagates into the simulation of actual evapotranspiration (AET) and other hydrologic processes. Moreover, lack of precision in capturing geo-spatial heterogeneity (e.g. topography, land use, soil texture, vegetation, anthropogenic management practices) also have serious implications. Despite using more reliable precipitation input which typically shows enhanced model performance, the above-indicated factors can persistently induce wrong spatio-temporal dynamics in the simulated AET (and hence, SMA). Some of this issues are rather practical than scientific, hence, these may not be avoided. In such context, spatially distributed direct ingestion of remotely sensed PET is found to provide a holistic solution. While the proposed approach is evaluated for a past period, the main motivation here is to serve the purpose of hydrologic forecasting once near real-time PET estimates become available.

5.4 Future Work

Although results from this dissertation are promising, application of the proposed approaches to address more science-based and practice-oriented questions would establish their functionality. Fully distributed spatial calibration of a large scale high resolution model using remotely sensed actual evapotranspiration would justify the use of multi-objective, intensive calibration protocol in an operational flood prediction system. Direct ingestion of remotely sensed potential evapotranspiration to

see the relative change in wetland hydrologic responses and associated effects on fill-spill volume could be another avenue to explore. Benefits of using the SMA-based CN method in near real-time 3 or 6-hourly flood forecasting also needs thorough evaluation. The enhanced prediction skills and reduced uncertainty of the SWAT model as shown in this dissertation can also contribute in studies related to sediment and nutrient transport, crop yield, as well as climate and land use impact assessments.

LIST OF REFERENCES

LIST OF REFERENCES

Abbaspour, K.C., 2015. SWAT-CUP 2012: SWAT calibration and uncertainty programs - a user manual. Available online at: http://swat.tamu.edu/software/swat-cup/

Abbaspour, K.C., Rouholahnejad, E., Vaghefi, S., Srinivasan, R., Yang, H., Kløve, B., 2015. A Continental-Scale Hydrology and Water Quality Model for Europe: Calibration and uncertainty of a high-resolution large-scale SWAT model. J. Hydrol. 524, 733–752. doi:10.1016/j.jhydrol.2015.03.027

Alighalehbabakhani, F., Miller, C. J., Selegean, J.P., Barkach, J., Abkenar, S.M.S., Dahl, T., Baskaran, M., 2017. Estimates of sediment trapping rates for two reservoirs in the Lake Erie watershed: Past and present scenarios. J. Hydrol. 544, 147–155.

Alvarez-Garreton, C., Ryu, D., Western, a. W., Su, C.-H., Crow, W.T., Robertson, D.E., Leahy, C., 2015. Improving operational flood ensemble prediction by the assimilation of satellite soil moisture: comparison between lumped and semi-distributed schemes. Hydrol. Earth Syst. Sci. 19, 1659–1676. doi:10.5194/hess-19-1659-2015

Aouissi, J., Benabdallah, S., Chabaâne, Z.L., Cudennec, C., 2016. Evaluation of potential evapotranspiration assessment methods for hydrological modelling with SWAT—Application in data-scarce rural Tunisia. Agricultural Water Management 174, 39-51.

Arnold, J., Moriasi, D., Gassman, P., Abbaspour, K., White, M., Srinivasan, R., Santhi, C., Harmel, R.D., Griensven, A. Van, 2012. SWAT: model use, calibration, and validation. Trans. ASABE 55, 1491–1508.

Arsenault, K.R., Houser, P.R., De Lannoy, G.J.M., Dirmeyer, P.A., 2013. Impacts of snow cover fraction data assimilation on modeled energy and moisture budgets. J Geophys Res.-Atmos. 118, 7489-7504.

Bastiaanssen, W.G.M., Menenti, M., Feddes, R.A., Holtslag, A.A.M., 1998. Remote sensing surface energy balance algorithm for land (SEBAL): 1. Formulation. J. Hydrol. 212-213(1-4), 198-212.

Bekele, E.G., Nicklow, J.W., 2007. Multi-objective automatic calibration of SWAT using NSGA-II. J. Hydrol. 341, 165–176. doi:10.1016/j.jhydrol.2007.05.014

Beven, K., 1993. Prophecy, reality and uncertainty in distributed hydrological modelling. Adv. Water Resour. 16, 41–51. doi:10.1016/0309-1708(93)90028-E

Beven, K., 2012. Rainfall-runoff modelling: The primer. 2nd edition, John Wiley & Sons Ltd, ISBN 978-0-470-71459-1.

Bieger, K., Arnold, J.G., Rathjens, H., White, M.J., Bosch, D.D., Allen, P.M., Volk, M., Srinivasan, R., 2017. Introduction to SWAT+, a completely restructured version of the Soil and Water Assessment Tool. Journal of the American Water Resources Association 53(1), 115-130. doi: 10.1111/1752-1688.12482

Boles, C.M.W., 2013. SWAT model simulation of bioenergy crop impacts in a tile-drained watershed. Open access theses, paper 23, Purdue University. Available

online at: http://docs.lib.purdue.edu/cgi/viewcontent.cgi?article=1022&context=open_access_theses (last cited on February 18, 2017)

Boles, C.M.W., Frankenberger, J.R., Moriasi, D., 2015. Tile drainage simulation in SWAT 2012: Parameterization and evaluation in an Indiana watershed. Trans. ASABE 58(5), 1201–1213. doi: 10.13031/trans.58.10589

Brocca, L., Moramarco, T., Melone, F., Wagner, W., Hasenauer, S., Hahn, S., 2012. Assimilation of surface- and root-zone ASCAT soil moisture products into rainfall-runoff modeling. IEEE Trans. Geosci. Remote Sens. 50, 2542–2555. doi:10.1109/TGRS.2011.2177468

Budyko, M.I., 1974. Climate and Life. Academic Press, p. 508.

Chen, F., Crow, W.T., Starks, P.J., Moriasi, D.N., 2011. Improving hydrologic predictions of a catchment model via assimilation of surface soil moisture. Adv. Water Resour. 34, 526–536. doi:10.1016/j.advwatres.2011.01.011

Cleugh, H.A., Dunin, F.X., 1995. Modelling sensible heat fluxes from a wheat canopy: an evaluation of the resistance energy balance method. Journal of Hydrology 164, 127–152.

Chiang, L.C., Yuan, Y., Mehaffey, M., Jackson, M., Chaubey, I., 2014. Assessing SWAT's performance in the Kaskaskia River watershed as influenced by the number of calibration stations used. Hydrol. Process. 28, 676–687. doi:10.1002/hyp.9589

Crow, W.T., Van den Berg, M., 2010. An improved approach for estimating observation and model error parameters in soil moisture data assimilation. Water Resour. Res. 46 (12). doi: DOI: 10.1029/2010WR009402

Daggupati, P., Pai, N., Ale, S., Douglas-Mankin, K. R., Zeckoski, R. W., Jeong, J., Parajuli, P. B., Saraswat, D., Youssef, M. A., 2015. A recommended calibration and validation strategy for hydrologic and water quality models. Trans. ASABE, 58(6), 1705-1719.

Daggupati, P., Deb, D., Srinivasan, R., Yeganantham, D., Mehta, V. M., Rosenberg, N.J., 2016. Large-scale fine-resolution hydrological modeling using parameter regionalization in the Missouri River Basin. Journal of the American Water Resources Association, 52(3), 648-666. doi: 10.1111/1752-1688.12413

Donohue, R.J., Roderick, M.L., McVicar, T.R., 2007. On the importance of including vegetation dynamics in Budyko's hydrological model. Hydrol. Earth Syst. Sc. 11, 983−995.

Evenson, G., Golden, H.E., Lane, C.R., D'Amico, E., 2016. An improved representation of geographically isolated wetlands in a watershed-scale hydrologic model. Hydrological Processes 30(22), 4168-4184.

Faramarzi, M., Abbaspour, K.C., Adamowicz, W.L., Lu, W., Fennel, J., Zehnder, A.J.B., Goss, G.G., 2017. Uncertainty based assessment of dynamic freshwater scarcity in semi-arid watersheds of Alberta, Canada. J. Hydrol.: Regional Studies 9, 48-68.

Favis-Mortlock, D., 2004. Self-organization and cellular automata models. In Wainright and Muuligan (Eds.), Environmental Modelling: Finding simplicity in complexity. John Wiley & Sons Ltd, ISBN 10-0-471-49618-9.

Fletcher, S.J., Liston, G.E., Hiemstra, C.A., Miller, S.D., 2012. Assimilating modis and AMSR-E snow observations in a snow evolution model. J Hydrometeorol 13, 1475-1492.

Friedl, M.A., McIver, D.K., Hodges, J.C.F., Zhang, X.Y., Muchoney, D., Strahler, A.H. et al., 2002. Global land cover mapping from MODIS: Algorithms and early results. Remote Sensing of Environment 83(1–2), 287−302.

Fuka, D.R., Walter, M.T., Macalister, C., Degaetano, A.T., Steenhuis, T.S., Easton, Z.M., 2014. Using the Climate Forecast System Reanalysis as weather input data for watershed models. Hydrol. Process. 28, 5613–5623. doi:10.1002/hyp.10073

Golden, H., Knightes, C., Conrads, P., Davis, G., Feaster, T., Journey, C., Benedict, S., Brigham, M., Bradley, P., 2012. Characterizing mercury concentrations and fluxes in a Coastal Plain watershed: insights from dynamic modeling and data. Journal of Geophysical Research 117, G01006. doi: 10.1029/2011JG001806

Grimaldi, S., Petroselli, A., Romano, N., 2013. Green-Ampt Curve-Number mixed procedure as an empirical tool for rainfall–runoff modelling in small and ungauged basins. Hydrol. Process. 27, 1253-1264.

Guerschman, J.P., van Dijk, A.I.J.M., Mattersdorf, G., Beringer, J., Hutley, L.B., Leuning, R., Pipunic, R.C., Sherman, B.S., 2009**.** Scaling of potential evapotranspiration with MODIS data reproduces flux observations and catchment water balance observations across Australia. J. Hydrol. 369 (1–2), 107–119.

Gupta, H. V., Kling, H., Yilmaz, K.K., Martinez, G.F., 2009. Decomposition of the mean squared error and NSE performance criteria: Implications for improving hydrological modelling. J. Hydrol. 377, 80–91. doi:10.1016/j.jhydrol.2009.08.003

Han, E., Merwade, V., Heathman, G.C., 2012a. Application of data assimilation with the Root Zone Water Quality Model for soil moisture profile estimation in the upper Cedar Creek, Indiana. Hydrol. Process. 26, 1707–1719. doi:10.1002/hyp.8292

Han, E., Merwade, V., Heathman, G.C., 2012b. Application of data assimilation with the Root Zone Water Quality Model for soil moisture profile estimation in the upper Cedar Creek, Indiana. Hydrol. Process. 26, 1707–1719. doi:10.1002/hyp.8292

Her, Y., Chaubey, I., 2015. Impact of the numbers of observations and calibration parameters on equifinality, model performance, and output and parameter uncertainty. Hydrol. Process. 29, 4220–4237. doi:10.1002/hyp.10487

Her, Y., Frankenberger, J., Chaubey, I., Srinivasan, R., 2015. Threshold effects in HRU definition of the Soil and Water Assessment Tool. Trans. ASABE, 58(2), 367-378. doi: 10.13031/trans.58.10805

Heathman, G.C., Starks, P.J., Ahuja, L.R., Jackson, T.J., 2003. Assimilation of surface soil moisture to estimate profile soil water content. Journal of Hydrology 279, 1-17.

Heathman, G.C., Cosh, M.H., Merwade, V., Han, E., 2012. Multi-scale temporal stability analysis of surface and subsurface soil moisture within the Upper Cedar Creek Watershed, Indiana. Catena 95, 91–103. doi:10.1016/j.catena.2012.03.008

Immerzeel, W.W., Droogers, P., 2008. Calibration of a distributed hydrological model based on satellite evapotranspiration. J. Hydrol. 349, 411–424. doi:10.1016/j.jhydrol.2007.11.017

Jacobsen, A., Hansen, B.U., 1999. Estimation of the soil heat fux/ net radiation ratio based on spectral vegetation indexes in high-latitude Arctic areas. Int. J. Remote Sensing 20(2), 445-461.

Kannan, N., Santhi, C., Williams, J.R., Arnold, J.G., 2008. Development of a continuous soil moisture accounting procedure for curve number methodology and its behaviour with different evapotranspiration methods. Hydrological Processes 22, 2114–2121.

Kling, H., Fuchs, M., Paulin, M., 2012. Runoff conditions in the upper Danube basin under an ensemble of climate change scenarios. J. Hydrol. 424-425, 264–277. doi:10.1016/j.jhydrol.2012.01.011

Kiniry, J.R., Jones, C.A., O'Toole, J.C., Blanchet, R., Cabelguenne, M., Spanel, D.A., 1989. Radiation-use efficiency in biomass accumulation prior to grain-filling for five grain-crop species. Field Crops Research 20, 51-64.

Kiniry, J.R., Rosenthal, W.D., Jackson, B.S., Hoogenboom, G., 1991. Chapter 5: Predicting leaf development of crop plants. In Hodges (ed.), Predicted crop phenology. CRC Press, Boca Raton, FL.

Kiniry, J.R., Major, D.J., Izaurralde, R.C., Williams, J.R., Gassman, P.W., Morrison, M., Bergentine, R., Zentner, R.P., 1995. EPIC model parameters for cereal, oilseed, and forage crops in the northern Great Plains region. Can. J. Plant Sci. 75, 679-688.

Körner, Ch., Scheel, J.A., Bauer, H., 1979. Maximum leaf diffusive conductance in vascular plants. Photosynthetica 13:45-82.

Kumar, S., Merwade, V., 2009. Impact of watershed subdivision and soil data resolution on SWAT model calibration and parameter uncertainty. J. Am. Water Resour. Assoc. 45, 1179–1196.

Kunnath-Poovakka, A., Ryu, D., Renzullo, L.Z., George, B., 2016. The efficacy of calibrating hydrologic model using remotely sensed evapotranspiration and soil moisture for streamflow prediction. J. Hydrol. 535, 509-524.

Larose, M., Heathman, G.C., Norton, L.D., Engel, B., 2007. Hydrologic and atrazine simulation of the Cedar Creek Watershed using the SWAT model. J. Environ. Qual. 36, 521–31. doi:10.2134/jeq2006.0154

Lin, P., Rajib, M.A., Somos-Valenzuela, M.A., Yang, Z.L., Merwade, V., Maidment, D.R., Wang, Y., Chen, L., 2017. Spatio-temporal evaluation of simulated evapotranspiration and streamflow over Texas in a WRF-Hydro-RAPID

modeling framework. Journal of the American Water Resources Association. [in press]

Long, D., Longuevergne, L., Scanlon, B.R., 2014. Uncertainty in evapotranspiration from land surface modeling, remote sensing, and GRACE satellites. Water Resour. Res. 50, 1131-1151. doi:10.1002/2013WR014581

Looper, J., Vieux, B., Moreno, M., 2012. Assessing the impacts of precipitation bias on distributed hydrologic model calibration and prediction accuracy. Journal of Hydrology 418, 110–122.

Matalas, N.C., 1967. Mathematical assessment of synthetic hydrology. Water Resources Res. 3(4), 937-945.

Meng, C.L., Zhang, C.L., Tang, R.L., 2013. Variational estimation of land-atmosphere heat fluxes and land surface parameters using modis remote sensing data. J Hydrometeorol. 14, 608-621.

Michel, C., Andréassian, V., Perrin, C., 2005. Soil Conservation Service Curve Number method: how to mend a wrong soil moisture accounting procedure? Water Resources Research 41. doi:10.1029/2004WR003191.

Moriasi, D. N., Gitau, M. W., Pai, N., Daggupati, P., 2015. Hydrologic and water quality models: Performance measures and evaluation criteria. Trans. ASABE, 58(6), 1763-1785.

Mu, Q., Heinsch, F.A., Zhao, M., Running, S.W., 2007. Development of a global evapotranspiration algorithm based on MODIS and global meteorology data. Remote Sensing of Environment 111, 519-536.

Mu, Q., Zhao, M., Running, S.W., 2011. Improvements to a MODIS Global Terrestrial Evapotranspiration Algorithm. Remote Sensing of Environment 115, 1781-1800.

Mu, Q., Zhao, M., Running, S.W., 2013. MODIS Global Terrestrial Evapotranspiration (ET) Product (NASA MOD16A2/A3): algorithm theoretical basis document collection 5. National Aeronautics and Space Administration Headquarters, Wahsnigton DC, USA. Available online at: http://www.ntsg.umt.edu/sites/ntsg.umt.edu/files/MOD16_ATBD.pdf (last cited on February 18, 2017)

Myneni, R. B., Hoffman, S., Knyazikhin, Y., Privette, J.L., Glassy, J., Tian, Y. et al., 2002. Global products of vegetation leaf area and fraction absorbed PAR from year one of MODIS data. Remote Sensing of Environment 83(1–2), 214−231.

NASS-CDL, 2016. National Agricultural Statistics Service – Cropland Data Layer. US Department of Agriculture – Agricultural Research Service CropScape Viewer. Available at: https://nassgeodata.gmu.edu/CropScape/. Accessed March 10, 2016.

NCAR-RDA, 2016. National Center for Atmospheric Research – Research Data Archive. doi: 10.5065/D6513W89

Neitsch, S.L., Arnold, J., Kiniry, J., Williams, J., 2011. Soil and Water Assessment Tool theoretical documentation version 2009. Texas A&M University System, College Station, TX, USA.

Nicks, A.D., Lane, L.J., Gander, G.A.. 1995. Chapter 2: Weather generator. In Flanagan and Nearing (Eds.) USDA-Water Erosion Prediction Project: Hillslope profile and watershed model documentation. National Soil Erosion Research Laboratory, Report No. 10, West Lafayette, IN, USA.

Nishida, K., Nemani, R.R., Glassy, J.M., Running, S.W., 2003a. Development of an evapotranspiration index from aqua/MODIS for monitoring surface moisture status. IEEE Transactions on Geoscience and Remote Sensing 41 (2), 493-501.

Nishida, K., Nemani, R.R., Running, S.W., Glassy, J.M., 2003b. An operational remote sensing algorithm of land surface evaporation. J. Geophys. Res. 108(D9). doi:10.1029/2002JD002062.

Pan, M., Wood, E., Wójcik, R., McCabe, M.F., 2008. Estimation of regional terrestrial water cycle using multi-sensor remote sensing observations and data assimilation. Remote Sens Environ 112, 1282–1294.

Parajka, J., Naeimi, V., Blöschl, G., Wagner, W., Merz, R., Scipal, K., 2006. Assimilating scatterometer soil moisture data into conceptual hydrologic models at the regional scale. Hydrol. Earth Syst. Sci. 10(3), 353-368.

Paul, M., Rajib, M.A., Ahiablame, L., 2017. Spatial and temporal evaluation of hydrological response to climate and land use change in three South Dakota watersheds. Journal of the American Water Resources Association 53(1), 69-88. doi: 10.1111/1752-1688.12483

Price, K., Purucker, T., Kraemer, K.R., Babendreier, J.E., Knightes, C.D., 2014. Comparison of radar and gauge precipitation data in watershed models across varying spatial and temporal scales. Hydrol. Process. 28, 3503-3520. doi:10.1002/hyp.9890

Rajib, M. A., Merwade., V., 2016. Improving soil moisture accounting and streamflow prediction in SWAT by incorporating a modified time-dependent SCS CN method. Hydrol. Process. 30, 603-624. doi: 10.1002/hyp.10639

Rajib, M.A., Merwade, V., Yu, Z., 2016a. Multi-objective calibration of a hydrologic model using spatially distributed remotely sensed/in-situ soil moisture. J. Hydrol. 536, 192-207.

Rajib, M.A., Merwade, V., Kim, I.L., Zhao, L., Song, C., Zhe, S., 2016b. SWATShare – A web platform for collaborative research and education through online sharing, simulation and visualization of SWAT models. Environ. Model. Softw. 75, 498–512. doi:10.1016/j.envsoft.2015.10.032

Rathjens, H., Oppelt, N., Bosch, D.D., Arnold, J.G., Volk, M., 2015. Development of a grid-based version of the SWAT landscape model. Hydrological Processes 29(6), 900-914.

Reichle, R.H., Koster, R.D., 2005. Global assimilation of satellite surface soil moisture retrievals into the NASA catchment land surface model. Geophys. Res. Lett. 32 (2). doi: 10.1029/2004GL021700

Renzullo, L.J., van Dijk, A.I.J.M., Perraud, J.M., Collins, D., Henderson, B., Jin, H., Smith, A.B., McJannet, D.L., 2014. Continental satellite soil moisture data assimilation improves root-zone moisture analysis for water resources assessment. J. Hydrol. 519 (Part D), 2747–2762.

Richardson, C.W., Wright, D.A., 1984. WGEN: a model for generating daily weather variables. US Department of Agriculture – Agricultural Research Service, Report ARS-8.

Rui, H., Mocko, D., 2014. README document for North American Land Data Assimilation System Phase 2 (NLDAS-2) products. Goddard Earth Sciences Data and Information Services Center (GES DISC). Available online at: https://hydro1.gesdisc.eosdis.nasa.gov/data/NLDAS/README.NLDAS2.pdf (last cited on Fenruary 17, 2017)

Schuol, J., Abbaspour, K. C., Srinivasan, R., Yang, H., 2008b. Estimation of freshwater availability in the West African sub-continent using the SWAT hydrologic model. Journal of Hydrology 352(1), 30-49.

Schneider, K., Ketzer, B., Breuer, L., Vache, K.B., Bernhofer, C., Frede, H.-G., 2007. Evaluation of evapotranspiration methods for model validation in a semi-arid watershed in northern China. Adv. Geosci. 11, 37–42.

Schierhorn, F., Müller, D., Prishchepov, A., Faramarzi, M., Balmann, A., 2014. The potential of Russia to increase its wheat production through cropland expansion and intensification. Global Food Security 3, 133-141.

Sellami, H., Jeunesse, I., Benabdallah, S., Baghdadi, N., Vanclooster, M., 2014. Uncertainty analysis in model parameters regionalization: a case study involving the SWAT model in Mediterranean catchments (Southern France). Hydrol. Earth Syst. Sci. 18, 2393–2413.

Silvestro, F., Gabellani, S., Rudari, R., Delogu, F., Laiolo, P., Boni, G., 2015. Uncertainty reduction and parameter estimation of a distributed hydrological model with ground and remote-sensing data. Hydrology and Earth System Sciences 19(4), 1727-1751.

Stockle, C.O., Kiniry, J.R., 1990. Variability in crop radiation-use efficiency associated with vapor-pressure deficit. Field Crops Res. 25, 171-181.

Strauch, M., Bernhofer, C., Koide, S., Volk, M., Lorz, C., Makeschin. F., 2012. Using precipitation data ensemble for uncertainty analysis in SWAT streamflow simulation. Journal of Hydrology 414, 413–424.

Su, Z., 2002. The surface energy balance system (SEBS) (for estimation of turbulent heat fluxes. Hydrology and Earth System Sciences 6, 85-99.

Tang, Q., Peterson, S., Cuenca, R.H., Hagimoto, Y., Lettenmaier, D.P. 2009. Satellite-based near-real-time estimation of irrigated crop water consumption. J Geophys Res.-Atmos. 114, doi: 10.1029/2008JD010854

USDA, 2016. Climatic data for the United States: 1950-2010. US Department of Agriculture – Agricultural Research Service. Metadata is available at: https://www.ars.usda.gov/ARSUserFiles/30980000/us_climatic_data/Standard_Data_Details.pdf. Accessed March 10, 2016.

USGS-NED, 2016. National Elevation Dataset: United States Geological Survey National Map Viewer. Available at: http://viewer.nationalmap.gov/viewer/. Accessed March 10, 2016.

USGS-NLCD, 2016. National Land Cover Database 2011: United States Geological Survey National Map Viewer. Available at: http://viewer.nationalmap.gov/viewer/. Accessed March 10, 2016.

Wang, X., Melesse, A.M., Yang, W., 2006. Influence of potential evapotranspiration estimation methods on SWAT's hydrologic simulation in a northeastern Minnesota watershed. Trans. ASABE 49(6), 1755–1771.

Wang, K. C., Dickinson, R.E., 2012. A review of global terrestrial evapotranspiration: Observation, modeling, climatology, and climatic variability, Rev. Geophys. 50, RG2005, doi:10.1029/2011RG000373

Yang, W., Tan, B., Huang, D., Rautiainen, M., Shabanov, N.V., Wang, Y. et al. 2006. MODIS leaf area index products: From validation to algorithm improvement. IEEE Transactions on Geoscience and Remote Sensing 44, 1885-1898.

Yin, J., Zhan, C., Ye,W., 2016. An experimental study on evapotranspiration data assimilation based on the hydrological model, Water Resour. Management. 30 (14), 5263-5279, doi: 10.1007/s11269-016-1485-5

Zang, C.F., Liu, J., Van Der Velde, M., Kraxner, F., 2012. Assessment of spatial and temporal patterns of green and blue water flows under natural conditions in inland river basins in Northwest China. Hydrol. Earth Syst. Sci. 16, 2859–2870. doi:10.5194/hess-16-2859-2012

Zhang, Y., Wegehenkel, M., 2006. Integration of MODIS data into a simple model for the spatial distributed simulation of soil water content and evapotranspiration. Remote Sens. Environ. 104 (4), 393–408.

Zhang, Y., Chiew, F.H.S., Zhang, L., Li, H. 2009. Use of remotely sensed actual evapotranspiration to improve rainfall–runoff modeling in Southeast Australia. J Hydrometeorol. 10, 969-980.

Zhang, Y., Chiew, F., Zhang, L., Leuning, R., Cleugh, H., 2008. Estimating catchment evaporation and runoff using MODIS leaf area index and the Penman–Monteith equation. Water Resour. Res. 44 (10), doi: 10.1029/2007WR006563

APPENDIX A

Derivation of the time-dependent SMA-based CN equation

$$V = V_0 + \frac{P(S + I_a) - {I_a}^2}{P - I_a + S}$$

$$\Longrightarrow P(S + I_a) - (V - V_0)P = (V - V_0)(S - I_a) + {I_a}^2$$

$$\Longrightarrow P = \frac{(V - V_0)(S - I_a) + {I_a}^2}{S + I_a - V + V_0} \ldots\ldots\ldots [A.1]$$

Equation [A.1] can be expanded as follows:

$$P - I_a = \frac{(V - V_0)(S - I_a) + {I_a}^2 - I_a(S + I_a - V + V_0)}{S + I_a - V + V_0}$$

$$\Longrightarrow P - I_a = \frac{(V - V_0)(S - I_a) - SI_a + VI_a - V_0I_a}{S + I_a - V + V_0}$$

$$\Longrightarrow P - I_a = \frac{S(V - V_0) - VI_a + V_0I_a - SI_a + VI_a - V_0I_a}{S + I_a - V + V_0}$$

$$\Longrightarrow P - I_a = \frac{S(V - V_0 - I_a)}{S + I_a - V + V_0} \ldots\ldots\ldots [A.2]$$

Again,

$$P - I_a + S = \frac{S(V - V_0 - I_a) + S(S + I_a - V + V_0)}{S + I_a - V + V_0}$$

$$\Longrightarrow P - I_a + S = \frac{VS - S(V_0 + I_a) + S(V_0 + I_a) - VS + S^2}{S + I_a - V + V_0}$$

$$\Longrightarrow P - I_a + S = \frac{S^2}{S + I_a - V + V_0} \ldots\ldots\ldots [A.3]$$

Similarly,

$$P - I_a + 2S = \frac{S^2 + S(S + I_a - V + V_0)}{S + I_a - V + V_0} \ldots\ldots\ldots [A.4]$$

Combining equation [A.2] – [A.4],

$$\frac{(P - I_a)(P - I_a + 2S)}{(P - I_a + S)^2} = \frac{\{V - (V_0 + I_a)\}(2S + I_a - V + V_0)}{S^2}$$

$$\Longrightarrow \frac{(P - I_a)(P - I_a + 2S)}{(P - I_a + S)^2} = \frac{\{V - (V_0 + I_a)\}}{S}\left[2 - \frac{V - (V_0 + I_a)}{S}\right]$$

Since $(V_0 + I_a) = V'$

$$\frac{dV}{dt} = \frac{dP}{dt} - \frac{dQ}{dt}$$

$$\Longrightarrow \frac{dV}{dt} = \frac{dP}{dt}\left[1 - \frac{V - V'}{S}\left[2 - \frac{V - V'}{S}\right]\right]$$

$$\Longrightarrow \frac{dV}{dt} = \frac{dP}{dt}\left[1 - 2\left[\frac{V - V'}{S}\right] + \left[\frac{V - V'}{S}\right]^2\right]$$

$$\Longrightarrow \frac{dV}{dt} = \frac{dP}{dt}\left[1 - \left[\frac{V - V'}{S}\right]\right]^2$$

$$\Longrightarrow \frac{dV}{\left[\frac{V - S - V'}{S}\right]^2} = \frac{dP}{dt}dt \ldots\ldots\ldots [A.5]$$

Now, producing limit integral of equation [A.5] after rearrangement,

$$\int_{V_0}^{V} \frac{dV}{[V - S - V']^2} = \int_{0}^{P} \frac{dP}{S^2}$$

$$\Longrightarrow \frac{1}{S + V' - V} - \frac{1}{S + V' - V_0} = \frac{P}{S^2}$$

which refers to equation (3.7) in section 3.3.

APPENDIX B**:** Table B1**.** Calibrated parameter values

Parameter [a]	Best estimate				
	Upper Wabash			Cedar Creek	
	Single-site calibration/ CFSR weather [b]	Multi-site calibration/ CFSR weather [b, c]	Multi-site calibration/ WGN weather [c]	SWAT [d]	SWAT-Process [d]
v_ALPHA_BF	0.85	0.68	0.20	0.95	0.83
v_CANMX	8.50	8.47	25.0	20.2	5.0
v_SURLAG	2.18	7.67	5.72	0.86	18.90
v_CH_K2	33.06	30.72	64.05	85.37	81.95
v_CH_N2	0.086	0.068	0.087	0.056	0.039
r_CN2	0.19	-0.18	0.13	0.09	-0.09
v_EPCO	1.0	0.70	0.42	0.38	0.50
v_ESCO	0.23	0.01	1.0	0.95	0.20
a_GW_DELAY	0.45	-10.0	4.80	-2.55	-0.35
v_GW_REVAP	0.11	0.01	0.06	0.01	0.07
v_GWQMN	4643.0	0.01	4162.0	723.0	3803.0
v_REVAPMN	247.0	244.0	81.0	450.0	9.0
r_SOL_K	-0.14	0.15	-0.04	-0.15	-0.1
r_SOL_AWC	0.12	0.15	0.08	0.14	-0.07
v_SFTMP [c]	1.37	4.13	4.43	2.55	1.54
v_SMFMN [c]	0.62	6.61	10.0	5.04	8.0
v_SMFMX [c]	4.05	0.85	4.40	8.32	5.87
v_SMTMP [c]	1.29	0.22	-2.0	-0.86	1.52
v_TIMP [c]	0.42	0.54	0.38	0.47	0.48

[a] Parameter definitions and their initial ranges are provided in Table 3. All calibrations are performed using the same initial range; [b] Modeling experiment 1; [c]Modeling experiment 2; [d] Modeling experiment 3

131

APPENDIX B**:** Table B2**.** Calibrated parameter values

Parameter [a]	**Cedar Creek**		**Saline River**	
	SWAT [b]	**SWAT-PET**	**SWAT**	**SWAT-PET**
v_ALPHA_BF	0.95	0.98	0.82	0.75
v_CANMX	20.2	15.5	18.8	15.75
v_SURLAG	0.86	0.80	0.41	0.77
v_CH_K2	85.37	98.0	58.5	78.6
v_CH_N2	0.056	0.035	0.052	0.05
r_CN2	0.09	0.12	0.24	0.19
v_EPCO	0.38	0.26	0.89	0.40
v_ESCO	0.95	0.63	0.72	0.07
a_GW_DELAY	-2.55	-6.12	0.81	-8.75
v_GW_REVAP	0.01	0.08	0.02	0.07
v_GWQMN	723.0	2643.0	4118.0	825.0
v_REVAPMN	450.0	182.0	397.0	468.0
r_SOL_K	-0.15	0.12	-0.05	-0.13
r_SOL_AWC	0.14	-0.15	0.5	0.13
v_SFTMP [c]	2.55	1.90		
v_SMFMN [c]	5.04	8.10		
v_SMFMX [c]	8.32	5.40		
v_SMTMP [c]	-0.86	1.77		
v_TIMP [c]	0.47	0.28		

[a] Parameter definitions and their initial ranges are provided in Table 3. All calibrations are performed using the same initial range; [b] Modeling experiment 1; [c] Modeling experiment 2; [d] Modeling experiment 3

VITA

VITA

Adnan Rajib was born in Dhaka, Bangladesh. He graduated with a BS in Civil Engineering (major in Environmental and Structural Engineering) in 2008 from Bangladesh University of Engineering and Technology (BUET), securing 2nd position out of 185 graduates. Right after his graduation, he started working as a lecturer in the Department of Civil Engineering at BUET. Adnan received his MS degree in Civil Engineering (major in Environmental Engineering) from the same institute in 2010. He joined the graduate program in the Lyles School of Civil Engineering at Purdue University in Fall 2012 and received Doctor of Philosophy degree in May, 2017.

Adnan's area of expertise covers multi-disciplinary problems involving large-scale computational hydrology, hydroinformatics, satellite remote sensing, and cyber-enabled decision support systems for natural hazards. He has served as the Student Coordinator in the National Oceanic and Atmospheric Administration's 2016 Innovators program, where he lead a large group of researchers to mobilize a new operational flood forecasting and emergency response framework for the continental United States. In Spring 2016, Adnan was named as the recipient of the prestigious Bilsland Dissertation Fellowship, a top honor by Purdue's College of Education, recognizing an outstanding PhD candidate for scholarly achievements and excellence in research.